



Climate of the Gulf Coast States

An examination of climate change's effects across the region



Tropical Storm Isaac (CC BY 2.0)

**FLOOD
WISE
COMMUNITIES**

(This page is intentionally left blank)

Climate of the Gulf Coast States

*An examination of climate change's effects
across the region*

FloodWise Communities

Southern Climate Impacts and Planning Program (SCIPP)

Great Lakes Integrated Sciences + Assessments (GLISA)

University of Oklahoma

Joshua “Jay” Wimhurst, Kimberly Channell, Omar Gates, and Mark Shafer

June 2021

Suggested Citation: Wimhurst, J.J., Channell, K., Gates, O., and Shafer, M. (2021). Climate of the Gulf Coast States: An examination of climate change's effects across the region. *FloodWise Communities*, 74pp. [Available online at https://www.southernclimate.org/wp-content/uploads/Gulf_Coast_Climate.pdf].

Preface

Climate of the Gulf Coast States uses observations and climate model data to produce an in-depth examination of the climate of the six states (TX, LA, AL, MS, GA, FL) surrounding the Gulf of Mexico. This report is intended as supplementary material for people seeking more details after reading their *City/County Climate Summary*, and for those with an interest in better understanding broader climate trends beyond their communities. City planners may also find including this report in the appendices of climate and flood risk management plans useful.

This report is broken down into four chapters. [Chapter 1](#) covers the average historical state of the Gulf Coast States' climate, summarizing the region's physical geography, major climate classifications, and spatial patterns in its average temperature and rainfall climatology. [Chapter 2](#) uses observations to detail how the climate of the Gulf Coast States has changed in the last several decades, while connecting these changes to the current scientific consensus on climate change. [Chapter 3](#) provides an introduction to climate modeling, how the climate data used to prepare this report and the *City/County Climate Summaries* were selected, and subsequently what changes are likely for the Gulf Coast States' climate by the late-21st Century. Finally, [Chapter 4](#) is comprised of three-page summaries of weather-related hazards that frequently impact the Gulf Coast States, while also discussing their sensitivity to climate change.

The first three chapters are introduced by a *Chapter Summary* that highlights key messages for the reader. Regarding Chapter 4, the three-page summary of each hazard is intended as a mini-document for standalone use, hence a *Chapter Summary* is not provided.

Definitions of technical terminology are provided in the [Glossary](#) at the end of this report. Links to this *Glossary* are provided throughout, wherever such terminology is used. Links for chapter headings are also provided for ease of navigation.

Climate of the Gulf Coast States was written by [FloodWise Communities](#) for recruited cities, counties, and parishes across the region. Special thanks to Joshua "Jay" Wimhurst, Mark Shafer, Kimberly Channell, Omar Gates, Darrian Bertrand, and Simone Speizer for writing and guiding the construction of this report.

Climate of the Gulf Coast States - Chapter 1: Geography and Average Climatology

[Chapter Summary](#) 3

[Geography of the Gulf Coast States](#) 4

[Classifying the Gulf Coast States' Climate](#) 5

 1. The Humid Subtropical Climate 5

 2. South Florida's Tropical Wet-Dry Climate 6

 3. West Texas' Desert/Steppe Climate 6

[Average State of the Current Climate](#) 7

 1. Average Temperature 7

 2. Minimum Temperature 8

 3. Maximum Temperature 10

 4. Rainfall 11

[References](#) 13

Chapter Summary

This chapter summarizes the key physical features of the Gulf Coast States (TX, LA, MS, AL, GA, and FL), in terms of both their geography and recent climatology.

- The Gulf Coast States' physical geography is marked by dry mountainous terrain to the west that transitions into coastal plains and marshlands to the east.
- According to the Köppen-Geiger Climate Classification System, the vast majority of the region possesses a "humid-subtropical" climate, characterized by warm, humid summers and mild winters, with rainfall that peaks in frequency and intensity during the summer months.
- The climate of West Texas is classed as "desert/steppe", given its warm, arid conditions that are broken up by persistent early summer to mid-autumn rainfall. The "tropical wet/dry" climate of South Florida also has definable wet and dry seasons, though being much wetter than West Texas overall.
- Average temperatures across the Gulf Coast States are greater to the south, along with the differences in summer and winter temperatures being smaller.
- Freezing conditions also become increasingly rare to the south, almost never happening in South Florida.
- Summer temperatures that reach over 100°F are not uncommon in Central Texas. By contrast, coastal summer temperatures are typically slightly lower, thanks to temperature regulation from the Gulf of Mexico's sea breezes.
- Although Florida on average experiences the most wet days per year in this region, the heaviest rainfall often occurs further west along the coast, thanks to frequent convective thunderstorms.
- Several meteorological features influence the Gulf Coast States' climate, two important ones being the North American Monsoon (brings summer/autumn rains to West Texas) and the Bermuda-Azores High (brings warm, moist air and hurricanes from the tropics).

Geography of the Gulf Coast States

The Gulf Coast States (TX, LA, MS, AL, GA, FL) possess a wide-ranging geography, from the flat marshlands of the Florida Everglades to the imposing Guadalupe Mountains of West Texas. Altitude and geographical landmarks of this region are summarized in Figure 1. Peaking at 8750 ft, the Guadalupe Mountains represent the greatest elevation of the Gulf Coast States, giving way eastward to the semi-arid, high tablelands of the Llano Estacado and the Edwards Plateau. Progression into East Texas leads to the Gulf Coastal Plain, characterized by hardwood forests and pines that transition toward the coast into grasslands, shrubs, and occasional coniferous forests. This coastal flora lies atop low rolling hills across much of South Texas, Louisiana, and Mississippi, flattening across Alabama and Florida.

As well as the interspersed forests, the terrain of the Gulf Coastal Plain is broken up by alluvial plains crafted by rivers that discharge into the Gulf of Mexico, occasionally producing valleys with gentle slopes. Many of the larger alluvial plains exist on the western side of the Gulf Coastal Plains, thanks to large rivers such as the Rio Grande and the Mississippi depositing large amounts of fertile silt and changing course over millions of years.

While much of the Gulf Coast States become increasingly flat and dominated by low-lying flora to the east, the exception is the Blue Ridge Mountains (part of the Appalachians), which find their southern tip in North Alabama and Georgia. Elevations within these states reach over 4,700 ft (Brasstown Bald, GA), becoming lower among the rolling hills of the Piedmont to the south, and eventually returning to the flat grasslands of the Gulf Coastal Plain. This far to the east, the coastal flora become dominated by marshes, especially along the Florida Peninsula. Miles of flooded, reed-like grasses are a common sight, particularly in South Florida, as are (sub)tropical forests that have adapted to a warmer, wetter climate.

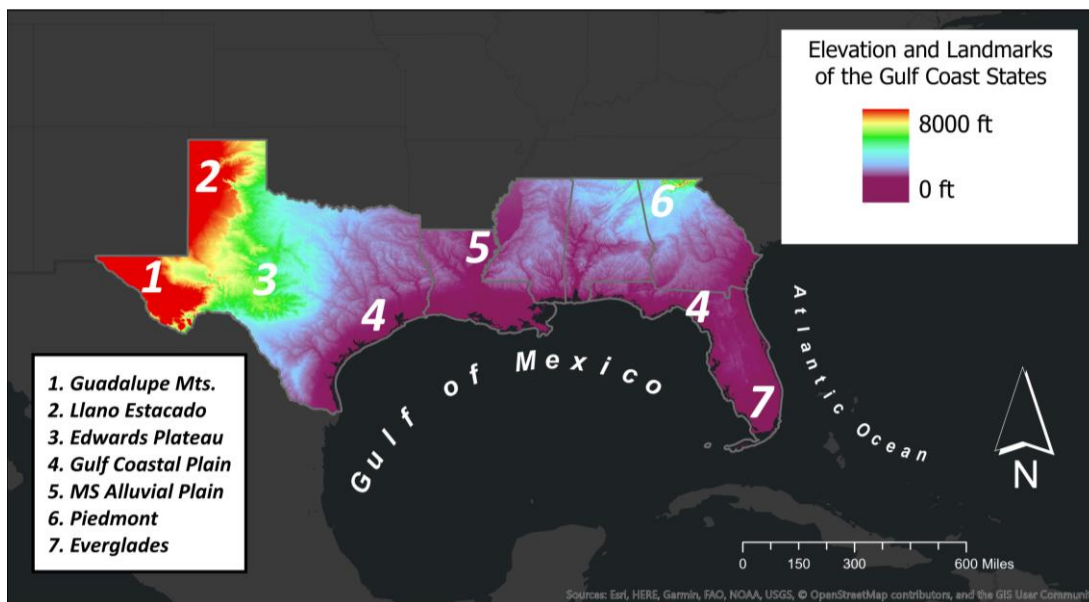


Figure 1: Map of elevation (in feet) and geographical landmarks of the Gulf Coast States. Meaning of white numbers is indicated by the bottom-left key. Data source: USGS (2007).

Classifying the Gulf Coast States' Climate

1. The Humid-Subtropical Climate

Most of the Gulf Coast States are classified as having a *humid-subtropical climate*, as shown in Figure 2 (Beck et al., 2018). Humid-subtropical climates feature warm, humid summers and mild winters that are typically drier further away from the coast. This climate is strongly influenced by the [Bermuda-Azores High](#), a large region of high-pressure air over the North Atlantic Ocean. Its clockwise motion steers warm, moist air from the tropics northwest towards the Gulf Coast States.

Across all seasons, temperatures in this climate region are often highest along the coast, with summer highs averaging 90°F or above in cities such as Houston, TX and Tampa, FL. Summer daytime temperatures in inland cities, like Atlanta, GA and Birmingham, AL, can be just as high if not higher. However, inland temperatures are less influenced by the slow heating and cooling of the Gulf of Mexico, allowing wind direction changes to significantly affect temperatures on subsequent days, especially in spring and autumn. Freezing temperatures are uncommon in humid-subtropical climates, with average winter lows usually remaining above 35°F. The retention of summer heat by the Gulf of Mexico's waters makes winter freezes along the coast a rare event. Further north, freezes are more common thanks to both proximity to the jet stream and the lack of a consistent wind from the south.

The region's humid air favors wetter conditions, with the frequency and intensity of rainfall peaking in summer months. Conditions are drier to the west, with East Texas receiving around 35 inches of rainfall per year. Further east, annual rainfall can exceed 60 inches per year, affecting cities such as New Orleans, LA and Mobile, AL. Much of the summer rainfall, especially nearer the coast, is convective (produced by daytime heating) and often yields thunderstorms. Although summer is generally the wettest season across the Gulf Coast States, there are some exceptions. For instance, seasonal thunderstorms peak in activity over inland Alabama and Mississippi in mid/late-spring. Secondly, hurricanes frequently pass over the Gulf Coast States in

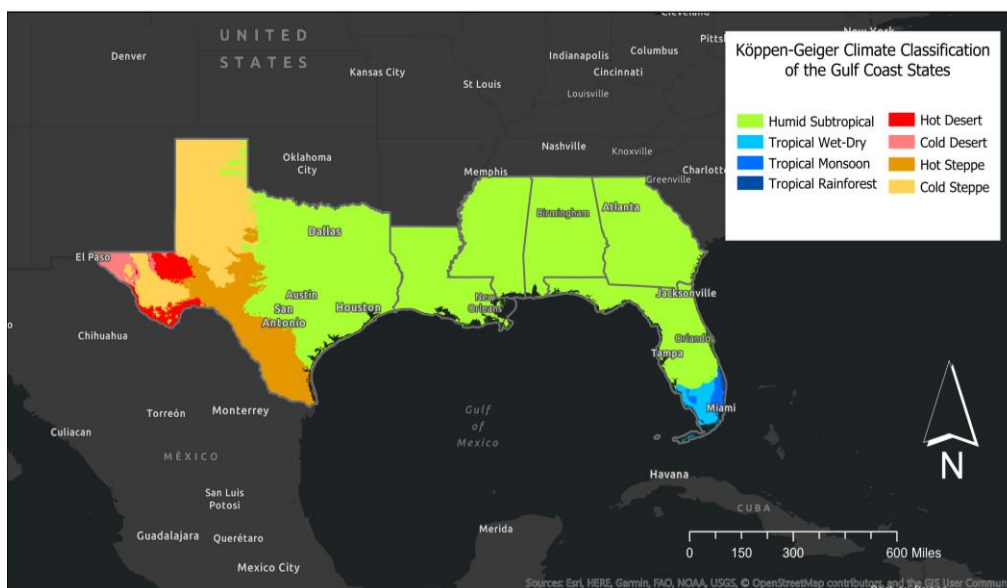


Figure 2: Map of current [Köppen-Geiger climate classifications](#) of the Gulf Coast States. Data source: Beck et al. (2018).

late-summer and autumn, bringing enhanced rainfall that is often most intense along the coast. The lack of below-freezing temperatures makes snowfall uncommon. Coastal cities experience snow every several years, though powerful snowstorms are much rarer, having historically happened around once every 100 years. Further inland, lower winter temperatures allow for more frequent snowfall, meaning cities like Dallas, TX receive an average of 1.7 inches of snow per year (NOAA, 2020).

2. South Florida's Tropical Wet-Dry Climate

While the climate of the Gulf Coast States is broadly humid-subtropical, South Florida is overall classed as having a *tropical wet-dry climate*. This climate class' features are average temperatures each month of at least 64°F (hot summers and warm winters), and definable wet and dry seasons in the summer (May-Oct) and winter (Nov-Apr) months respectively. South Florida's dry season is produced by westward expansion of the Bermuda-Azores High in winter, bringing drier and more settled weather. The wet season is produced by northward movement of equatorial rain belts in summer, bringing intense convective rainfall to the state.

Despite being further south, summer temperatures in South Florida are similar to those in the humid-subtropical areas of the Gulf Coast States. Cities such as Naples and Key West experience summer daytime temperatures above 90°F and nighttime lows in the mid/low-70s, similar to cities such as Houston, TX and New Orleans, LA. Daytime temperatures at this time of year are regulated by the bodies of water surrounding the Florida Peninsula: the Gulf of Mexico (west), the Straits of Florida (south), and the Atlantic Ocean (east). Conversely, winters in tropical wet-dry climates are warmer than their humid-subtropical counterparts. Winter highs above 70°F are common in South Florida, thanks to its low latitude, warm Atlantic winds from the east, and slow release of heat from its surrounding waters. Similarly, winter lows usually remain above 50°F, with lows near-freezing being rare. Below-freezing conditions occur just once every several decades.

Powerful wet season thunderstorms occur regularly in South Florida. According to the Florida Climate Center, Florida reports the most thunderstorm days of anywhere in the United States, averaging up to 80 days per year (FCC, 2020). South Florida's wet season rainfall often occurs in heavy bursts, with annual amounts reaching over 60 inches in Fort Lauderdale and Miami, and smaller annual rainfall totals further south (e.g., the Florida Keys) of around 40 inches. Wet season rainfall is enhanced in late-summer and autumn by hurricanes directed towards South Florida by the Bermuda-Azores High. Conversely, rainfall in the dry season is less common and less intense, almost never falling as snow. If snow falls in South Florida, it occurs as part of Nor'easters (cold-season storms that impact the Atlantic Coast) that swing especially far southward, last reaching as far south as Miami in 1977 (NOAA, 2012).

3. West Texas' Desert/Steppe Climate

West Texas possesses both a *desert climate* and a *steppe (semi-arid) climate*. These climates are characterized by low rainfall amounts year-round, with most rainfall occurring in warmer months, as well as by hot summers and mild to cool winters. Desert climates are mostly found in the high altitudes of far-west Texas, with steppe climates being further east on the tablelands

of the Llano Estacado and the Edwards Plateau. Although steppe climates experience more annual rainfall than desert climates, their temperature characteristics are very similar.

Summer daytime temperatures above 90°F are common across West Texas, especially to the south. Temperatures at night typically fall just below 70°F, meaning cities like El Paso have a similar summer temperature profile to other cities across the Gulf Coast States. Profile differences become apparent in winter, with milder daytime temperatures closer to 50°F in the Texas Panhandle, and 60°F further south. Winter temperatures frequently drop below freezing at night, especially in the high-altitude deserts.

West Texas is mountainous, meaning its climate is influenced by a “rain-shadow” effect from the nearby Sierra Madre Oriental Mountains. Rain from the west falls on the mountains’ windward side, thus not reaching West Texas, creating dry conditions. Another important driver of this desert/steppe climate is the [North American Monsoon](#). West Texas’ inland location means summer temperatures exceed those of the Gulf of Mexico. This inland heating shifts the wind direction and brings warm, moist air over land, and thus West Texas’ summer rains.

West Texas, particularly in winter, is much drier than the rest of the Gulf Coast States. Late-spring brings rainfall from thunderstorms, mostly to the northern steppes, hence the May/June rainfall maximum of West Texas cities such as Amarillo and Lubbock. The North American Monsoon is the biggest contributor to the region’s rainfall, bringing powerful evening convective thunderstorms in summer. The desert climate of the far-west experiences, on average, below 10 inches of rainfall per year, whereas the steppe climate of the high plateaus typically receives 10-25 inches per year, with the amount increasing further east. Although winter is the driest season of West Texas, heavy snow occasionally happens, thanks to incoming storms and below-freezing temperatures at high altitudes. Desert cities like El Paso receive around 7 inches of snow per year (US Climate Data, 2020¹), much less than steppe cities further north, such as Amarillo, at 19 inches per year (US Climate Data, 2020²).

Average State of the Current Climate

1. Average Temperature

Average temperature across the Gulf Coast States consistently increases from north to south, as shown in Figure 3a. From 1981-2010, annual average temperatures were below 60°F in the Texas Panhandle, West Texas, and North Alabama/Georgia, the region’s altitude extremes. Annual average temperatures above 70°F were common across South Texas and Florida. Increasing average temperatures to the south follows a progression from the cold to hot steppe, and the humid-subtropical to tropical wet-dry, climates illustrated in Figure 2.

Seasonal patterns of average temperature were not as consistent. Figure 3b shows average summer and winter temperatures for 16 of the region’s cities, ordered from north to south. Northern cities possessed greater seasonal temperature variation, with Amarillo, TX and Atlanta, GA having winters on average 35-40°F colder than their summers. By contrast, southern cities, such as Corpus Christi, TX and Miami, FL, possessed a smaller seasonal temperature range, with winters 15-25°F colder than summers. Seasonal temperature variation

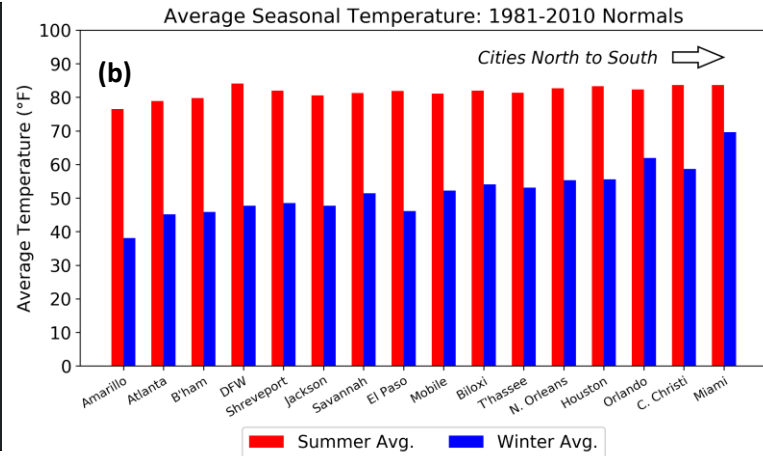
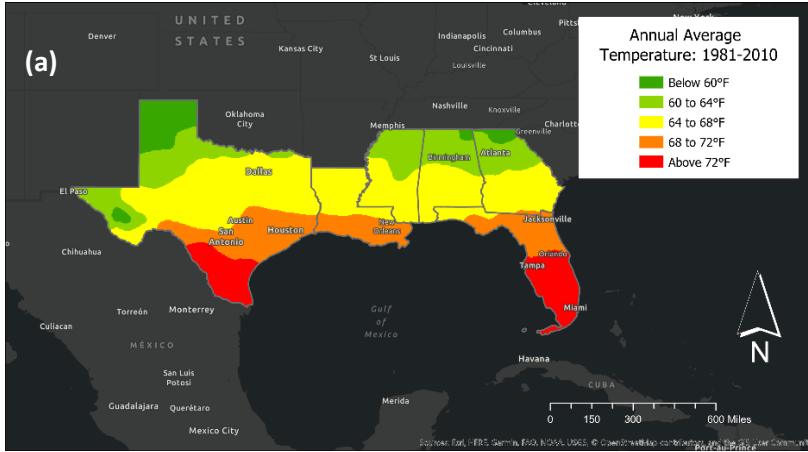


Figure 3: Annual average temperatures across the Gulf Coast States (3a, left) and average summer (red) and winter (blue) temperatures in 16 cities ordered from north to south (3b, right), both in °F, from 1981-2010. Data sources: NOAA PSL (2020¹); Arguez et al. (2010).

seems to be mostly produced by average winter temperature differences, increasing from below 40°F in Amarillo to about 70°F in Miami. By contrast, average summer temperatures possess a fairly small range of 75 to 85°F. Inland cities become much colder in the winter due to their distance from the relatively warmer oceans and how rapidly land heats up and cools down, hence their seasonal temperature range is much larger than the southern coastal cities.

2. Minimum Temperature

As with average temperature, minimum temperature (based on 1981-2010) also consistently increases from north to south. According to Figure 4, annual minimum temperatures below 8°F occurred notably in the Texas Panhandle, with below-freezing temperatures having occurred on average up to 120 days per year. This frequency is in contrast with coastal cities such as New Orleans, LA that experienced just 5 such days per year. The coldness of the Texas Panhandle and the Piedmont is explained by higher altitude and proximity to the jet stream. South Florida is the only area south of the 32°F line, with temperatures in some places having just fallen below 40°F. In this 30-year period, Miami experienced only 4 days with below-freezing temperatures, exemplifying how rare such cold conditions are in South Florida.

With such differences in the occurrence of below-freezing temperatures, it is unsurprising that freezing conditions persist later in the year in certain areas. Figure 5 summarizes the median date of first autumn freeze (5a) and last spring freeze (5b), as a percentage of the Gulf Coast States' total area (from 1981-2010). The most common date for first autumn freeze (first minimum temperature below 32°F) was late-November, accounting for over 40% of the region. Most of Florida (~60%) and the southern tip of Texas rarely experienced freezing conditions, meaning no date for a first autumn freeze ("No Freeze" column). Moreover, Louisiana's first autumn freeze happened slightly later in the year (late-November and early-December) than in most other states, thanks to late freezes nearer its coast.

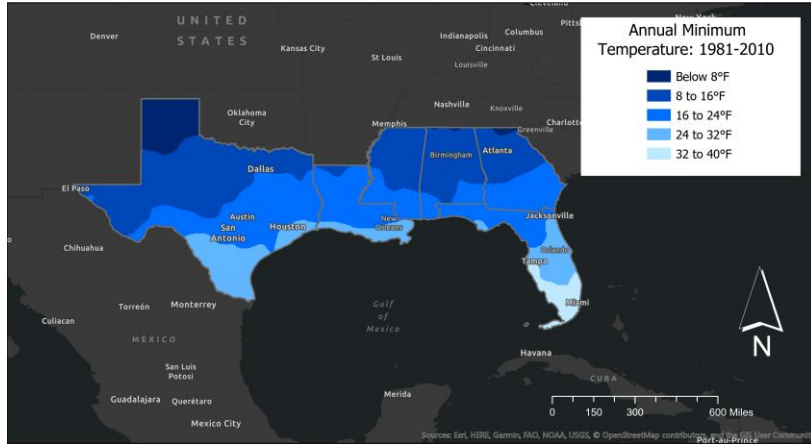


Figure 4: Annual minimum temperatures across the Gulf Coast States in °F, from 1981-2010. Data source: NOAA PSL (2020¹).

Louisiana also experienced its last spring freeze earlier than most other states, with over half of the state having had its last freeze in February. March was the most common month of last spring freeze for the other states (except Florida), representing 65% of the region. The same portion of South Florida again did not freeze, with most of the state having experienced its last freeze by early-February. The latest last spring freezes occurred in early-April, almost entirely confined to the Texas Panhandle and the Blue Ridge Mountains area of Alabama and Georgia. These same locations experienced the earliest first autumn freezes of late-October. Overall, higher minimum temperatures and earlier (later) last spring (first autumn) freezes typically occur at lower latitudes, lower altitudes, and closer to the Gulf of Mexico.

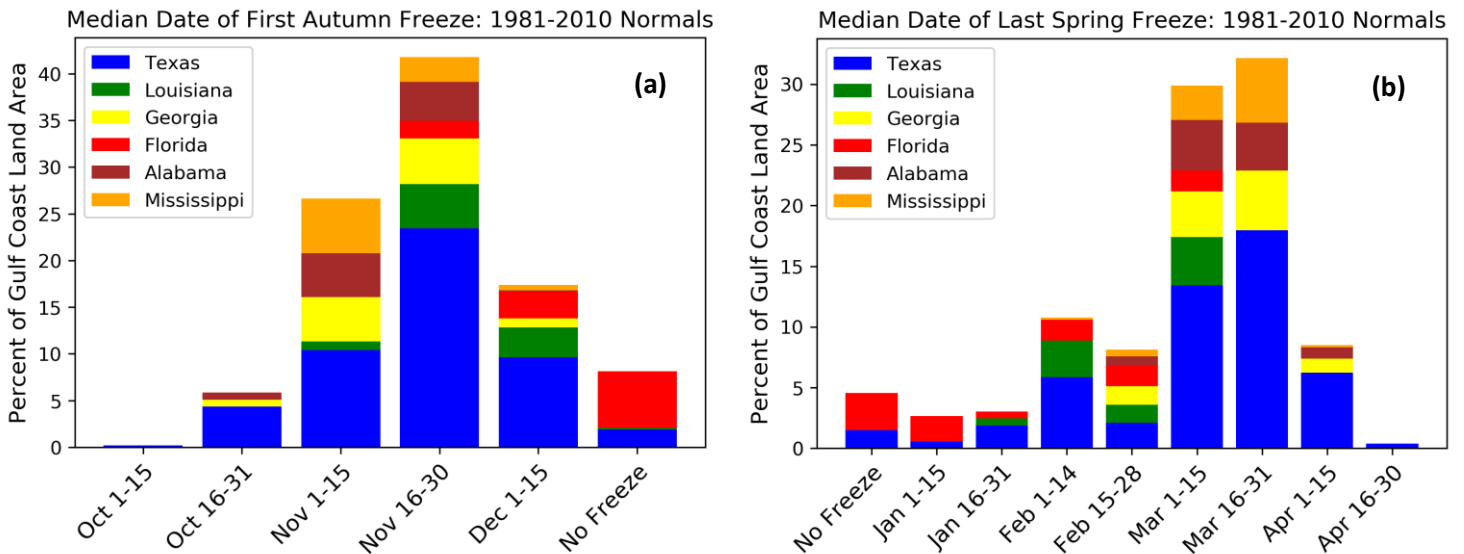


Figure 5: Median date of the first autumn freeze (5a, left) and the last spring freeze (5b, right) expressed as a percentage of the total Gulf Coast States area, from 1981-2010. Each color indicates the percent area of a different state. Data source: NOAA PSL (2020¹).

3. Maximum Temperature

Unlike average and minimum temperature, annual maximum temperature does not increase consistently with latitude, as shown in Figure 6a. Maximum temperatures from 1981-2010 typically did not exceed 98°F along the coast due to the oceans’ cooling effect in summer. Greater annual maximum temperatures occurred inland, particularly in West Texas, in some places having exceeded 104°F, affecting cities such as Lubbock, Midland, and El Paso. The importance of ocean proximity as a regulator of maximum temperature is apparent.

Insight into maximum temperatures also comes from their frequency and duration. Figure 6b summarizes state-averaged annual frequency of days with temperatures above 95°F (red), and the annual average length of the longest period of days above 95°F (blue). In agreement with Figure 6a, Texas experienced the greatest annual frequency, averaging almost 45 days per year. Due to Texas’ size, this value varied across the state, with places near Mexico having experienced up to 107 days per year, much more than the 36 days per year around Houston. The number of days above 95°F was quite consistent when comparing other states, at around 15 days per year. The range of frequency in these states was smaller than in Texas, with the number of days in Louisiana having ranged from 26 days per year in its north to 2 days per year in its south. Florida experienced the least days above 95°F, at 7 days per year. This infrequency was common along its coast, with cities like St. Petersburg, FL even having experienced no days above 95°F for several consecutive years.

The same pattern occurred for the annual average longest period of days above 95°F, with Texas having experienced the longest (~15 days per year), Florida the shortest (~2 days per year), and all other states in between (~6 days per year). Almost all of Texas experienced average maximum temperatures exceeding 95 Fahrenheit in four or five months of the year, therefore a high number of consecutive days above 95°F is expected. Such high monthly averages are less common elsewhere, occurring only in July and August in cities such as Atlanta, GA and New Orleans, LA, and not at all in cities further south like Tampa, FL. Maximum

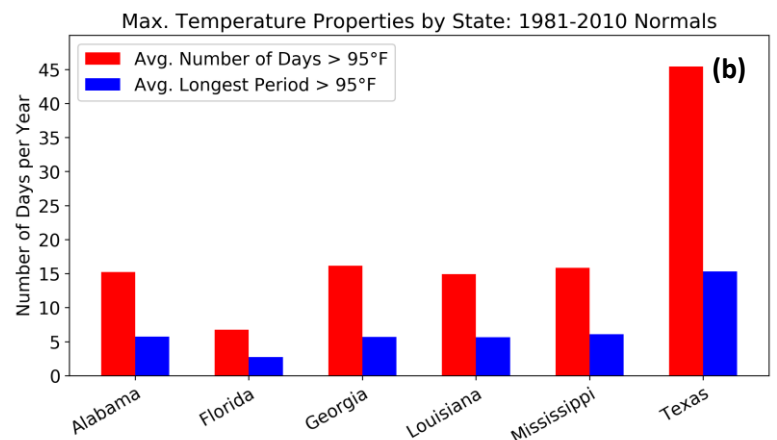
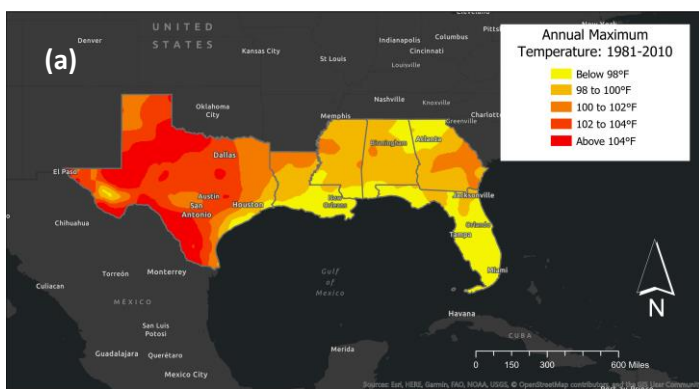


Figure 6: Annual maximum temperatures across the Gulf Coast States in °F (6a, left); state-averaged annual frequency (red) and annual average longest period (blue) of days above 95°F (6b, right) from 1981-2010. Data source: NOAA PSL (2020¹).

temperatures in the west of the Gulf Coast States were thus not only higher in magnitude from 1981-2010, but were also consistently high.

4. Rainfall

Rainfall amounts across the Gulf Coast States increase from west to east, peaking along the coast. The pattern of annual average rainfall amount from 1981-2010 is illustrated in Figure 7a, showing that West Texas was much drier than the rest of the region. Experiencing less than 20 inches per year, West Texas' rainfall was consistent with its desert/steppe climate. Conditions become wetter to the east, as altitude decreases and proximity to the warm, moist air of the Gulf of Mexico increases. Although Florida is known for thunderstorms and hurricanes, the greatest rainfall amounts actually occurred along the coasts of Louisiana, Mississippi, and Alabama, having exceeded 60 inches per year. This rainfall amount can be especially high in individual years, such as New Orleans, LA having received 96 inches in 1991. Even drier years along the coast, such as Mobile, AL having seen only 41 inches in 2000, were still wetter than the west of the region.

Florida does not have the highest rainfall amount, but it does have the highest rainfall frequency. Figure 7b shows the Gulf Coast States' annual average rainfall frequency (days per year with ≥ 0.01 inches of rainfall), which places Southeast Florida's frequency at over 200 days per year. This frequency maximum was associated with some especially wet years, such as Miami having reached up to 257 rainfall days in 1994. Unlike other states, almost all of Florida possessed an average rainfall frequency of above 175 days per year. In Louisiana, average rainfall frequency maximized at 185 days per year near the coast, and some places in West Texas did not even experience 100 days of rainfall per year. While rainfall frequency, like rainfall amount, does therefore increase from west to east, it is noteworthy that peak amount and peak frequency are not in the same locations. As such, while rainfall frequency over this period was greatest in Florida, the heaviest rainfall events most likely occurred over the coasts of Louisiana, Mississippi, and Alabama.

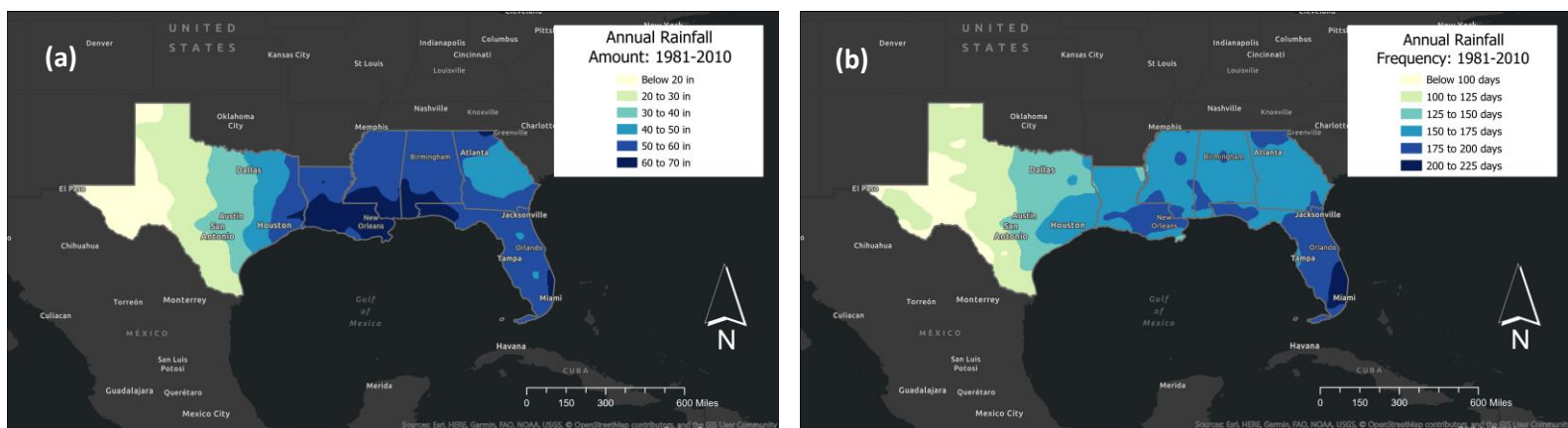


Figure 7: Annual rainfall amount in inches (7a, left) and annual rainfall frequency in days (7b, right) for the Gulf Coast States from 1981-2010. Data source: NOAA PSL (2020²).

Another important aspect of rainfall frequency is how long periods of rainfall last. Figure 8 shows state-averaged annual longest dry (red) and wet (blue) periods, with 0.01 inches of rain distinguishing wet from dry days. The average longest wet periods follow a similar pattern to Figure 7b; Florida possessed the longest annual wet period (~28 days per year), Texas the shortest (~10 days per year), with all other states in the middle (~13-14 days per year). This pattern reverses near-perfectly for longest annual dry period, except for Florida's value being comparable to other states at around 17 days per year. However, like temperature, rainfall can vary significantly, with wet period length often having peaked in areas of high rainfall amount/frequency. For instance, North Mississippi possessed an average longest wet period of around 11 days per year, but this increased to 20 days per year along the coast. Rainfall thus occurs more intensely, more frequently, and more consecutively closer to the Gulf of Mexico.

The Gulf Coast States also have notable monthly and seasonal rainfall patterns, as shown in Figure 9, charts of average monthly rainfall amounts for a selection of the region's cities from 1981-2010. The effects of the North American Monsoon can be seen in the chart for El Paso, TX, with rainfall having peaked at two inches in August, but being much lower outside of summer. Texan cities further east, namely Dallas and Houston, showed an elevated annual rainfall amount in the warmer months. However, whereas more northern cities like Dallas receive much of their rainfall from thunderstorms associated with the jet stream, southern cities like Houston are more influenced by the warm, moist air over the Gulf of Mexico.

Other cities along the coast, such as New Orleans, LA and Tallahassee, FL, possessed the region's characteristic peak in summer rainfall, which reached up to 8 inches per month. Miami, FL is representative of South Florida's typical rainfall climate, with its well-defined wet season in the warmer months and a high annual rainfall amount. The inland cities to the east, such as Birmingham, AL, and Atlanta, GA, are interesting because they experienced no definable peak in monthly or seasonal rainfall, instead having received around 3.5 to 5.5 inches each month.

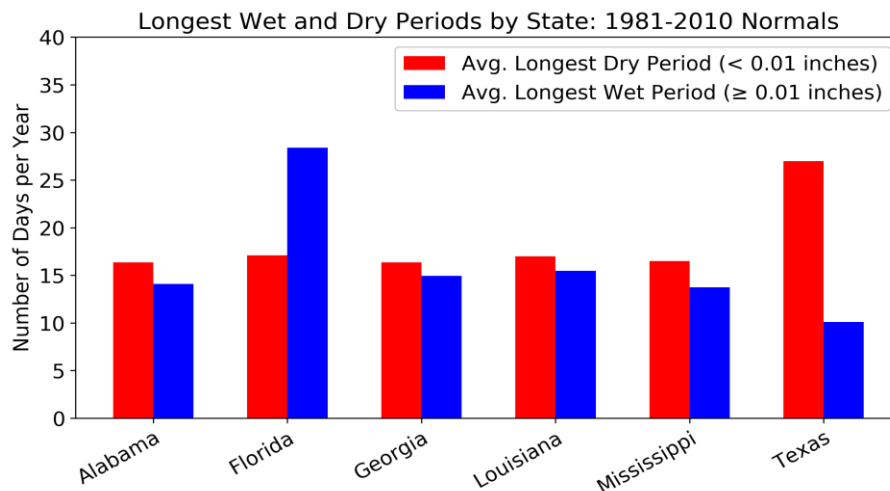


Figure 8: State-averaged annual longest dry (red) and wet (blue) periods using a rainfall criterion of 0.01 inches, from 1981-2010. Data source: NOAA PSL (2020²).

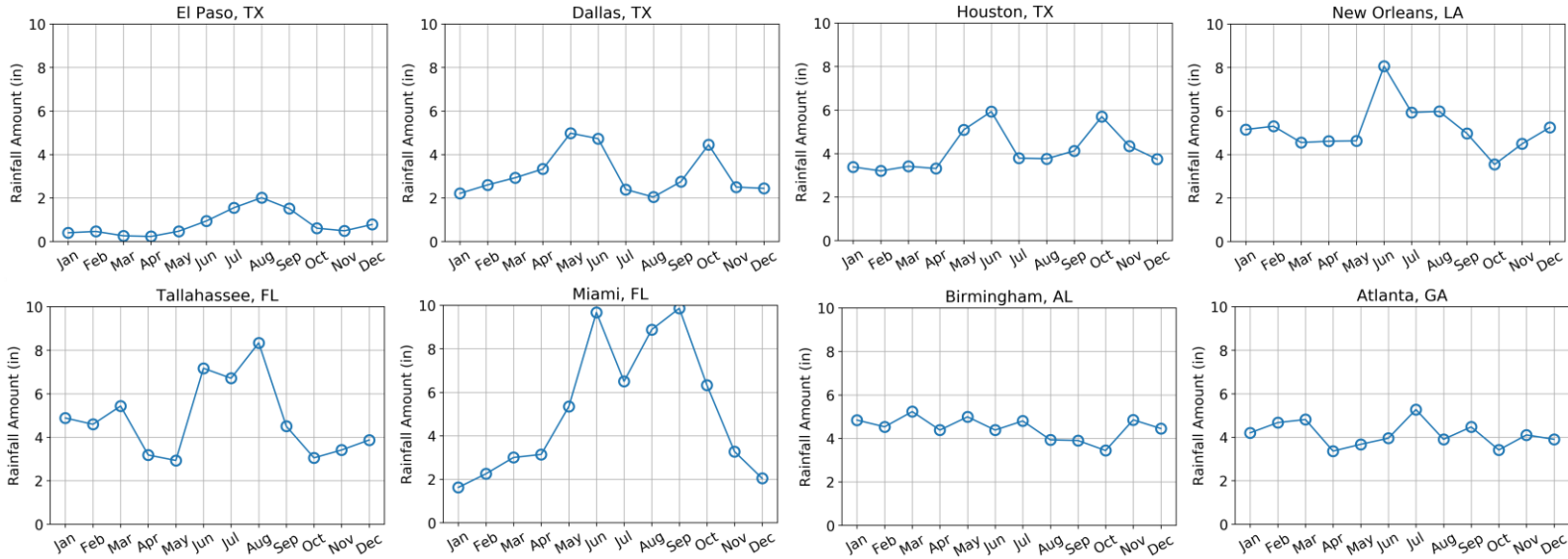


Figure 9: Average monthly rainfall amounts (in inches) for a selection of cities across the Gulf Coast States, from 1981-2010. Data source: Arguez et al. (2010).

Despite not having a rainfall maximum, these inland cities still experienced annual rainfall amounts and frequencies comparable to cities along the coast, as seen in Figure 7. These figures together therefore show how the nature of the region’s rainfall climate changes when moving further away from the coast.

References

Arguez, A., Durre, I., Applequist, S., Squires, M., Vose, R., Yin, X., and Bilotta, R. (2010). NOAA’s U.S. Climate Normals (1981-2010) – NOAA National Centers for Environmental Information, doi: 10.7289/V5PN93JP. Accessed July 13 2020.

Beck, H.E., Zimmermann, N.E., McVicar, T.R., Vergopolan, N., Berg, A., and Wood, E.F. (2018). Present and future Köppen-Geiger climate classification maps at 1-km resolution. *Scientific Data*, 5, 1-12, doi: 10.1038/sdata.2018.214.

FCC. (2020). Topics: Thunderstorms. Accessed July 18 2020. Available online at <https://climatecenter.fsu.edu/topics/thunderstorms>.

NOAA. (2012). Miami-South Florida NWS Forecast Office – 40th Anniversary of Snow in South Florida. Accessed July 18 2020. Available online at <https://www.weather.gov/media/mfl/news/SnowArticleSouthFlorida40th.pdf>.

NOAA. (2020). Dallas/Fort Worth - Normals (1981-2010), Means, and Extremes. Accessed July 18 2020. Available online at <https://www.weather.gov/fwd/dfwann>.

NOAA PSL. (2020¹). CPC Global Temperature data provided by the NOAA Physical Sciences Laboratory, Boulder, Colorado, USA. Accessed July 13 2020. Available online at <https://psl.noaa.gov/data/gridded/data.cpc.globaltemp.html>.

NOAA PSL. (2020²). CPC Global Unified Precipitation data provided by the NOAA Physical Sciences Laboratory, Boulder, Colorado, USA. Accessed July 13 2020. Available online at <https://psl.noaa.gov/data/gridded/data.cpc.globalprecip.html>.

US Climate Data. (2020¹). Climate El Paso – Texas. Accessed July 18 2020. Available online at <https://www.usclimatedata.com/climate/el-paso/texas/united-states/ustx0413>.

US Climate Data. (2020²). Climate Amarillo – Texas. Accessed July 18 2020. Available online at <https://www.usclimatedata.com/climate/amarillo/texas/united-states/ustx0029>.

USGS. (2007). North America Elevation 1-Kilometer Resolution GRID. Accessed July 13 2020. Available online at <https://www.sciencebase.gov/catalog/item/4fb5495ee4b04cb937751d6d>.

Climate of the Gulf Coast States - Chapter 2: Observed Changes in the Climate

<u>Chapter Summary</u>	16
<u>Observed Temperature Changes</u>	17
1. How/Why Has Temperature Changed?	17
2. Change in Average Temperature	19
3. Change in Ocean Temperature	20
4. Change in Number of Hot Days	21
5. Change in Number of Warm Nights	22
6. Change in Longest Freeze-Free Period	23
7. Temperature Change Summary	23
<u>Observed Rainfall Changes</u>	24
1. How/Why Has Rainfall Changed?	24
2. Change in Rainfall Amount	25
3. Change in Rainfall Frequency	26
4. Change in Heavy Rainfall Frequency	26
5. Change in Longest Wet and Dry Periods	27
6. Rainfall Change Summary	28
<u>References</u>	29

Chapter Summary

This chapter covers observed changes in the Gulf Coast States' climate that have taken place in the last 40 years, as well as the consistency of these changes with the expected impacts of climate change.

- Global average temperatures have increased by 2°F since the 1880s, and has largely been attributed to humans' influence on the climate. What is concerning about this increase is the rate at which it is happening, and how large it is compared to temperatures derived from 420,000 years of ice core records.
- Climate change is already affecting the Gulf Coast States in several ways, such as heat stress altering patterns of crop production, groundwater contamination from sea level rise, and coastal cities raising floodwater defenses to protect against storm surges from strengthening hurricanes.
- In the last 40 years, average temperatures across the Gulf Coast States have increased by around 1°F, mostly due to warmer winters, with increases being greater to the west.
- Hot days (days above 95°F) and warm nights (nights above 75°F) have both become more common as summers have warmed, and are more attributable to climate change than to the urban heat island effect.
- Freezing conditions have become less common in every part of the Gulf Coast States, especially along the coast itself.
- Trends in rainfall are not as spatially consistent as those for temperature, because rainfall is more variable by nature. That being said, the overall trend across the region has been annual rainfall amount reductions of up to -6 inches. Moreover, while annual rainfall frequency has decreased by up to -24 days in many places, the frequency of heavy (above-three-inch) rainfall events has seen a small increase.
- One consistent rainfall trend across the Gulf Coast States is consecutive days with rainfall becoming shorter and those without rainfall becoming longer, suggesting drying conditions for the last 40 years. This drying has been most pronounced over Florida and Texas.
- Although possessing more variability than temperature, the consensus is that rainfall in the Gulf Coast States has become heavier and less frequent, which is consistent with currently accepted theories about climate change's impacts.

Observed Temperature Changes

1. How/Why Has Temperature Changed?

Changes in the climate are certainly not new in Earth's history. Cycles of solar output, volcanic eruptions, and changes in Earth's orbit around the Sun have driven Earth's climate variability for millions of years. The concerning features of the current warming trend, however, are its rate and magnitude of change. Earth's natural climate drivers either take too long to produce changes (changes in orbit), do not produce long-term changes (volcanic eruptions), or produce changes too small (solar output) to explain the 2°F global average surface temperature increase since the 1880s (NASA, 2019). According to the [Intergovernmental Panel on Climate Change](#) (IPCC), observed temperature increases over the last several decades are best explained by a combination of human and natural climate change drivers, as shown in Figure 1 (EPA, 2014).

Emission of [greenhouse gases](#) (e.g., carbon dioxide and methane) is considered the most important human climate change driver. These gases are produced naturally to an extent, whether from biological processes or gradual release from the land/oceans. However, production of these gases has increased in the last 170 years due to manufacturing, agriculture, transportation, and many other human sources. This excess production has disturbed Earth's natural cycling of these gases, leading to their accumulation in the atmosphere (IPCC, 2013).

The [greenhouse effect](#), the natural process by which these gases trap heat released from Earth's surface into the atmosphere, has therefore been enhanced, preventing more heat from escaping into space and thus increasing global temperatures. Ice core records dating back 420,000 years show the consistent link between atmospheric carbon dioxide concentration and temperature (Figure 2 – Nord (2010)), hence the greenhouse effect's importance for maintaining temperatures that support life on Earth. This concentration reached 418 parts per million in 2020 (NOAA ESRL, 2020), much larger than any value in Figure 2, and continues to

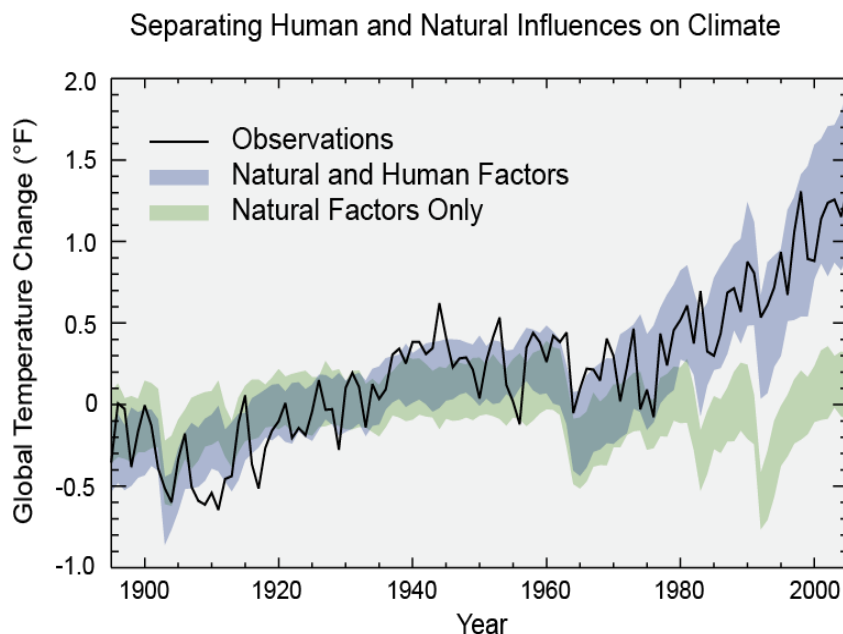


Figure 1: Record of observed global average temperature change (in °F) throughout the 20th Century (black). Model simulations of this observed change using natural (green) and human and natural (blue) drivers are also shown (EPA, 2014).

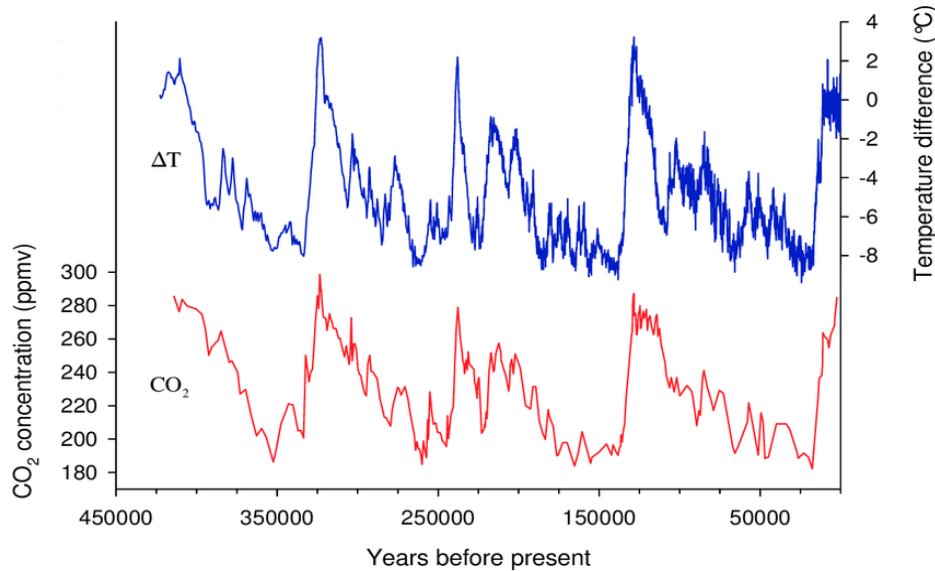


Figure 2: Temperature (red) and carbon dioxide concentration (blue) data derived from the Vostok ice core, from 420,000 years ago to now (Nord, 2010).

increase year after year. Combine this elevated concentration with the recently observed temperature increases (Figure 1), and the current climate change trend appears unprecedented during the Common Era.

Increased global temperatures present several risks to the economy, ecosystems, and survival of people across the Gulf Coast States, risks that are already beginning to present themselves:

- *Changes to crop-growing seasons.* Over time, temperature increases could allow crops that flourish in warmer climates, such as oranges and tomatoes, to be grown further north. Conversely, there is the concern of heat stress, and consequent soil erosion and irrigation demands, should temperatures become too high. This concern is rising in Florida, as its already high temperatures increasingly threaten the length and yield of the growing season of heat-sensitive crops, such as peanuts, sorghum, and rice (Gu Her et al., 2017).
- *Spread of vector-borne diseases.* *Aedes Aegypti*, a mosquito species capable of transmitting diseases like chikungunya, dengue, and Zika, can survive and has potential to infect human populations across the Gulf Coast States. Higher winter temperatures due to climate change could allow this mosquito to be active for longer periods of the year, particularly in the warm, moist areas nearer the coast (Butterworth et al., 2017).
- *Contributions to sea level rise.* Increasing global temperatures have contributed to a loss of land ice volume and to thermal expansion of ocean water, resulting in sea level rise around the world (see [Chapter 4: Sea Level Rise](#)). Sea level rise presents several challenges to the Gulf Coast States, such as property and livelihood damage to coastal cities, particularly in low-lying states like Florida (Wdowinski et al., 2016). Another challenge is saltwater intrusion into groundwater supply, notably the Gulf Coast Aquifer underneath Louisiana and Texas, which has become more saline in the last 25 years in part due to rising sea levels flooding the aquifer (Anderson and Al-Thani, 2016).
- *Frequency and intensity of hazardous weather.* The Gulf Coast States experience several forms of hazardous weather, such as droughts, tornadoes, and hurricanes. Higher temperatures due to climate change have been linked to more frequent and intense

hazardous weather across the region, such as the depletion of salamander populations by drought in Northwest Florida (Walls et al., 2013), and the powerful rainfall and property damage along the Texas coast due to Hurricane Harvey (Trenberth et al., 2018). Higher temperatures also lead to more heatwaves, and their associated infrastructural and human health impacts. Indeed, the Southeast United States has recently experienced more heatwaves than any other region in the country (Smith et al., 2013), hence the concern for heatwaves becoming more frequent and intense. Chapter 4 covers hazardous weather mechanisms and their responses to climate change in detail.

Note about Methodology: The effects of climate change on temperature, based on these examples, are already being felt in ways that directly affect people’s lives. To get an idea of how much the climate has already changed, the analyses below assess several temperature change indicators over the last several decades across the region. All analyses in this chapter were conducted over the period 1979-2019 (unless otherwise stated), by fitting best-fit trend lines to observed Climate Prediction Center data (NOAA PSL, 2020^{1,2}) using linear least-squares regression. This approach was also used for data analyses presented in Chapters 3 and 4.

2. Change in Average Temperature

Increase of average temperature is a fundamental indicator of climate change’s recent effects. The pervasiveness of this increase can be seen in Figure 3a, a map of the change of annual average temperature across the Gulf Coast States from 1979-2019. Temperature increases of over 1°F in just 40 years are commonplace, especially further west, with some areas of the West Texas deserts/steppes having become over 2°F warmer in that time. Increases were somewhat smaller to the south-east, especially in Florida, likely due to being surrounded by the ocean and being closer to the equator, where recent warming has tended to be smaller (IPCC, 2013). These increases of annual average temperature have been largely consistent over this period, as shown by regional 5-year average temperatures in Figure 3b. While the warming trend slowed down in the 2000s, the average temperature across the region still increased overall by 2.21°F.

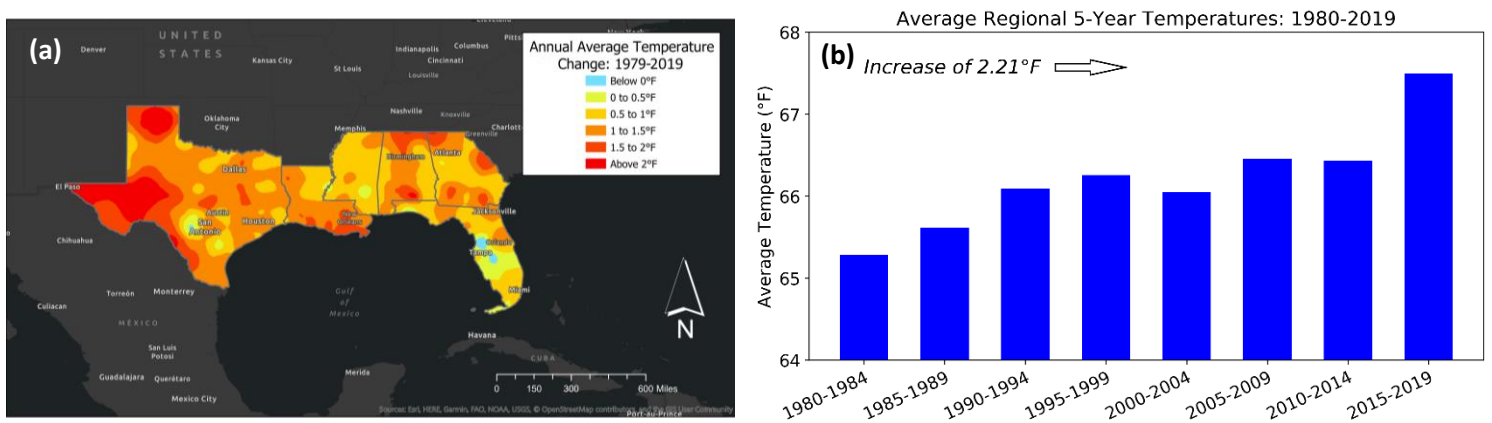


Figure 3: Change of annual average temperature across the Gulf Coast States from 1979-2019 (3a, left) and regionally-averaged 5-year average temperatures from 1980-2019 (3a, right), both in °F. Data source: NOAA PSL (2020¹).

Breaking down these average temperature increases by season reveals the times of year that influenced Figure 3’s annual trends the most. This seasonal breakdown from 1979-2019 is given for four cities across the Gulf Coast States in Figure 4, each one representing a different [Köppen-Geiger classification](#) – tropical wet/dry (Miami, FL), coastal humid-subtropical (New Orleans, LA), inland humid-subtropical (Atlanta, GA), and desert/steppe (El Paso, TX). These seasonal temperature increases are mostly larger than the annual increases in Figure 3, with El Paso having experienced an increase of above 4°F in spring, summer, and autumn. This figure also shows that seasonal temperature increases were largest in the warmer seasons in desert cities like El Paso, as opposed to the cooler seasons in wetter cities like Atlanta and New Orleans. Figure 4 thus suggests that the greater temperatures across much of the Gulf Coast States were mostly due to warmer winters than 40 years ago, assuming that the trends in this figure hold across the region.

3. Change in Ocean Temperature

Since the waters of the Gulf of Mexico are important for regulating temperatures on land ([discussed in Chapter 1](#)), it is worth examining how the temperature of the waters themselves has changed in recent years. Unfortunately, reliable ocean temperature observations are hard to find, and those that exist have been kept consistently for just 30 years. As such, Figure 5 presents two charts of annual average ocean temperatures since the 1990s, for a coastal station in southeast Florida (5a) and an open ocean buoy off the Texas coast (5b).

Two differences between these charts stand out. Firstly, average temperatures were lower at the open ocean buoy than the coastal station, by around 3 to 4°F. Secondly, ocean temperatures increased much more at the coastal station, rising by 1.73°F over 30 years, compared to the much smaller 0.69°F increase at the open ocean buoy. With land being further away at the open ocean buoy, the greater water volume surrounding it requires more heat and time to increase in temperature, hence the lower average temperatures and smaller

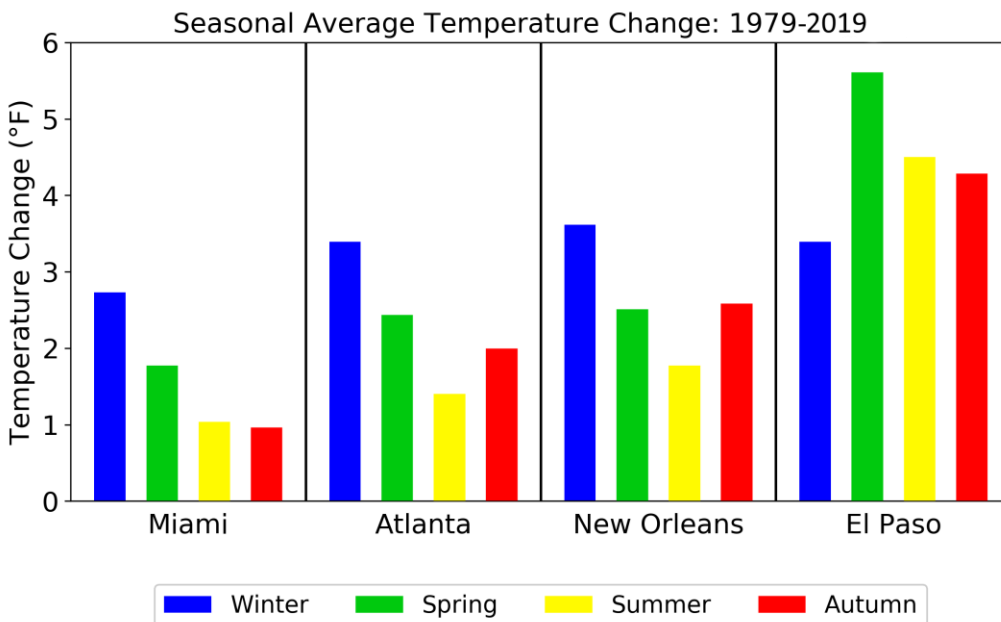


Figure 4: Seasonal average temperature change for four cities across the Gulf Coast States, in °F, from 1979-2019. Data source: NOAA PSL (2020¹).

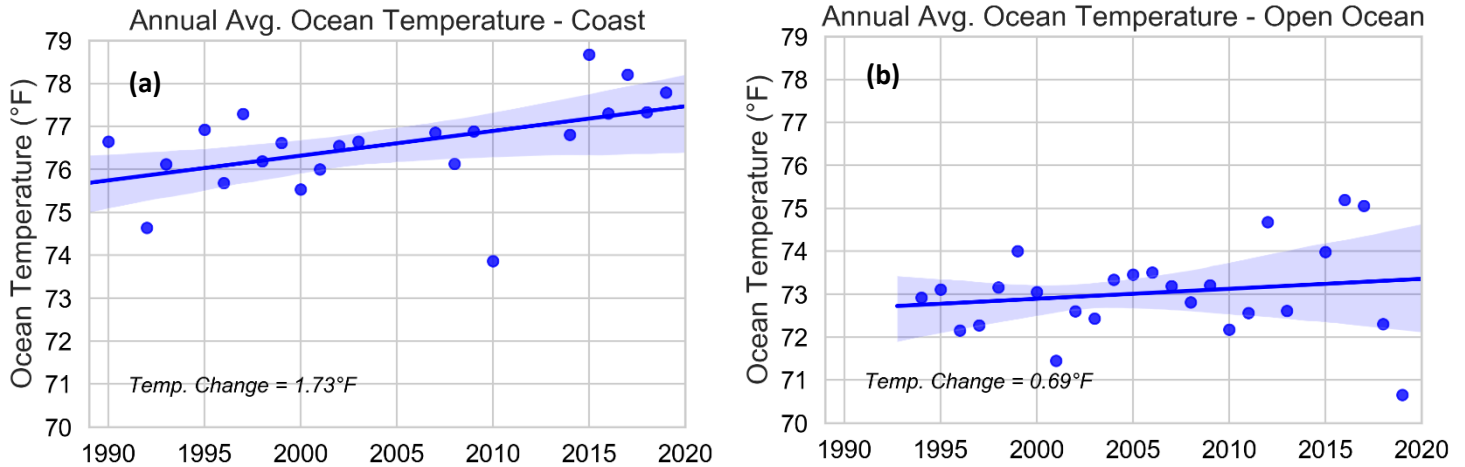


Figure 5: Change in annual average ocean temperature at a coastal ocean station (5a, left) and an open ocean buoy (5b, right), both in °F, from the early 1990s to 2019. The blue line is the trend line, and the blue shading is the confidence interval of the trend line’s slope. Data source: NOAA NBDC (2020).

temperature increase than at the coastal station. Although 0.69°F sounds small compared to the warming over land, this increase has resulted from a massive oceanic heat intake, with the Gulf of Mexico gaining more heat per square mile than much of the world’s oceans (Johnson et al., 2020). The oceans are gradually releasing this heat into the atmosphere, which will lead to temperature increases potentially much larger than those that the Gulf Coast States have already observed.

4. Change in Number of Hot Days

Much like the US Fourth National Climate Assessment (Carter et al., 2018), a hot day is defined for the Gulf Coast States as a day on which the maximum temperature exceeds 95°F. The change in the number of hot days thus measures the change in maximum temperature and the change in the duration of extreme heat events. Figure 6a shows that in the last 40 years, the

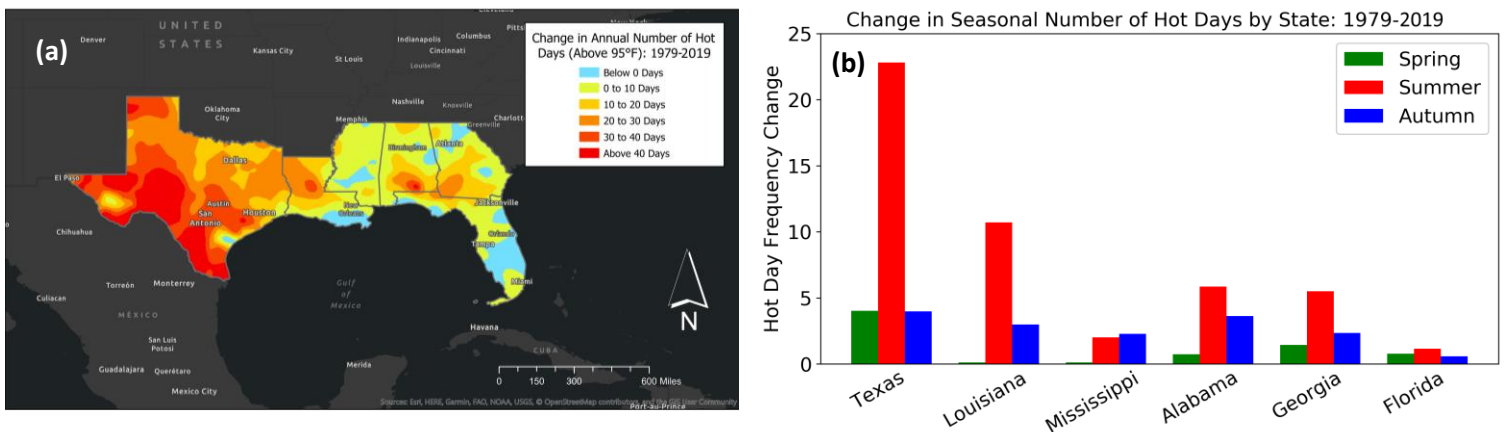


Figure 6: Change in annual number of hot days (days with maximum temperatures above 95°F) across the Gulf Coast States (6a, left) and state-averaged change in seasonal number of hot days (6b, right), both from 1979-2019. Data source: NOAA PSL (2020¹).

Gulf Coast States' largest increases in annual hot day frequency have occurred to the west, with most of Texas and North Louisiana now experiencing over 20 additional hot days in a single year. To the east, hot day increases were smaller, with places like South Louisiana/Florida and inland Georgia and Mississippi having experienced small decreases. Maximum temperature analysis in Chapter 1 showed that the eastern half of the region, and the coastline itself, possessed lower annual maximum temperatures ([Chapter 1, Figure 6a](#)), hence days above 95°F have historically been less common in these locations. It is therefore expected that the western half of the Gulf Coast States will have experienced a greater observed increase in hot day frequency. What is true of all states (except Mississippi), however, is that these increases in hot day frequency have been mostly influenced by warmer summers, as shown in Figure 6b.

5. Change in Number of Warm Nights

Along with hot day frequency, change in the number of warm nights is also considered, a warm night (in the Gulf Coast States) being a day on which the minimum temperature remains above 75°F (Carter et al., 2018). Examining the change in number of warm nights thus accounts for the change in the highest minimum temperatures over the last several decades. Figure 7 shows by how much the annual warm night frequency changed from 1979-2019. Figure 7 follows somewhat of a rural-urban pattern, as opposed to the east-west pattern of Figure 6a. The greatest increases in warm night frequency occurred around rapidly growing urban areas, particularly the Texas Triangle and several of Florida's cities, with an additional 40 warm nights per year being common.

Increased warm nights in urban areas suggests that a strengthened urban heat island effect may be a contributing factor. Cities release large amounts of heat from buildings, vehicles, lights, and accumulated daytime heat from man-made surfaces, meaning that urban areas are typically warmer at night than nearby rural areas. Urban expansion intensifies the urban heat island effect (Huang et al., 2019), thus contributing to warm night increases in urban areas. However, some increases in Figure 7 appear to have also happened outside of the region's largest cities. For that reason, increased temperatures produced by climate change are still an

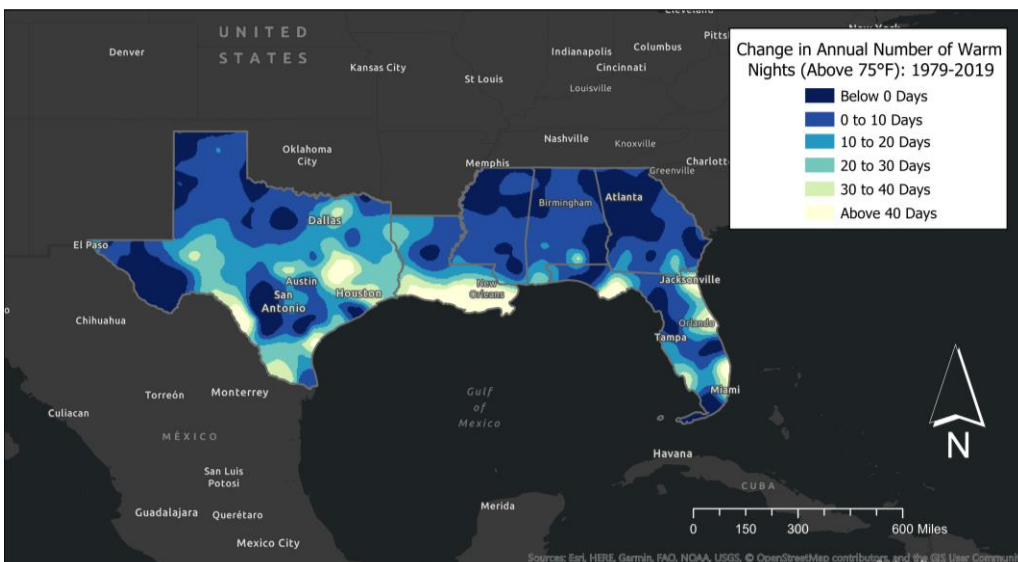


Figure 7: Change in annual number of warm nights (days with minimum temperatures above 75°F) across the Gulf Coast States, from 1979-2019. Data source: NOAA PSL (2020¹).

important driver of increased warm night frequency. Furthermore, not every large city or metropolitan area has observed an increase in the number of warm nights. Cities such as Atlanta, GA and San Antonio, TX seemed to have experienced decreases of warm night frequency, thus the role of the urban heat island effect should not be overstated.

6. Change in Longest Freeze-Free Period

The final considered temperature change indicator is the change in longest annual freeze-free period, defined as the longest run of consecutive days in a year without minimum temperature falling below 32°F. The longer this period becomes, the fewer days that experience freezing conditions. Figure 8 shows how the longest annual freeze-free period across the Gulf Coast States has changed in the last 40 years. Increases occurred in every part of the region, meaning that freezes have become less common in recent years. The biggest increases in freeze-free period have happened further south and closer to the coast, becoming over two months longer in some places. While this increase seems large, recall from [Chapter 1](#) that freezing conditions are rare along the coast itself, and barely happen at all in South Florida. As such, if freezing conditions changed from occurring once or twice per year 40 years ago to zero times per year today, such a large increase in freeze-free period length is conceivable.

7. Temperature Change Summary

Temperature trends of the last 40 years tell a story of consistent warming (Figure 3), greater temperature extremes (Figure 6), seasonality of temperature increases (Figure 4), and significantly warmer nighttime conditions (Figure 7, Figure 8). Some of these changes have notable patterns across the region, such as the largest temperature/hot day frequency increases having happened to the west, and the largest freeze-free period increases having been to the south. Climate change's role in increasing temperatures can be seen across these indicators. The maps and charts in these figures thus contextualize how much of an impact human activity is having on the climate system, and why the climate change impacts discussed at the beginning of this chapter are already having effects on people.

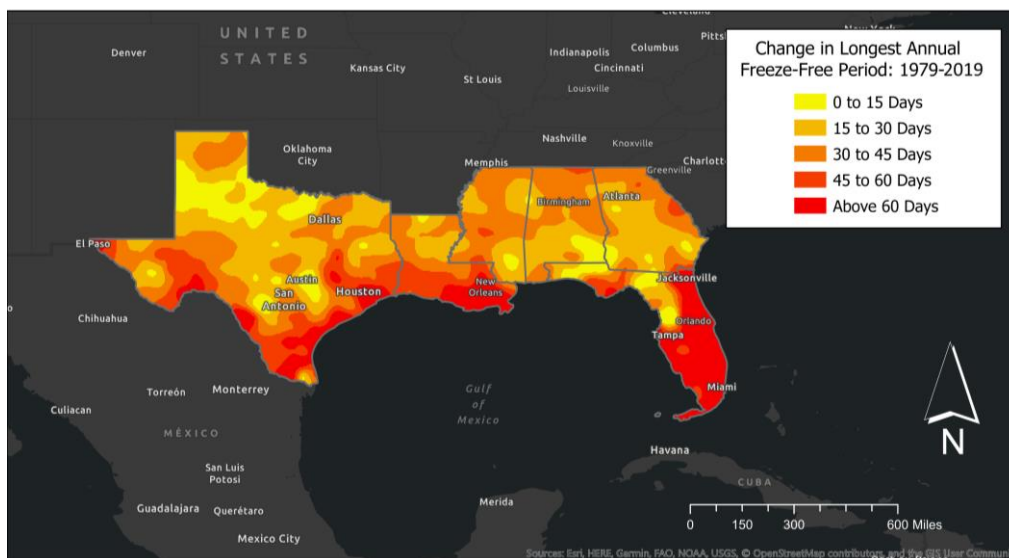


Figure 8: Change in the longest annual freeze-free period (longest run of days with minimum temperatures above 32°F) across the Gulf Coast States, from 1979-2019. Data source: NOAA PSL (2020¹).

Observed Rainfall Changes

1. How/Why Has Rainfall Changed?

Climate change's effects on rainfall are largely a consequence of its effects on temperature. An enhanced greenhouse effect results in a warmer atmosphere, allowing more water from the oceans and land to be held in the air as clouds and water vapor. Since a warmer atmosphere can hold more water, bigger clouds can form before the air is saturated, resulting in more powerful but less frequent rainfall events (Trenberth, 2011). Climate change is therefore associated with heavier bursts of rainfall that are broken up by longer droughts.

Not only does climate change encourage more extreme rainfall, but it can also affect where rainfall happens. A warmer climate means changes to the atmosphere and ocean circulations that transport excess heat away from the equator and toward the poles. These changes have consequences for rainfall distribution, most notably a poleward shift of the world's rain belts (Putnam and Broecker, 2017), thus making some areas of the globe wetter and others drier. There are, however, many exceptions to this consensus among climate scientists, since even areas in proximity can experience quite different changes in rainfall characteristics (IPCC, 2013). It is thus important to not disregard the variability of rainfall trends in the context of climate change, whether for the Gulf Coast States or otherwise.

As with temperature, climate change's effects on rainfall have several social, economic, and environmental consequences, which are already posing a threat to the Gulf Coast States:

- *Effects on groundwater recharge.* Rainfall is vital for the recharge of groundwater reserves. The more rainfall runoff that occurs along the land, the more an aquifer can be refilled. The Edwards Aquifer in Central Texas, for example, is highly dependent on rainfall runoff, and is a critical water supply for drinking and irrigation. Reduced rainfall runoff due to climate change could threaten local economies and clean water access (Mace and Wade, 2008).
- *Flood risk from heavy rainfall.* Rainfall that occurs in heavy bursts increases the risk of flood events. Such events are not uncommon in the Gulf Coast States, particularly along the coast where warm-season thunderstorms are a frequent occurrence, significantly increasing the risk of damage to property and livelihoods. Climate change is increasing this flood risk as rainfall events become heavier, which was highlighted by the catastrophic flooding and damages across South Louisiana in 2016 (van der Wiel et al., 2017).
- *Worsening of drought.* There is some evidence to suggest that droughts across the Gulf Coast States may be becoming more severe. In the last few decades, the region has seen several record-breaking droughts (USDA, 2017), and summer rainfall amounts have almost consistently fallen for the last 100 years (Kunkel et al., 2013). With summer being the wettest season for much of the region ([Chapter 1, Figure 9](#)), drought produced by reduced rainfall can place stress on agriculture, domestic water use, energy generation, and many other sectors.
- *Stress on existing stormwater management infrastructure.* As rainfall associated with powerful storms becomes more intense and thus increases flood risk, greater stress is placed on infrastructure that minimizes stormwater damage. This stress is compounded

along coastlines by sea level rise, hence cities such as Miami, FL have drafted multi-billion-dollar flood-proofing plans with new and elevated stormwater defenses (Allen, 2020).

The recent flood and drought intensity, as well as action to adapt to a wetter, more hazardous climate, show that climate change’s effects on rainfall may already be impacting the region’s people. The next thing to ascertain is the extent of these effects over the last few decades.

2. Change in Rainfall Amount

The amount of rainfall across the Gulf Coast States is considered first in Figure 9a, a map of change in annual average rainfall amount from 1979-2019. This map shows no progression of change from east-west or north-south, but reductions of rainfall amount have occurred throughout the region. These reductions are inconsistent in magnitude, though most rarely exceeded a decrease of 6 inches, i.e., half a foot less of rainfall per year than 40 years ago. Slight increases of rainfall amount occurred in the east and west of the region, namely across Georgia, South Florida, and Central Texas. Decreases of more than 6 inches were more common in Mississippi and Louisiana. Although less spatially consistent than the recent changes in temperature (Figure 3), the overall slight reduction of rainfall is clear, and by extension the potential influence of climate change.

One part of Figure 9a that stands out is a small area of South Louisiana where the annual rainfall amount dropped by over two feet. Figure 9b presents monthly average rainfall amounts from 1980-1999 and 2000-2019 for this area, thus illustrating the months of greatest rainfall amount loss. The biggest losses took place in January through to July, reaching up to 2.5 inches in a single month. This area of South Louisiana is situated in the state’s bayou swamps, which receive an average of over 50 inches of rainfall per year (Chapter 1, Figure 7). With its climate being so wet, South Louisiana is likely vulnerable to even slight increases in temperature (e.g., the cooler seasons becoming warmer in nearby New Orleans, LA – Figure 4), and consequently losses of rainfall, hence this area was worth examining specifically.

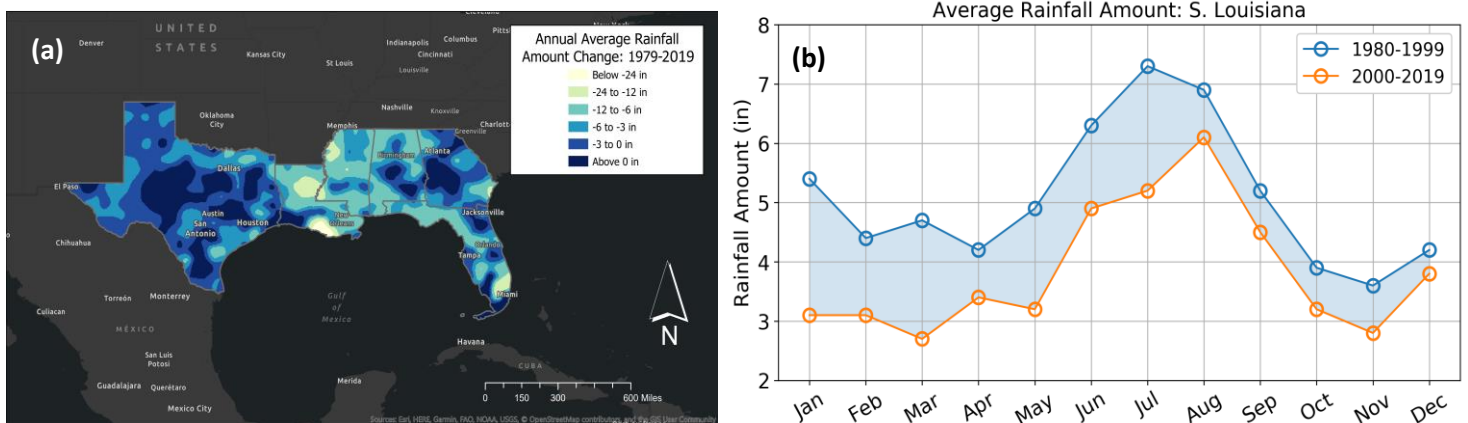


Figure 9: Change in annual average rainfall amount across the Gulf Coast States from 1979-2019 (9a, left) and average monthly rainfall amounts from 1980-1999 (blue) and 2000-2019 (orange) in South Louisiana (9b, right), both in inches. Data source: NOAA PSL (2020²).

3. Change in Rainfall Frequency

In accordance with expectations under climate change, decreases of annual average rainfall frequency have happened across the entirety of the Gulf Coast States, as shown in Figure 10 for 1979-2019. Frequency decreases of over 24 days were common, especially in Louisiana, Mississippi, Alabama, and Georgia. Decreases of rainfall frequency were smaller in South Florida and West Texas. Much like Figure 9a, there is no spatial pattern to these changes of annual rainfall frequency, but the loss of rainfall days in the last 40 years can be seen. Moreover, looking at Figures 9a and 10 together shows that several areas, such as West Georgia, the south tip of Florida, and Central-East Texas, have decreased in rainfall frequency but slightly increased in rainfall amount. These areas line up well with the expectation that climate change encourages less frequent rainfall in heavier bursts.

4. Change in Heavy Rainfall Frequency

To convey how much rainfall now occurs in these bursts, this chapter also considers change in heavy rainfall frequency. A heavy rainfall day is defined as one that experiences at least three inches of rainfall, as defined by the US Fourth National Climate Assessment (Carter et al., 2018). Figure 11a maps out changes in annual average heavy rainfall frequency from 1979-2019. These frequency changes were small, as expected, since above-three-inch rainfall events are uncommon. Many places have gained less than one more day of heavy rainfall over the last several decades, which still represents an increase in likelihood of occurrence. Heavy rainfall events have become more common across East Texas and most of Alabama, Georgia, and Florida, with some increases having exceeded more than one day. Although Figure 11a lacks spatial consistency, like the previous rainfall maps, most changes in heavy rainfall frequency were increases, contrasting the reductions of rainfall frequency in Figure 10. The theory that climate change produces less frequent, heavier rainfall bursts again holds generally true for the Gulf Coast States.

Something else of note in Figure 11a is that increases of heavy rainfall frequency have a more consistent magnitude over Alabama, Georgia, and Florida than the other states. This consistency may reflect in the seasonality of these increases, which is explored in Figure 11b, a

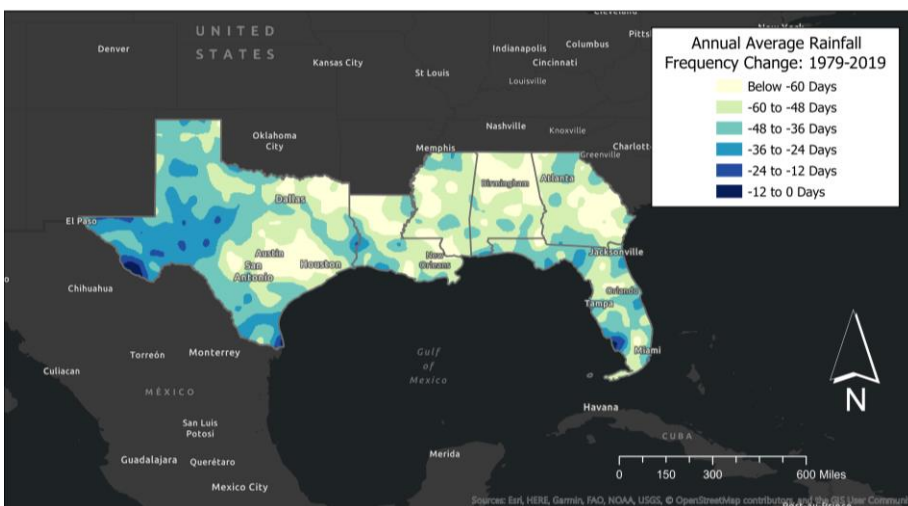


Figure 10: Change in annual average rainfall frequency across the Gulf Coast States in days, from 1979-2019. Data source: NOAA PSL (2020²).

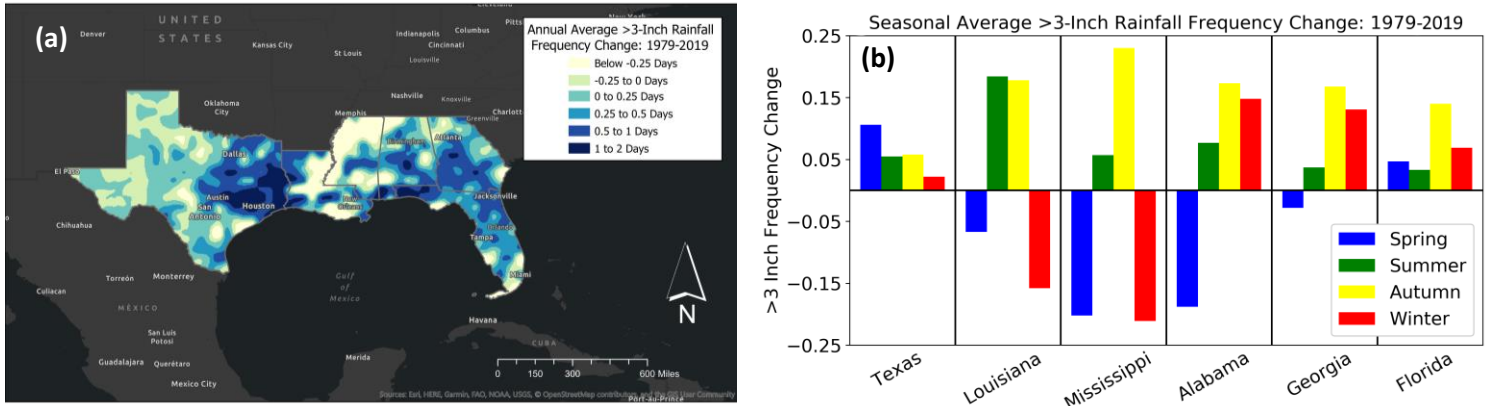


Figure 11: Change in annual average heavy rainfall frequency across the Gulf Coast States (11a, left) and change in state-averaged seasonal average heavy rainfall frequency (11b, right), both in days, from 1979-2019. Data source: NOAA PSL (2020²).

chart of state-averaged changes in seasonal average heavy rainfall frequency. While these seasonal changes are low in magnitude (within ± 0.25 days), the majority of changes that have occurred are increases. Changes of heavy rainfall frequency were positive in summer and autumn in all six states, with Alabama, Georgia, and Florida indeed having been consistent in terms of the sign of their experienced changes (except for spring). Figure 11b suggests that much of these increases in heavy rainfall frequency have happened outside of winter, mostly during warmer months of the year.

5. Change in Longest Wet and Dry Periods

Like the change in Longest Freeze-Free Period (Figure 8), examining changes in longest wet and dry periods provides insight into how much longer droughts (and how much shorter rainfall periods) have become as rainfall patterns have changed. The longest wet (dry) period is defined as the longest run of consecutive days where rainfall amount is at least (less than) 0.01 inches, the standard smallest measurable rainfall amount (NOAA NCEI, 2018). Figure 12 presents maps of change in longest annual wet (12a) and dry (12b) periods from 1979-2019, and what stands out is the large reduction of longest annual wet period across inland Florida, being over 20 days shorter than 40 years ago. Given Florida's increase of heavy rainfall frequency (Figure 11a), this reduction of longest wet period has likely affected the state's wet season, resulting in fewer overall days of rain, instead occurring in heavier downpours. Decreases of longest annual wet period happened all over the Gulf Coast States, but the largest decreases of 5 days or more typically happened closer to the coastline.

As for longest annual dry periods, increases happened for most of the region, but with lower magnitude than the change in longest annual wet periods. Changes maximized at 16 additional dry days in West Texas, and above 4 additional days across most of Georgia and Florida. Change in longest annual dry period also possesses less of a spatial pattern than change in longest annual wet period. However, the two maps show that the number of days without consecutive rainfall across the region has increased in recent years, suggesting a less reliable rainfall supply.

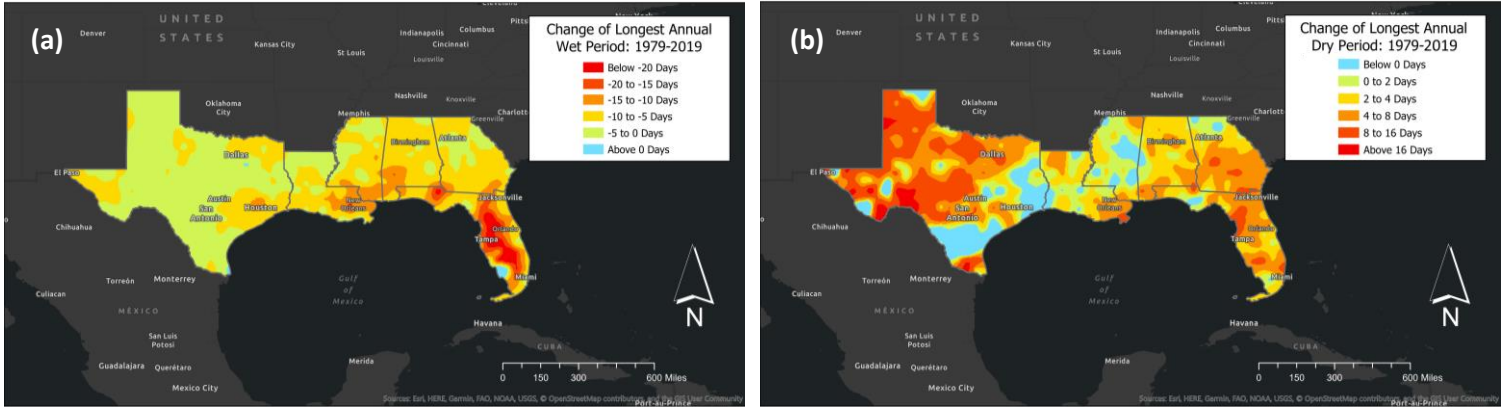


Figure 12: Change in longest annual wet period (12a, left) and longest annual dry period (12b, right) across the Gulf Coast States, both in days, from 1979-2019. Data source: NOAA PSL (2020²).

From these two maps, the areas of the Gulf Coast States that experienced the largest changes are inland Florida (Figure 12a) and Northwest Texas (Figure 12b). Recall from Chapter 1 that these areas experience significant rainfall due to wet season thunderstorms and winter storms respectively. It is thus worth determining whether these changes in wet/dry period lengths have occurred at these times of year. Table 1 summarizes the change in longest seasonal wet and dry periods for inland Florida and Northwest Texas respectively from 1979-2019. Inland Florida did indeed experience its greatest reduction in wet period length in summer, becoming over 16 days shorter in 40 years. Similarly, Northwest Texas’ longest dry period increased the most in winter, becoming 9.5 days longer. Periods of consistent rainfall seem to have become shorter and more sporadic in these regions.

6. Rainfall Change Summary

Although recent changes of rainfall have more spatial variability than those for temperature, noteworthy changes in the Gulf Coast States’ rainfall climate have taken place. Specifically, the region has experienced pervasive reductions of rainfall frequency (Figure 10), increases of heavy rainfall events in warmer seasons (Figure 11), and shorter consecutive rainfall periods (Figure 12, Table 1). These changes in rainfall characteristics amount to fewer and heavier rainfall events with less regularity, which fits in well with expectations for how climate change is considered to affect rainfall patterns. The flooding, drought, and groundwater recharge risks mentioned earlier in this chapter could therefore become more serious, and affect larger human populations, should the rainfall trends of the last several decades continue.

Season	Wet Period Change: Inland Florida	Dry Period Change: Northwest Texas
Winter	-2.5 days	9.5 days
Spring	-3.3 days	3.9 days
Summer	-16.3 days	0.6 days
Autumn	-4.7 days	-2.3 days

Table 1: Change in longest seasonal wet period for inland Florida, and longest seasonal dry period for Northwest Texas, both in days, from 1979-2019 (Data source: NOAA PSL (2020²)).

References

- Allen, G. (2020, June 13). A \$4.6 Billion Plan To Storm-Proof Miami. *National Public Radio*. Available online at <https://www.npr.org/2020/06/13/875725714/a-4-6-billion-plan-to-storm-proof-miami>.
- Anderson, F., and Al-Thani, N. (2016). Effect of Sea Level Rise and Groundwater Withdrawal on Seawater Intrusion in the Gulf Coast Aquifer: Implications for Agriculture. *Journal of Geoscience and Environment Protection*, 4(4), 116-124, <http://dx.doi.org/10.4236/gep.2016.44015>.
- Butterworth, M.K., Morin, C.W., and Comrie, A.C. (2017). An Analysis of the Potential Impact of Climate Change on Dengue Transmission in the Southeastern United States. *Environmental Health Perspectives*, 125(4), 579-585, <https://doi.org/10.1289/EHP218>.
- Carter, L., Terando, A., Dow, K., Hiers, K., Kunkel, K.E., Lascurain, A., Marcy, D., Osland, M., and Schramm P. (2018). *Southeast. In Impacts, Risks, and Adaptation in the United States: Fourth National Climate Assessment, Volume II* [D.R. Reidmiller, C.W. Avery, D.R. Easterling, K.E. Kunkel, K.L.M. Lewis, T.K. Maycock, and B.C. Stewart (Eds.)]. U.S. Global Change Research Program, Washington, DC, USA, 66pp.
- EPA. (2014). Climate Change Science – Causes of Climate Change. Accessed August 26 2020. Available online at <https://archive.epa.gov/epa/climate-change-science/causes-climate-change.html>.
- Gu Her, Y., Boote, K.J., Migliaccio, K.W., Fraisse, C., Leston, D., Mbuya, O., Anandhi, A., Chi, H., Ngatia, L., and Asseng, S. (2017). Climate Change Impacts and Adaptation in Florida’s Agriculture. In E.P. Chassignet, J.W. Jones, V. Misra, and J. Obeysekera (Eds.). *Florida’s Climate: Changes, Variations, & Impacts* (pp. 235-267). Gainesville, FL: Florida Climate Institute. <https://doi.org/10.17125/fci2017.exsum>.
- Huang, K., Li, X., Liu, X., and Seto, K.C. (2019). Projecting global urban land expansion and heat island intensification through 2050. *Environmental Research Letters*, 14, 1-12, <https://doi.org/10.1088/1748-9326/ab4b71>.
- IPCC. (2013). *Climate Change 2013: The Physical Science Basis. Contribution of Working Group I to the Fifth Assessment Report of the Intergovernmental Panel on Climate Change* [Stocker, T.F., D. Qin, G.-K. Plattner, M. Tignor, S.K. Allen, J. Boschung, A. Nauels, Y. Xia, V. Bex and P.M. Midgley (Eds.)]. Cambridge University Press, Cambridge, United Kingdom and New York, NY, USA, 1535 pp.
- Johnson, G.C., Lyman, J.M., Boyer, T., Cheng, L., Domingues, C.M., Gilson, J., Ishii, M., Killick, R.E., Monselesan, D., Purkey, S.G., and Wijffels, S.E. (2020). Ocean Heat Content [in “State of the Climate in 2019”]. *Bulletin of the American Meteorological Society*, 101(8), S163-S169, <https://doi.org/10.1175/BAMS-D-20-0105.1>.
- Kunkel, K.E., Stevens, L.E., Stevens, S.E., Sun, L., Janssen, E., Wuebbles, D., Konrad II, C.E., Fuhrmann, C.M., Keim, B.D., Kruk, M.C., Billot, A., Needham, H., Shafer, M., and Dobson, J.G. (2013). *Regional Climate Trends and Scenarios for the U.S. National Climate Assessment – Part*

2. *Climate of the Southeast U.S.* Available online at the South East Regional Climate Center website: https://sercc.com/NOAA_NESDIS_Tech_Report_Climate_of_the_Southeast_U.S.pdf.

Mace, R.E., and Wade, S.C. (2008). In Hot Water? How Climate Change May (or May Not) Affect the Groundwater Resources of Texas. *Gulf Coast Association of Geological Societies Transactions*, 58, 655-668, https://www.edwardsaquifer.org/wp-content/uploads/2019/02/2002_MaceWade_ClimateChangeTexasGroundwater.pdf.

NASA. (2020). Global Climate Change – Vital Signs: Global Temperature. Accessed August 26 2020. Available online at <https://climate.nasa.gov/vital-signs/global-temperature/>.

NOAA ESRL. (2020). Trend in Atmospheric Carbon Dioxide – Monthly Average Mauna Loa CO₂. Accessed 26 August 2020. Available online at <https://www.esrl.noaa.gov/gmd/ccgg/trends/mlo.html>.

NOAA NBDC. (2020). National Data Buoy Center – Station List. Accessed August 27 2020. Available online at https://www.ndbc.noaa.gov/to_station.shtml.

NOAA NCEI. (2018). *Comparative Climate Data For The United States Through 2018* [Brochure]. Available online at <https://www.ncdc.noaa.gov/sites/default/files/attachments/CCD-2018.pdf>.

NOAA PSL. (2020¹). CPC Global Temperature data provided by the NOAA Physical Sciences Laboratory, Boulder, Colorado, USA. Accessed July 13 2020. Available online at <https://psl.noaa.gov/data/gridded/data.cpc.globaltemp.html>.

NOAA PSL. (2020²). CPC Global Unified Precipitation data provided by the NOAA Physical Sciences Laboratory, Boulder, Colorado, USA. Accessed July 13 2020. Available online at <https://psl.noaa.gov/data/gridded/data.cpc.globalprecip.html>.

Nord, L.O. (2010). *Pre-Combustion CO₂ capture: Analysis of integrated reforming combined cycle* (Doctoral dissertation, Norwegian University of Science and Technology, Trondheim, Norway). Available online at https://www.researchgate.net/publication/259791199_Pre-combustion_CO2_capture_Analysis_of_integrated_reforming_combined_cycle.

Putnam, A.E, and Broecker, W.S. (2017). Human-induced changes in the distribution of rainfall. *Science Advances*, 3(5), 1-14, <https://doi.org/10.1126/sciadv.1600871>.

Smith, T.T., Zaitchik, B.F., and Gohlke, J.M. (2013). Heat waves in the United States: definitions, patterns and trends. *Climatic Change*, 118, 811-825, <https://doi.org/10.1007/s10584-012-0659-2>.

Trenberth, K.E. (2011). Changes in precipitation with climate change. *Climate Research*, 47, 123-138, <https://doi.org/10.3354/cr00953>.

Trenberth, K.E., Cheng, L., Jacobs, P., Zhang, Y., Fasullo, J. (2018). Hurricane Harvey Links to Ocean Heat Content and Climate Change Adaptation. *Earth's Future*, 6(5), 730-744, <https://doi.org/10.1029/2018EF000825>.

USDA. (2017). *Drought Impacts in the Southern Region* [Brochure]. Available online at https://www.climatehubs.usda.gov/sites/default/files/droughtfactsheet_r8_022018_508_0.pdf

van der Wiel, K., Kapnick, S.B., van Oldenborgh, G.J., Whan, K., Philip, S., Vecchi, G.A., Singh, R.K., Arrighi, J., and Cullen, H. (2017). Rapid attribution of the August 2016 flood-inducing extreme precipitation in south Louisiana to climate change. *Hydrology and Earth System Sciences*, 21, 897-921, <https://doi.org/10.5194/hess-21-897-2017>.

Walls, S.C., Baricovich, W.J., Brown, M.E., Scott, D.E., and Hossack, B.R. (2013). Influence of Drought on Salamander Occupancy of Isolated Wetlands on the Southeastern Coastal Plain of the United States. *Wetlands*, 33, 345-354, <https://doi.org/10.1007/s13157-013-0391-3>.

Wdowinski, S., Bray, R., Kirtman, B.P., and Wu, Z. (2016). Increasing flooding hazard in coastal communities due to rising sea level: Case Study of Miami Beach, Florida. *Ocean & Coastal Management*, 126, 1-8, <http://dx.doi.org/10.1016/j.ocecoaman.2016.03.002>.

Climate of the Gulf Coast States - Chapter 3: Climate Modeling and Future Climate Change

<u>Chapter Summary</u>	33
<u>Climate Modeling – An Introduction</u>	34
1. What is the Purpose of Climate Models?	34
2. How do Climate Models Work?	34
3. How is Climate Model Reliability Assured?	35
4. How were FloodWise Communities’ Climate Data Selected?	36
<u>Future of the Gulf Coast States’ Climate</u>	39
1. Future Average Temperature	39
2. Future Hot Day Frequency	40
3. Future Warm Night Frequency	41
4. Future Rainfall Amount and >3-Inch Rainfall Frequency	42
5. Summary of the Gulf Coast States’ Future Climate	43
<u>References</u>	44

Chapter Summary

This chapter provides a basic overview of how climate models work, how the climate models used to project the Gulf Coast States' future climate for this report were selected, and what these models suggest about the region's climate by the late-21st Century.

- Climate models are an equation-based approach to answering complex questions about the climate system's past, current, and future state. Common analyses performed with climate models are their ability to realistically capture past climates, projections of a range of possible future climates, and the relative importance of human and natural climate forcings.
- Multiple research institutes around the world build climate models and run them to contribute to publicly accessible online climate databases.
- Climate models are constructed and tested with common standards, but the equations, initial conditions, and resolutions that they use vary. While these variations allow us to assess a range of possible past and future climates, the reliability of these assessments must be ensured.
- Several strategies are commonly employed by climate model developers and users to ensure a model's reliability: comparison of outputs against observations, bias correction, and downscaling.
- This report and the *City/County Climate Summaries* made use of climate model datasets maintained by the NA-CORDEX (The North American Coordinated Regional Downscaling Experiment) project, due to their ability to better capture the Gulf Coast States' past temperature and rainfall than similar datasets.
- In a future with little global effort to reduce greenhouse gas emissions (RCP 8.5), average temperatures across the Gulf Coast States could increase by over 6°F by the late-21st Century, and by over 7.5°F further inland.
- The number of hot days (above 95°F) and warm nights (above 75°F) could also increase greatly, with increases nearer the coast modulated slightly by sea breezes from the Gulf of Mexico.
- Projected changes in rainfall by the late-21st Century are more spatially variable than those for temperature, but greater rainfall amounts in heavier bursts are projected by most climate models. These increases could be greatest in the north and center of the Gulf Coast States, where over 4 more inches of rain per year are expected.

Climate Modeling – An Introduction

1. What is the Purpose of Climate Models?

A climate model is a collection of mathematical equations applied to a gridded surface representing the Earth, built to better understand the complexity of Earth's climate system. By including processes like air-ocean heat exchange and global carbon cycles, climate models allow climatologists to answer important questions about the previous and future state of Earth's climate, and the relative importance of human (see [Chapter 2's discussion](#) of the [greenhouse effect](#)) versus natural [climate forcing](#) (NOAA GFDL, 2020). Climate models are an essential tool in the race to address global climate change; their projections inform political and economic decisions that minimize human impacts on the climate. Climate modeling is not guesswork, but a rapidly developing area of science based on cutting-edge knowledge of everything from sea ice dynamics to atmospheric trace gases, which are incorporated into the models' equations and variables. Even though globally coordinated development of climate models, most famously the [Coupled Model Intercomparison Project](#) (CMIP; Eyring et al., 2016), has been common since the 1990s, climate models are not perfect, hence consideration of their assumptions and limitations (e.g., making localized projections, processes not included/depicted in a model) is necessary when selecting climate models for a specific purpose (UCAR SciEd, 2020).

2. How do Climate Models Work?

Most climate models are built by leading research institutes, such as the National Oceanic and Atmospheric Administration's (NOAA) Geophysical Fluid Dynamics Laboratory (United States; NOAA GFDL, 2020) and the Met Office's Hadley Centre (United Kingdom; Met Office, 2020). These institutes contribute to global climate research projects, such as CMIP and the [Intergovernmental Panel on Climate Change's](#) (IPCC) Assessment Reports (IPCC, 2020). With so much emphasis on collaboration, climate models from these institutes are built in a similar manner, depicting Earth as a ball of three-dimensional grid cells. Each grid cell represents either the atmosphere, land, ocean, or ice, as illustrated by Figure 1 (NOAA Climate, 2020). The model's equations are applied to each grid cell, thus recreating (past) or projecting (future) the general climate state, hence these models are also called [General Circulation Models](#) (GCMs).

[Initial conditions](#) for each grid cell (e.g., rainfall, ocean salinity, soil carbon content) are provided to these equations, giving the GCMs a starting point

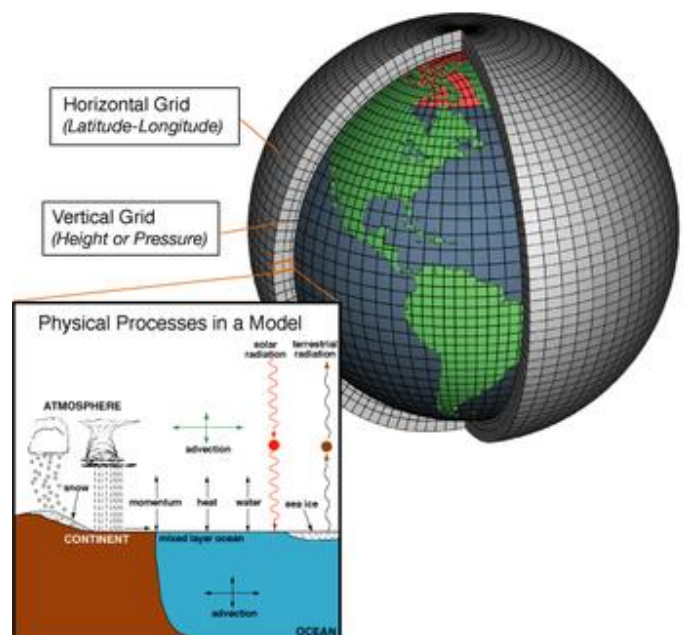


Figure 1: Representation of the three-dimensional grid used by General Circulation Models. Processes simulated within grid cells are also illustrated (NOAA Climate, 2020).

that is based in observed reality. Starting from the initial conditions, the GCMs are run over a specified timeframe, with anything from a minute-long to an annual timestep. The changing climate state across timesteps is driven by [Representative Concentration Pathway](#) (RCP) emission scenarios (van Vuuren et al., 2011), which account for the human contributions to the greenhouse effect (e.g., the effects of carbon dioxide emissions) in these GCMs. From these model runs, variables that represent the state of the climate (such as temperature) are averaged to compute [climate normals](#), conventionally over a 30-year period (World Meteorological Organization, 2017). By computing and comparing 30-year climate normals over two non-overlapping timeframes, one can determine the extent of climate change based on specific variables over a given spatial and temporal domain (e.g., heavy rainfall frequency change in the Gulf Coast States between the late-20th and late-21st Century). Due to variations in model construction, whether in equation structure, initial conditions, or model [resolution](#), different GCMs recreate and project different climate states, hence assurance of model reliability is vital.

3. How is Climate Model Reliability Assured?

Having data outputs from multiple climate models is useful for decision makers, since these outputs together suggest a range of future climate conditions (of varying likelihood) for which to prepare, and past conditions from which to learn. However, some of this range in outputs comes from unrealistic behavior simulated by climate models, due to our incomplete understanding of Earth's climate system and the limits of computational power. However, GCMs have long possessed high skill in simulating temperature (Hausfather et al., 2019), and new means to improve (Thornes, 2016) and measure (Baumberger et al., 2017) climate model reliability are constantly being developed. Below are strategies available to climatologists for increasing GCM reliability:

- *Comparing GCM outputs to observational data.* Observations are used both to provide initial conditions for a GCM's equations and to test the realism of its outputs. Climate models are often run over an historical timeframe (e.g., the years 1981-2010) for which observational data are available, thus allowing a GCM's [simulation](#) of a particular variable to be compared against these observations (Zhao et al., 2016). This comparison allows GCM errors to be identified, and systematic biases to be addressed, such as by correcting model equations accordingly (Cowtan et al., 2015; NOAA Climate, 2020). If a GCM possesses little error or [bias](#) when compared to the observed historical climate, the GCM is likely to be more reliable in its simulation of the historical and future climate state.
- *[Bias correction.](#)* This second means to increase model reliability goes beyond comparison against observations, instead correcting unrealistic behaviors in GCMs rather than simply identifying them. Biases in GCM outputs exist for several reasons, such as low model resolution, poor observational data quality, or incorrect initial conditions (Heo et al., 2019), which can cause a climate model to mischaracterize the true climate state, rendering the model unsuitable for application. Sometimes these biases are systematic, meaning that a GCM consistently over or underestimates a particular variable (e.g., underestimating average temperature across the Gulf Coast States by 2°F), hence a simple addition or

subtraction to a GCM's data output is sufficient. Such a correction works well for temperature, but not for more stochastic (random) variables like rainfall (CCAFS, 2014). Bias correction of stochastic variables is done with quantile mapping, which identifies GCM bias at all magnitudes of a given climate variable, and consequently corrects the identified bias at each magnitude, such as correcting the “drizzle problem” (simulation of too many light rain events) shared by many GCMs (Maraun, 2013). Whilst these two techniques do remove systematic biases from climate models, they both inherently assume that variability (continuous variation with space and time) in the historical and future climate is the same. Ultimately, the decision to use a climate dataset should consider whether its enlisted GCMs were bias corrected and how this correction was done.

- [Downscaling](#). This term refers to increasing the spatial or temporal resolution of a GCM's output by using a smaller grid cell size or a smaller timestep respectively. Downscaling therefore creates more data about the historical and future climate states, while also increasing a GCM's reliability by capturing smaller-scale processes, such as cloud dynamics (Schneider et al., 2019). Increasing computational power is allowing higher-resolution GCMs to be run more quickly and easily, though a trade-off between resolution and computing power is still a limiting factor to a GCM's reliability (UCAR SciEd, 2020), hence the importance of downscaling. Downscaling is typically done in one of two ways, the first being dynamical downscaling, which applies GCMs to one or several [Regional Climate Models](#) (RCMs). These RCMs use the same equations and assumptions as the original GCMs, but apply them to a three-dimensional grid with a higher resolution, allowing for better representation of local climate features and processes while still capturing relevant global-scale processes (Cooney, 2012). The second option is statistical downscaling, which constructs a statistical relationship between observations and a GCM's depiction of the historical climate to construct a high-resolution GCM dataset. While statistical downscaling is the less computationally expensive of these two methods, it depends heavily on having a long record of robust observations to construct the statistical relationship (Tang et al., 2016). The differences between these two downscaling approaches can lead to quite different simulations of the same region's climate, hence selecting a reliable climate dataset also depends on whether and how the data were downscaled.

4. *How were FloodWise Communities' Climate Data Selected?*

Improving model reliability is the role of climate research organizations, such as the World Climate Research Program's CORDEX (Coordinated Regional Downscaling Experiment) project (WCRP, 2020), or the University of California San Diego's LOCA (Localized Constructed Analogs) project (UCSD, 2020), rather than the institutes who constructed the original GCMs. These organizations build in-house downscaling and bias correction procedures to improve the reliability of GCM datasets. Reliability can be increased further by weighting and averaging datasets to produce [multi-model ensembles](#), allowing these organizations to improve performance compared to individual models, and to better summarize GCMs' simulated climate state (Hagedorn et al., 2005; Crawford et al., 2019). The difference in approaches to correcting

and downscaling GCMs means that the climate dataset used by [FloodWise Communities](#) had to be both publicly available and realistic in its depiction of the Gulf Coast States' climate.

Even though GCM datasets from CMIP's current sixth phase (CMIP6; Eyring et al., 2016) are publicly available, very few downscaled and bias corrected versions of these datasets currently exist, hence datasets from the CMIP5 generation (Taylor et al., 2012) have been used here instead. LOCA and the North American CORDEX (NA-CORDEX) projects (Mearns et al., 2017) have released climate products for the conterminous United States in recent years, albeit prepared in different ways. LOCA is a statistically downscaled collection of 32 GCMs, which are bias corrected using quantile mapping. This product is distinctive for its high spatial resolution of 0.0625 degrees, or a 7-kilometer grid cell size (UCSD, 2020). Conversely, NA-CORDEX is a dynamically downscaled product that uses 9 GCMs and 7 RCMs paired in varying GCM-RCM combinations, also using quantile mapping and some of the same GCMs as LOCA (Mearns et al., 2017). Although NA-CORDEX's resolution is lower (0.5 degrees, or 55-kilometer grid cell size), its resolution equals that of temperature and rainfall observations kept by NOAA's Climate Prediction Center (CPC; NOAA PSL, 2020^{1,2}). By [regridding](#) LOCA to this same resolution and extracting daily historical data from a period common to these three products (1979-2005), the following question can be answered: *which climate model dataset, out of LOCA and NA-CORDEX, agrees the most with CPC observations of the Gulf Coast States' historical climate, hence which dataset is better for projecting its future climate state?*

Firstly, the multi-model ensembles of the two climate datasets were compared against CPC, with ensembles computed by taking the average (mean) of the two datasets' GCM outputs; no weighting scheme was applied. As in Chapters 1 and 2 (which also used CPC), focus was on changes in indicators of temperature and rainfall (average temperature, hot day (>95°F) frequency, warm night (>75°F) frequency, rainfall amount, and >3-inch rainfall frequency), with climate normals from 1979-2005 calculated for these indicators using NA-CORDEX, LOCA, and CPC. Differences between CPC and the two climate datasets were averaged by state and are summarized in Table 1, where numbers in red represent the dataset for which the error compared to CPC was larger. For temperature, NA-CORDEX's ensemble error tended to exceed LOCA's for warm night and hot day frequency, however this difference in error maximized at under 3 days for hot day frequency in Texas (8.63 days for NA-CORDEX, versus 5.85 days for

State	Avg Temp Error (°F)		Hot Days Error (Days)		Warm Nights Error (Days)		Rain Amount Error (in)		>3 in Frequency Error (Days)	
	LOCA	NA-CORDEX	LOCA	NA-CORDEX	LOCA	NA-CORDEX	LOCA	NA-CORDEX	LOCA	NA-CORDEX
Texas	-0.26	0.25	5.85	8.63	-8.48	-6.51	-2.01	-0.70	-0.10	-0.03
Louisiana	-0.13	0.50	3.70	4.80	-5.31	6.83	-2.18	-0.71	-0.50	-0.13
Mississippi	-0.35	0.14	3.29	3.98	-2.79	-1.54	-1.67	-0.20	-0.40	-0.06
Alabama	-0.55	-0.09	2.04	1.31	-0.76	-0.91	-0.80	0.18	-0.32	-0.04
Georgia	-0.05	0.43	2.33	3.58	-0.91	-1.06	0.49	-0.46	-0.19	0
Florida	-0.10	0.38	3.11	3.59	-6.67	-3.98	-1.05	0.43	-0.13	-0.05

Table 1: State-averaged multi-model ensemble error for LOCA and NA-CORDEX compared to CPC, from 1979-2005. This error was computed for several annual temperature and rainfall statistics, and numbers in red represent the multi-model ensemble and state for which error compared to CPC was larger. Data sources: Mearns et al. (2017); UCSD (2020); NOAA PSL (2020^{1,2}).

LOCA). Differences in average temperature error were similarly small, with neither ensemble exceeding $\pm 0.55^{\circ}\text{F}$ versus CPC, hence both ensembles are similarly realistic in simulating the Gulf Coast States' historical temperature. By contrast, LOCA's ensemble consistently possessed greater error than NA-CORDEX's in simulating rainfall indicators, which is clear from all red numbers being in LOCA columns for rainfall amount and >3 -inch rainfall frequency. Although both ensembles tended to underestimate rainfall indicators, this error is several times greater for LOCA than NA-CORDEX, such as the former underestimating rainfall amount by -2.18 inches in Louisiana, versus -0.71 inches by NA-CORDEX. Even though LOCA captures heavy rainfall events better than other statistically downscaled climate products (Pierce et al., 2014), NA-CORDEX's ensemble simulates rainfall indicators closer to CPC-derived values in all six states.

There are several potential reasons to explain why NA-CORDEX outperforms LOCA in simulating past rainfall across the Gulf Coast States. Perhaps dynamically downscaled models are better at resolving convective rainfall (of which there is much along the Gulf Coast itself), or perhaps some of the models in LOCA's ensemble perform especially poorly over this region. The error produced by individual models, rather than the multi-model ensemble, may provide clarification, as presented in Figure 2, boxplots illustrating the number of surface grid cells over the Gulf Coast States in which historical runs (1979-2005) of NA-CORDEX and LOCA's individual models exceeded error limits compared to CPC. All three of these datasets possess 538 surface

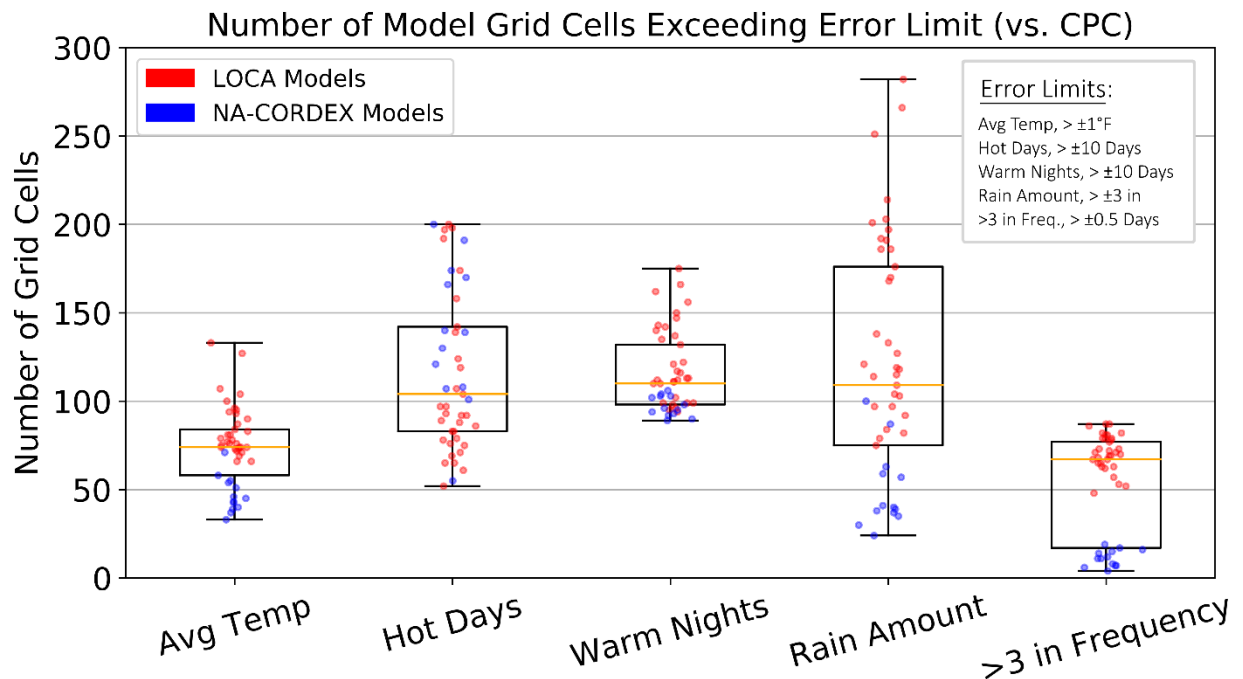


Figure 2: Boxplots showing the number of surface grid cells (out of 538 cells) over the Gulf Coast States for which NA-CORDEX and LOCA critically over/underestimate the CPC-derived historical value of each climate indicator. Indicators are based on computed climate normals from 1979-2005. Points that comprise the boxplots are shown, each representing a single model in the LOCA (red) or NA-CORDEX (blue) product. The error limits permitted for each indicator are given in the top-right box. Average (median) values for each boxplot are given by the orange lines. Data sources: Mearns et al. (2017); UCSD (2020); NOAA PSL (2020^{1,2}).

grid cells over the Gulf Coast States, thus the larger the number in Figure 2, the greater an individual model's (red points = LOCA models, blue points = NA-CORDEX models) error in simulating these climate indicators. As in Table 1, there is less difference in LOCA and NA-CORDEX's performance for the temperature indicators. The range of grid cells exceeding the error limit compared to CPC is relatively small for warm night frequency (± 10 Days) and average temperature ($\pm 1^\circ\text{F}$), at 86 and 100 grid cells respectively, and there are individual models within both LOCA and NA-CORDEX with up to 200 grid cells that exceeded the hot day frequency error limit (± 10 Days). For the rainfall indicators, there is clearer separation in LOCA and NA-CORDEX's performance. All models that simulated more than 150 grid cells over the error limit for rainfall amount (± 3 in) were part of LOCA, and all of the models in NA-CORDEX produced fewer than 20 grid cells that exceeded the error limit for >3 -inch rainfall frequency (± 0.5 Days). Furthermore, several models that performed poorly against CPC for a single climate indicator also performed poorly for other indicators, and many of these frequently erroneous models were used in LOCA but not in NA-CORDEX. As such, differences in ensemble members could partially explain NA-CORDEX's closer agreement with CPC, plus the effects of chosen downscaling and bias correction methods. Based on the presented analysis and its ease of availability, NA-CORDEX was chosen as the product to project the Gulf Coast States' future climate.

Future of the Gulf Coast States' Climate

1. Future Average Temperature

For all climate indicators, datasets from NA-CORDEX (Mearns et al., 2017) were used to project climate change in the Gulf Coast States between a future (Fut; 2071-2100) and an historical (Hist; 1976-2005) climate normal. These normals were computed using climate models driven by the RCP 8.5 emissions scenario, which is used to project climate change that assumes little effort to reduce global [greenhouse gas](#) emissions (van Vuuren et al., 2011), in contrast to other scenarios (RCP 6.5, RCP 4.0, and RCP 2.6) that assume increasing global efforts to reduce them. Of the several commonly used RCP scenarios, RCP 8.5 is the highest-emissions scenario, hence the analysis below represents one of several possible futures for the Gulf Coast States' climate. As such, Figure 3a maps the projected change in annual average temperature across the region in the coming decades (for NA-CORDEX's multi-model ensemble). Greater temperatures are expected throughout, with increases of up to 6.5°F along the coast and over 7.5°F inland. Temperature increases tend to be smaller nearer coastlines and the equator, so this pattern of future temperature increases is expected ([Chapter 2, Figure 3](#)). However, this pattern is much smoother than the observed temperature increases in Chapter 2; climate models offer a general picture of the climate system, especially with coarse spatial resolution, hence local temperature trends can easily be missed.

As Figure 2 showed, climate models from the same product can possess a wide projection range, hence it is worth considering more than the multi-model ensemble. Figure 3b therefore charts the projection range for annual average temperature change in four Gulf Coast cities, two further inland (Dallas, TX and Atlanta, GA) and two along the coast (New Orleans, LA and Miami, FL). Much like in Figure 3a, the inland cities could experience larger temperature increases (7.81°F in Dallas versus 6.20°F in Miami), but the inland cities also possess a larger

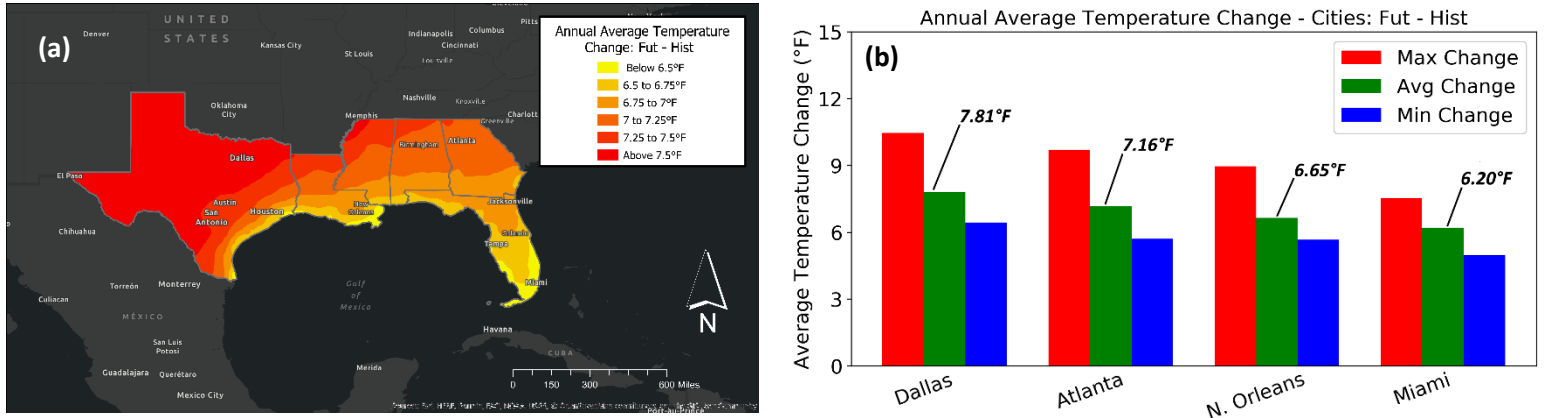


Figure 3: Projected change in annual average temperature between the Future (2071-2100) and the Historical (1976-2005) climate normals, forced by the RCP 8.5 emissions scenario. Projections are expressed as a map of change in NA-CORDEX's multi-model ensemble across the Gulf Coast States (3a, left), and the range of model projections for two coastal and two non-coastal cities (3b, right), both in °F. Data source: Mearns et al. (2017).

projection range (Max Change minus Min Change) from individual models, being close to 4°F in Dallas and Atlanta and more like 3°F in New Orleans and Miami. Furthermore, regardless of coastal proximity, this projection range typically comes from the same climate models, with the largest increases coming from the UK's HadGEM2 models (Collins et al., 2011) and Canada's CanESM2 models (Chylek et al., 2011), and the smallest from the US's GFDL models (Donner et al., 2011). Figure 3b therefore suggests that projection range is proportional to average projected change, and that the edges of these projection ranges are defined by the same NA-CORDEX models in both coastal and inland areas, assuming that the trends in these four cities hold across the Gulf Coast States.

2. Future Hot Day Frequency

Greater average temperatures would understandably result in greater hot day frequency, which is verified by Figure 4a, the change in annual hot day frequency between the two climate normals. Indeed, increases of 50 or more days above 95°F are expected across much of the region by the late-21st Century. [Chapter 1](#) showed that the highest maximum temperatures in this region tend to be inland, hence hot day frequency increases being largest nearer the coast is not very surprising. These increases could be largest in Florida, with most of the state seeing over 100 additional days above 95°F per year in several decades' time. Although Florida is warm year-round, days of extreme heat have long been less common than in states like Texas and Louisiana, though NA-CORDEX and Dahl et al. (2019) both suggest Florida's future climate becoming noticeably harder to tolerate.

Nevertheless, the increase in Florida's hot day frequency suggested by Figure 4a is anomalously high compared to the other Gulf Coast States, perhaps due to a specific model's performance within NA-CORDEX's multi-model ensemble, or due to hot day frequency trends in a specific season. A seasonal breakdown of the projection range for Florida's hot day frequency change (averaged across the state) is given in Figure 4b, with winter excluded since days above 95°F almost never occur. Being its warmest season, most of Florida's increase in seasonal hot days is

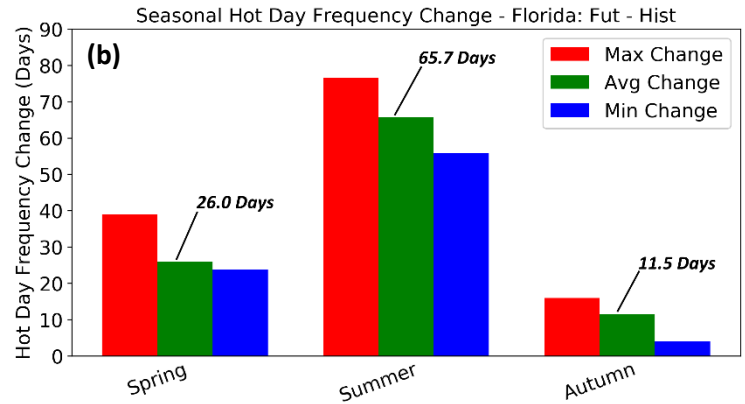
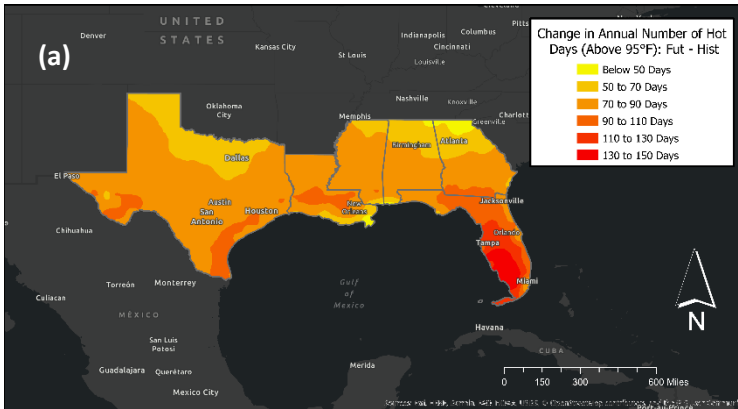


Figure 4: Projected change in annual hot day frequency between the Future (2071-2100) and the Historical (1976-2005) climate normals, forced by the RCP 8.5 emissions scenario. Projections are expressed as a map of change in NA-CORDEX’s multi-model ensemble across the Gulf Coast States (4a, left), and the range of seasonal model projections for the state of Florida (4b, right), both measured in Days. Data source: Mearns et al. (2017).

expected in summer, with a state-averaged increase of 65.7 days. The range of projections by different climate models is also largest in summer, being almost 19 days, compared to 15 days in spring and 12 days in autumn. Since projection range seems proportional to the average increase of hot day frequency, NA-CORDEX’s models arguably project hot day frequency with consistent reliability for each season. However, as in Figure 3b, specific models often represent the extremes of Figure 4b’s projection range, particularly CanESM2 and HadGEM2 on the high end, and GFDL and Europe’s EC-EARTH model (Hazeleger et al., 2010) on the low end. This result suggests that a climate model within NA-CORDEX that projects a large change for one temperature indicator will likely do the same for related indicators.

3. Future Warm Night Frequency

The pattern of projected changes for warm night frequency is similar to that of hot day frequency, as shown by Figure 5a. NA-CORDEX’s multi-model ensemble projects increasing annual warm night frequency across the Gulf Coast States, again peaking in South Florida at over 130 additional nights above 75°F per year. Another feature of this map that stands out is warm night frequency increasing by less in coastal areas than just inland, especially along the Texas coast. Hot day frequency also possesses this feature (Figure 4a), albeit less prominently, likely resulting from the cooling effect produced by the Gulf of Mexico.

This cooling effect is mostly due to sea breezes created by the temperature difference between the warm land and the cooler ocean water. When warm air over land rises, cooler air over the ocean moves to replace it (i.e., the sea breeze), thus regulating coastal temperatures (Banta et al., 2005; White and Kozaira, 2018). Land temperatures in the Gulf Coast States are highest in summer ([Chapter 1, Figure 3](#)), leading to stronger sea breezes, hence examining seasonal warm night frequency could be revealing. Figure 5b illustrates the projection range for seasonal warm night frequency change in two coastal (Tampa, FL and Houston, TX) and two inland (Orlando, FL and San Antonio, TX) Gulf Coast cities, winter again excluded as in Figure 4b. In all four cities,

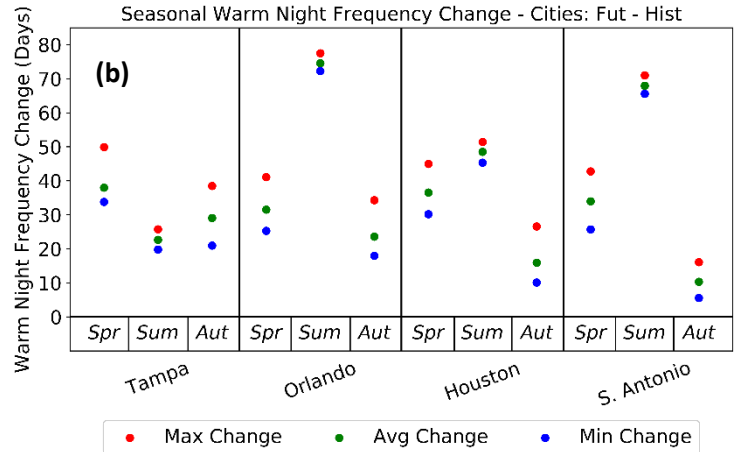
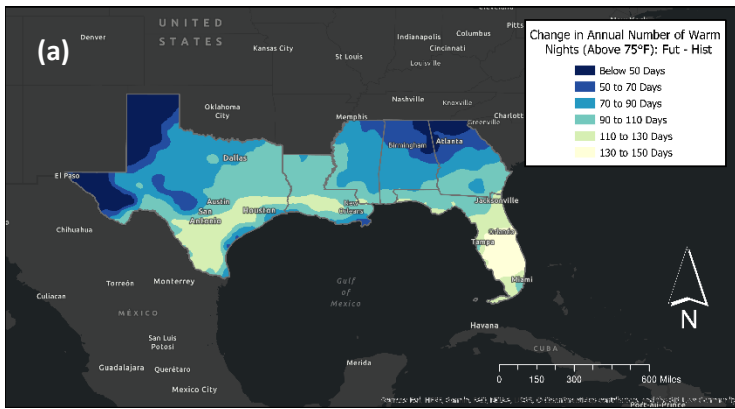


Figure 5: Projected change in annual warm night frequency between the Future (2071-2100) and the Historical (1976-2005) climate normals, forced by the RCP 8.5 emissions scenario. Projections are expressed as a map of change in NA-CORDEX’s multi-model ensemble across the Gulf Coast States (5a, left), and the range of seasonal model projections for two coastal and two non-coastal cities (5b, right), both measured in Days. Data source: Mearns et al. (2017).

projection ranges are smallest in summer at 5-6 days; the climate models within NA-CORDEX that produced these seasonal projection ranges are the same as in the previous Figures (HadGEM2, CanESM2, GFDL). Figure 5b’s most important result, however, is increases of average warm night frequency being larger in summer for the inland cities (Orlando = 74.6 days, San Antonio = 67.9 days) than for the coastal cities (Houston = 48.5 days, Tampa = 22.6 days). This difference in seasonal increases is much smaller in spring and autumn, suggesting the importance of summertime sea breezes strengthened by climate change for explaining warm night (and hot day) frequency increasing less along the coast than further inland.

4. Future Rainfall Amount and >3-Inch Rainfall Frequency

NA-CORDEX slightly underestimates historical rainfall indicators (Table 1), not as much as LOCA, but this tendency should be remembered during this section. Figure 6 maps projected change

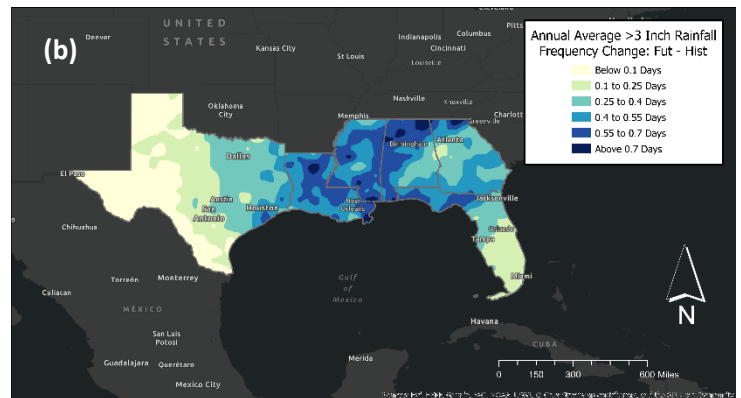
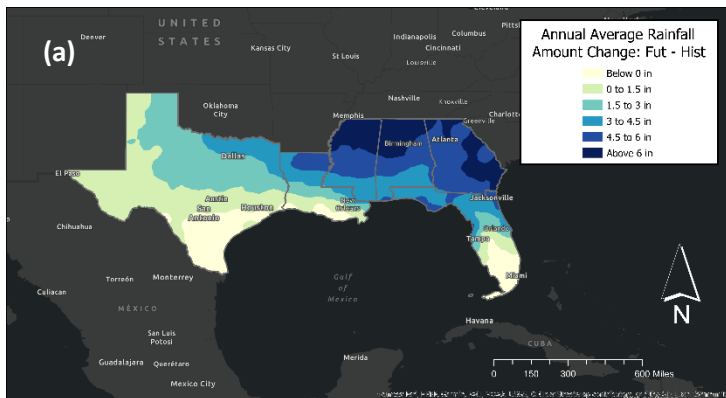


Figure 6: Projected change in rainfall indicators between the Future (2071-2100) and the Historical (1976-2005) climate normals, forced by the RCP 8.5 emissions scenario. Projections are expressed as a map of annual average rainfall amount change in inches (6a, left) and >3-inch rainfall frequency change in Days (6b, right), both applying NA-CORDEX’s multi-model ensemble across the Gulf Coast States. Data source: Mearns et al. (2017).

in annual average rainfall amount (6a) and >3-inch rainfall frequency (6b) for the Gulf Coast States between the two climate normals, according to the NA-CORDEX multi-model ensemble. These two maps point to increasing rainfall in heavier bursts in the decades to come, peaking in the north and center of the region with over 4 more inches of rainfall and over 0.5 more days of >3-inch rainfall per year. Conversely, the coast itself and the south of the region could see decreases of rainfall in the future, despite still experiencing a slight increase in >3-inch rainfall frequency. A warmer atmosphere due to climate change can hold more water vapor (Trenberth, 2011), resulting in fewer and heavier rainfall events. This phenomenon is important for explaining thunderstorm activity in the Gulf of Mexico, particularly in spring (Trapp et al., 2007; Molina et al., 2016), hence the expected rainfall patterns along the coast in Figure 6a.

As with the other climate indicators examined, a multi-model ensemble conveys little about the range of possibilities for the future climate state, and this range for rainfall is often large. Table 2 summarizes NA-CORDEX's projection range for annual average rainfall amount and >3-inch rainfall frequency by state. As in Figure 6, the biggest projected changes are for states in the center of the region, i.e., Mississippi and Alabama, which could see up to 11.2 more inches of rainfall per year by the late-21st Century. Projection range seems to be smallest in the drier states, with Texas' >3-inch rainfall frequency having a range of 0.39 days (0.05 to 0.44 days), much smaller than the wetter state of Louisiana with a range of 1.21 days (0.12 to 1.33 days). Despite differences in projection range, the average changes in both rainfall indicators are positive in all 6 states, suggesting that most of NA-CORDEX's models project both more and heavier rainfall for the Gulf Coast States. However, some models project rainfall amount decreases, such as the CanESM2 and GFDL models projecting decreases of over 5 inches in Florida (-5.29 in) and Louisiana (-6.32 in). Climate change trends for rainfall are often less clear than those for temperature, since most rainfall in this region is convective (Jiang and Yang, 2012; Liu et al., 2012), hence the projection ranges in Table 2 being large is not unexpected.

5. Summary of the Gulf Coast States' Future Climate

Much like many other parts of the world, climate change is expected to bring warmer conditions to the Gulf Coast States, potentially increasing temperatures by up to and over 7°F

		Texas	Louisiana	Mississippi	Alabama	Georgia	Florida
Annual Rainfall Amount (in)	Max Change	6.97	9.19	11.11	11.2	9.72	8.52
	Avg Change	1.51	2.44	5.76	5.43	5.77	1.62
	Min Change	-1.67	-6.32	-2.41	-1.24	0.55	-5.29
Annual >3 in Rainfall Frequency (days)	Max Change	0.44	1.33	1.66	1.89	1.15	0.63
	Avg Change	0.18	0.55	0.62	0.65	0.46	0.31
	Min Change	0.05	0.12	0.02	0.16	0.21	0.09

Table 2: State-averaged projection range for annual average rainfall amount (in inches) and annual average >3-inch rainfall frequency (in days) between the Future (2071-2100) and the Historical (1976-2005) climate normals, forced by the RCP 8.5 emissions scenario. For each state, the maximum, minimum, and average projected change according to NA-CORDEX's individual models has been given. Data source: Mearns et al. (2017).

(Figure 3). Despite temperature increases being smaller nearer the coast, this area will see some of the biggest increases in hot day (Figure 4) and warm night (Figure 5) frequency, although sea-breezes along the coast itself could slightly modulate these changes. There is less confidence in future changes in rainfall, since NA-CORDEX's climate models project both increases and decreases in rainfall amount in future decades (Table 2), and these models are consistently biased to underestimate heavy rainfall in particular (Table 1). That being said, a future with more rainfall in heavier bursts seems to be the most likely (Figure 6). It is important to remember, however, that this picture of the Gulf Coast States' future climate was created using the highest greenhouse gas emissions scenario (RCP 8.5; van Vuuren et al., 2011), hence other outcomes are possible depending on the trajectory of future emissions, and on the climate model product used to project these outcomes (i.e., a product other than NA-CORDEX).

References

- Banta, R.M., Senff, C.J., Nielsen-Gammon, J., Darby, L.S., Ryerson, T.B., Alvarez, R.J., Sandberg, S.P., Williams, E.J., and Trainer, M. (2005). A Bad Air Day in Houston. *Bulletin of the American Meteorological Society*, 86(5), 657-670, <https://doi.org/10.1175/BAMS-86-5-657>.
- Baumberger, C., Knutti, R., and Hadorn, G.H. (2017). Building confidence in climate model projections: an analysis of inferences from fit. *WIREs Climate Change*, 8(3), e454, <https://doi.org/10.1002/wcc.454>.
- CCAFS. (2014). Bias Correction. Accessed December 23 2020. Available online at http://www.ccafs-climate.org/bias_correction/.
- Chylek, P., Li, J., Dubey, M.K., Wang, M., and Lesins, G. (2011). Observed and model simulated 20th century Arctic temperature variability: Canadian Earth System Model CanESM2. *Atmospheric Chemistry and Physics Discussions*, 11, 22893-22907, <https://doi.org/10.5194/acpd-11-22893-2011>.
- Collins, W.J., Bellouin, N., Doutriaux-Boucher, M., Gedney, N., Halloran, P., Hinton, T., Hughes, J., Jones, C.D., Joshi, M., Liddicoat, S., Martin, G., O'Connor, F., Rae, J., Senior, C., Sitch, S., Totterdell, I., Wiltshire, A., and Woodward, S. (2011). Development and evaluation of an Earth-System model – HadGEM2. *Geoscientific Model Development*, 4, 1051-1075, <https://doi.org/10.5194/gmd-4-1051-2011>.
- Cooney, C.M. (2012). Downscaling Climate Models: Sharpening the Focus on Local-Level Changes. *Environmental Health Perspectives*, 120(1), a22-a28, <https://dx.doi.org/10.1289%2Fehp.120-a22>.
- Cowtan, K. Hausfather, Z., Hawkins, E., Jacobs, P., Mann, M.E., Miller, S.K., Steinman, B.A., Stolpe, M.B., and Way, R.G. (2015). Robust comparison of climate models with observations using blended land air and ocean sea surface temperatures. *Geophysical Research Letters*, 42(15), 6526-6534, <https://doi.org/10.1002/2015GL064888>.
- Crawford, J., Venkataraman, K., and Booth, J. (2019). Developing climate model ensembles: A comparative case study. *Journal of Hydrology*, 568, 160-173, <https://doi.org/10.1016/j.jhydrol.2018.10.054>.

- Dahl, K., Licker, R., Abatzoglou, J.T., and Delet-Barreto, J. (2019). Increased frequency of and population exposure to extreme index heat days in the United States during the 21st century. *Environmental Research Communications*, 1, 075002, <https://doi.org/10.1088/2515-7620/ab27cf>.
- Donner, L.J., Wyman, B.L., Hemler, R.S., Horowitz, L.W., Ming, Y., Zhao, M., Golaz, J.-C., Ginoux, P., Lin, S.-J., Schwarzkopf, M.D., Austin, J., Alaka, G., Cooke, W.F., Delworth, T.L., Freidenreich, S.M., Gordon, C.T., Griffies, S.M., Held, I.M., Hurlin, W.J., Klein, S.A., Knutson, T.R., Langenhorst, A.R., Lee, H.-C., Lin, Y., Magi, B.I., Malyshev, S.L., Milly, P.C.D., Naik, V., Nath, M.J., Pincus, R., Ploshay, J.J., Ramaswamy, V., Seman, C.J., Shevliakova, E., Sirutis, J.J., Stern, W.F., Stouffer, R.J., Wilson, R.J., Winton, M., Wittenberg, A.T., and Zeng, F. (2011). The Dynamical Core, Physical Parameterizations, and Basic Simulation Characteristics of the Atmospheric Component AM3 of the GFDL Global Coupled Model CM3. *Journal of Climate*, 24(13), 3484-3519, <https://doi.org/10.1175/2011JCLI3955.1>.
- Eyring, V., Bony, S., Meehl, G.A., Senior, C.A., Stevens, B., Stouffer, R.J., and Taylor, K.E. (2016). Overview of the Coupled Model Intercomparison Project Phase 6 (CMIP6) experimental design and organization. *Geoscientific Model Development*, 9, 1937-1958, <https://doi.org/10.5194/gmd-9-1937-2016>.
- Hagedorn, R., Doblas-Reyes, F., and Palmer, T.N. (2005). The rationale behind the success of multi-model ensembles in seasonal forecasting – I. Basic Concept. *Tellus A: Dynamic Meteorology and Oceanography*, 57(3), 219-233, <https://doi.org/10.3402/tellusa.v57i3.14657>.
- Hausfather, Z., Drake, H.F., Abbott, T., and Schmidt, G.A. (2019). Evaluating the Performance of Past Climate Model Projections. *Geophysical Research Letters*, 47(1), e2019GL085378, <https://doi.org/10.1029/2019GL085378>.
- Hazeleger, W., Severijns, C., Semmler, T., Ștefănescu, S., Yang, S., Wang, X., Wyser, K., Dutra, E., Baldasano, J.M., Bintanja, R., Bougeault, P., Caballero, R., Ekman, A.M.L., Christensen, J.H., van den Hurk, B., Jimenez, P., Jones, C., Kållberg, P., Koenigk, T., McGrath, R., Miranda, P., van Noije, T., Palmer, T., Parodi, J.A., Schmith, T., Selten, F., Storelvmo, T., Sterl, A., Tapamo, H., Vancoppenolle, M., Viterbo, P., and Willén, U. (2010). EC-EARTH – A Seamless Earth-System Prediction Approach in Action. *Bulletin of the American Meteorological Society*, 91(10), 1357-1364, <https://doi.org/10.1175/2010BAMS2877.1>.
- Heo, J.-H., Ahn, H., Shin, J.-Y., Kjeldsen, T.R., and Jeong, C. (2019). Probability Distributions for a Quantile Mapping Technique for a Bias Correction of Precipitation Data: A Case Study to Precipitation Data Under Climate Change. *Water*, 11(7), 1475, <https://doi.org/10.3390/w11071475>.
- IPCC. (2020). IPCC – Reports. Accessed December 23 2020. Available online at <https://www.ipcc.ch/reports/>.
- Jiang, X., and Yang, Z.-L. (2012). Projected changes of temperature and precipitation in Texas from downscaled global climate models. *Climate Research*, 53(3), 229-244, <https://doi.org/10.3354/cr01093>.

Liu, L., Hong, Y., Hocker, J.E., Shafer, M.A., Carter, L.M., Gourley, J.J., Bednarczyk, C.N., Yong, B., and Adhikari, P. (2012). Analyzing projected changes and trends of temperature and precipitation in the southern USA from 16 downscaled global climate models. *Theoretical and Applied Climatology*, 109, 345-360, <https://doi.org/10.1007/s00704-011-0567-9>.

Maraun, D. (2013). Bias Correction, Quantile Mapping, and Downscaling: Revisiting the Inflation Issue. *Journal of Climate*, 26(6), 2137-2143, <https://doi.org/10.1175/JCLI-D-12-00821.1>

Mearns, L., McGinnis, S., Korytina, D., Arritt, R., Biner, S., Bukovsky, M., Chang, H.-I., Christensen, O., Herzmann, D., Jiao, Y., Kharin, S., Lazare, M., Nikulin, G., Qian, M., Scinocca, J., Winger, K., Castro, C., Frigon, A., and Gutowski, W. (2017). *The NA-CORDEX dataset*, version 1.0. NCAR Climate Data Gateway, Boulder CO. Accessed December 27 2020. Available online at <https://doi.org/10.5065/D6SJ1JCH>.

Met Office. (2020). Met Office Hadley Centre for Climate Science and Services. Accessed December 23 2020. Available online at <https://www.metoffice.gov.uk/weather/climate/met-office-hadley-centre/index>.

Molina, M.J., Timmer, R.P., and Allen, J.T. (2016). Importance of the Gulf of Mexico as a climate driver for U.S. severe thunderstorm activity. *Geophysical Research Letters*, 43(23), 12295-12304, <https://doi.org/10.1002/2016GL071603>.

NOAA Climate. (2020). Climate Models. Accessed December 23 2020. Available online at <https://www.climate.gov/maps-data/primer/climate-models>.

NOAA GFDL. (2020). Climate Modeling. Accessed December 23 2020. Available online at https://www.gfdl.noaa.gov/wp-content/uploads/files/model_development/climate_modeling.pdf.

NOAA PSL. (2020¹). CPC Global Temperature data provided by the NOAA Physical Sciences Laboratory, Boulder, Colorado, USA. Accessed July 13 2020. Available online at <https://psl.noaa.gov/data/gridded/data.cpc.globaltemp.html>.

NOAA PSL. (2020²). CPC Global Unified Precipitation data provided by the NOAA Physical Sciences Laboratory, Boulder, Colorado, USA. Accessed July 13 2020. Available online at <https://psl.noaa.gov/data/gridded/data.cpc.globalprecip.html>.

Pierce, D.W., Cayan, D.R., and Thrasher, B.L. (2013). Statistical Downscaling Using Localized Constructed Analogs (LOCA). *Journal of Hydrometeorology*, 15(6), 2558-2585, <https://doi.org/10.1175/JHM-D-14-0082.1>.

Schneider, T., Kaul, C.M., and Pressel, K.G. (2019). Possible climate transitions from breakup of stratocumulus decks under greenhouse warming. *Nature Geoscience*, 12, 163-167, <https://doi.org/10.1038/s41561-019-0310-1>.

Tang, J., Niu, X., Wang, S., Gao, H., Wang, X., and Wu, J. (2016). Statistical downscaling and dynamical downscaling of regional climate in China: Present climate evaluations and future climate projections. *Journal of Geophysical Research – Atmospheres*, 121(5), 2110-2129, <https://doi.org/10.1002/2015JD023977>.

- Taylor, K.E., Stouffer, R.J., and Meehl, G.A. (2012). An overview of CMIP5 and the experiment design. *Bulletin of the American Meteorological Society*, 93(4), 485-498, <https://doi.org/10.1175/BAMS-D-11-00094.1>.
- Thornes, T. (2016). Can reducing precision improve accuracy in weather and climate models? *Weather*, 71(6), 147-150, <https://doi.org/10.1002/wea.2732>.
- Trapp, R.J., Diffenbaugh, N.S., Brooks, H.E., Baldwin, M.E., Robinson, E.D., and Pal, J.S. (2007). Changes in severe thunderstorm environment frequency during the 21st century caused by anthropogenically enhanced global radiative forcing. *PNAS*, 104(50), 19719-19723, <https://doi.org/10.1073/pnas.0705494104>.
- Trenberth, K.E. (2011). Changes in precipitation with climate change. *Climate Research*, 47, 123-138, <https://doi.org/10.3354/cr00953>.
- UCAR SciEd. (2020). Climate Modeling. Accessed December 23 2020. Available online at <https://scied.ucar.edu/learning-zone/how-climate-works/climate-modeling>.
- UCSD. (2020). University of California San Diego – LOCA Statistical Downscaling. Accessed December 27 2020. Available online at <http://loca.ucsd.edu/>.
- van Vuuren, D.P., Edmonds, J., Kainuma, M., Riahi, K., Thomson, A., Hibbard, K., Hurtt, G.C., Kram, T., Lamarque, J.-F., Masui, T., Meinshausen, M., Nakicenovic, N., Smith, S.J., and Rose, S.K. (2011). The representative concentration pathways: an overview. *Climatic Change*, 109, 5, <https://doi.org/10.1007/s10584-011-0148-z>.
- WCRP. (2020). World Climate Research Program – CORDEX. Accessed December 27 2020. Available online at <https://cordex.org/>.
- White, L.D., Kozaira, M. (2018). Surface Thermodynamic Gradients Associated with Gulf of Mexico Sea-Breeze Fronts. *Advances in Meteorology*, 2018, 2601346, <https://doi.org/10.1155/2018/2601346>.
- World Meteorological Organization. (2017). *WMO Guidelines on the Calculation of Climate Normals* (Report No. WMO-No. 1203). World Meteorological Organization.
- Zhao, S., Deng, Y., and Black, R.X. (2016). Warm Season Dry Spells in the Central and Eastern United States: Diverging Skill in Climate Model Representation. *Journal of Climate*, 29(15), 5617-5624, <https://doi.org/10.1175/JCLI-D-16-0321.1>.

Climate of the Gulf Coast States - Chapter 4: Climate Hazards

[Sea Level Rise](#)49

 1. How does Sea Level Rise Happen? 49

 2. Climatology of Sea Level Rise 50

[Hurricanes](#) 52

 1. How do Hurricanes Form?52

 2. Climatology of Hurricanes52

[Droughts and Floods](#) 55

 1. How do Droughts and Floods Happen?55

 2. Climatology of Droughts and Floods 56

[Tornadoes](#) 58

 1. How do Tornadoes Form?58

 2. Climatology of Tornadoes59

[Wildfires](#) 61

 1. How do Wildfires Happen?61

 2. Climatology of Wildfires 61

[References](#)64

Note: A *Chapter Summary* has not been provided for Chapter 4, since each hazard’s three-page summary is intended as a mini-document for standalone use.

Sea Level Rise

1. How does Sea Level Rise Happen?

Sea level rise is the changing height of the oceans over a period of time, often in the context of climate change. Being a more visible and threatening consequence of climate change, sea level rise is often used as one indicator of how much the climate has changed. Since 1880, global average sea level has increased by 8-9 inches, with some of the fastest rates of sea level rise around the United States occurring in the Gulf of Mexico (NOAA Climate, 2020¹).

There are two mechanisms that explain most recent sea level rise, which are illustrated in Figure 1. These mechanisms result from heating of the land and sea, with heat coming from the Sun and excess heat from a human-enhanced [greenhouse effect](#) (see [Chapter 2](#)). The first mechanism, thermal expansion, describes the direct absorption of this heat by the world's oceans. As heat is absorbed, water molecules gain energy and move faster, causing the oceans to expand, much like how metal expands when held above an open flame. The only way oceans can expand is upward and onshore, hence thermal expansion produces sea level rise. According to the [Intergovernmental Panel on Climate Change](#) (IPCC), thermal expansion is now the biggest single contributor to global sea level rise, which was not true a few decades ago (IPCC, 2013).

The second sea level rise mechanism is the melting of land ice, whether the melting of ice sheets in Antarctica and Greenland or of glaciers in mountain ranges. As land ice absorbs heat, this ice will either melt or break off into the oceans, increasing ocean volume and producing sea level rise. Sea ice does not cause sea level rise when it melts, since it already sits atop the oceans. Sea level rise occurs when too much land ice melts, or when the world's oceans absorb too much heat, such are the effects of a human-enhanced greenhouse effect, hence why sea level rise serves as a common indicator of climate change.

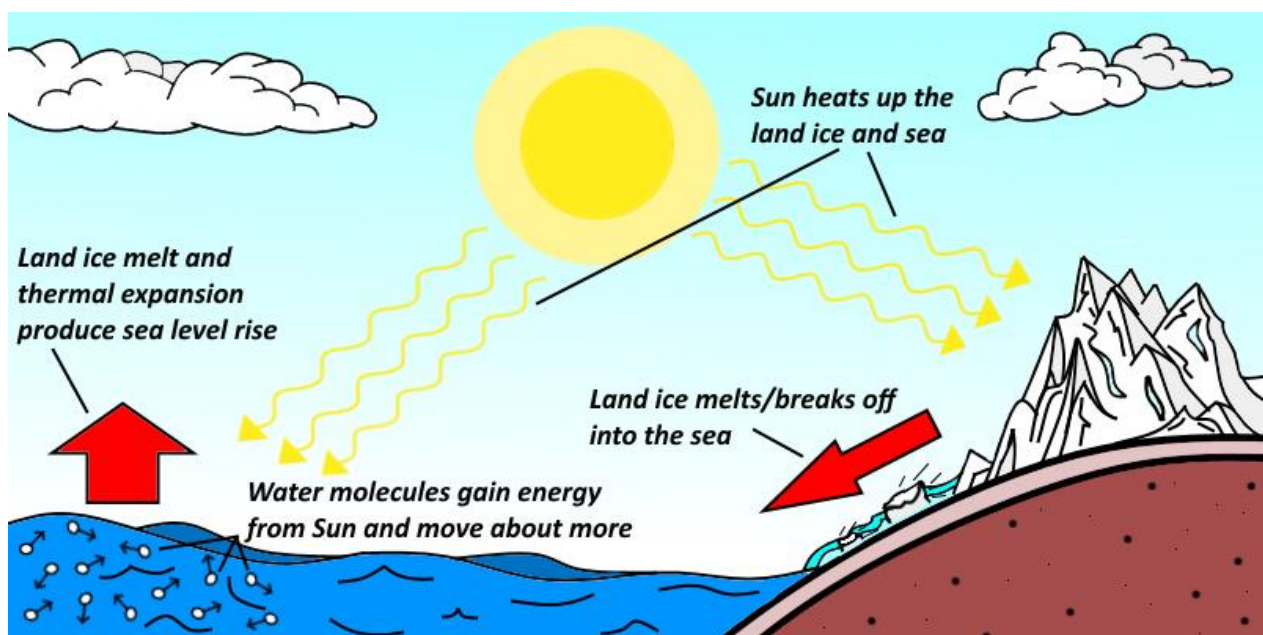


Figure 1: Sketch of the two major sea level rise mechanisms.

2. Climatology of Sea Level Rise

Sea level rise trends in the Gulf of Mexico are among the fastest affecting the United States, with trends in Louisiana and Texas accelerating in recent years (Boon et al., 2018). Figure 2a shows sea level rise measured at tide gauges across the Gulf Coast States since 1980, with increases above 1 foot affecting the Mississippi River Delta and low-lying towns along the Texas coast. In context, 1 foot of sea level rise in 40 years, or around 0.35 in/year (8.89mm/year), has seldom happened in the Gulf of Mexico since the last ice age (Donoghue, 2011), which is made more concerning by how much human settlement now exists along the coast. This rapid sea level rise is compounded by land subsidence, the sinking of land *relative* to sea level, as opposed to the *absolute* sea level rise produced by the mechanisms in Figure 1. Land subsidence from over-pumping groundwater along the Texas and Louisiana coast is among the fastest in the United States, reaching up to 0.2 in/year (5 mm/year) and thus exacerbating the sea level rise already produced by land ice melt and thermal expansion (Argus et al., 2018)

With sea level rise comes an increased risk of tidal flooding (floods that occur during high tide), which the Gulf Coast States now see more frequently than a few decades ago. Figure 2b illustrates the increase of annual tidal flooding frequency across the region since 1994, with some places (e.g., the Houston, TX area and the Mississippi coast) now experiencing over an additional week of tidal flooding days than 25 years ago. Some tide gauges in the Gulf Coast States possess records going as far back as the 1920s, all of which suggest long-term increases in tidal flooding frequency, especially along the western half of the coast (Sweet et al., 2018).

Consequences of sea level rise and tidal flooding are already being felt across the Gulf Coast States. Coastal ecosystems are especially [vulnerable](#) to sea level rise, such as the freshwater forests of West Florida (DeSantis et al., 2007; Langston et al., 2017), and the disappearing marshlands of the Mississippi River Delta (Burkett et al., 2005; Törnqvist et al., 2020). These ecosystems are an important natural defense against coastal flooding, so their loss increases the urgency to either evacuate infrastructure and people inland or to invest in multi-billion-dollar coastal defenses. Indeed, the Texas state government (CBS News, 2018) and Miami, FL (Allen, 2020) have both proposed expensive floodwall projects, symbolizing the palpable threat

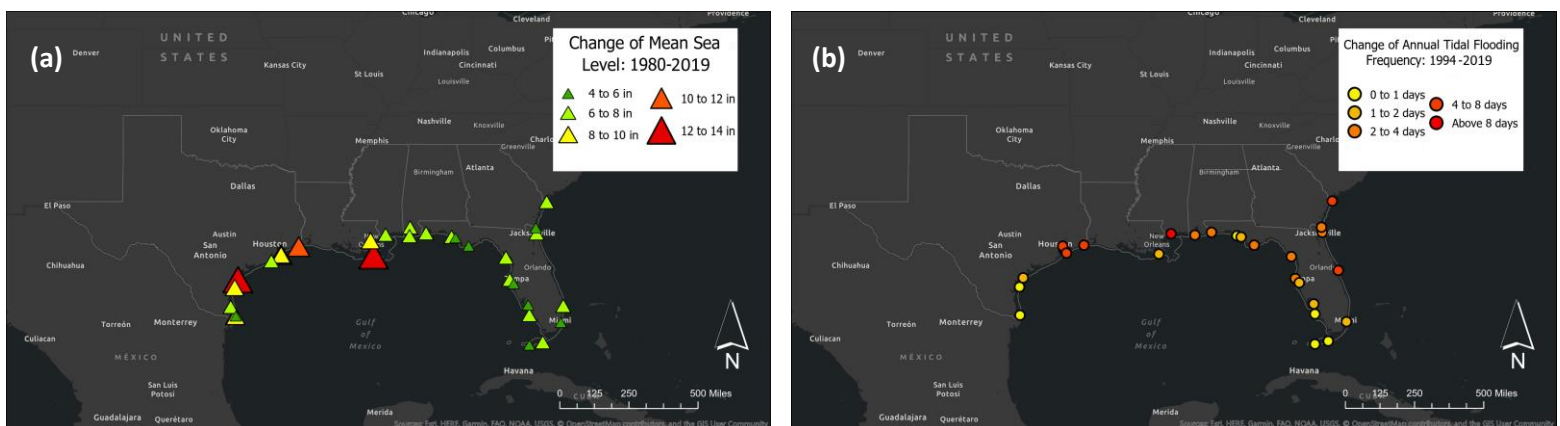


Figure 2: Change of average sea level in inches from 1980-2019 (2a, left), and change of annual frequency of tidal flooding days from 1994-2019 (2b, right). Data source: NOAA Inundation Dashboard (2020).

sea level rise now poses to the Gulf Coast States. The interaction of increased tidal flooding and hurricane storm surges pushes this threat even higher. A slight increase (+1.05 ft) in the height of Gulf Coast hurricane storm surges since 1950 is shown in Figure 3, although high tide's effects on storm surges in the Gulf of Mexico have been historically limited (Marsooli and Lin, 2018). It is clear, nonetheless, that sea level rise represents an increasing ecological, infrastructural, and economic [hazard](#) to the Gulf Coast States.

As sea level rise continues into the future, difficulty in maintaining existing infrastructure and ecosystems will increase. Blum and Roberts (2009) pointed out that without sufficient sediment input from upstream, sea level rise could drown most of the Mississippi River Delta by 2100. Additionally, Dahl et al. (2017) find that by 2045, several Gulf Coast locations that historically experienced almost no tidal flooding could experience up to 60 tidal floods per year, especially along the Texas coast. Increased tidal flooding due to sea level rise could thus threaten low-lying Gulf Coast cities in future decades, something that is already affecting cities like Miami Beach, FL (Wdowinski et al., 2016). In fact, climate models project that sea levels in the Gulf of Mexico could rise anywhere from 0.7 m (2.30 ft; IPCC, 2013) to up to 3 m (10 ft; NOAA SLR Viewer, 2020) by 2100, an increase that would submerge major cities like Miami, FL and New Orleans, LA.

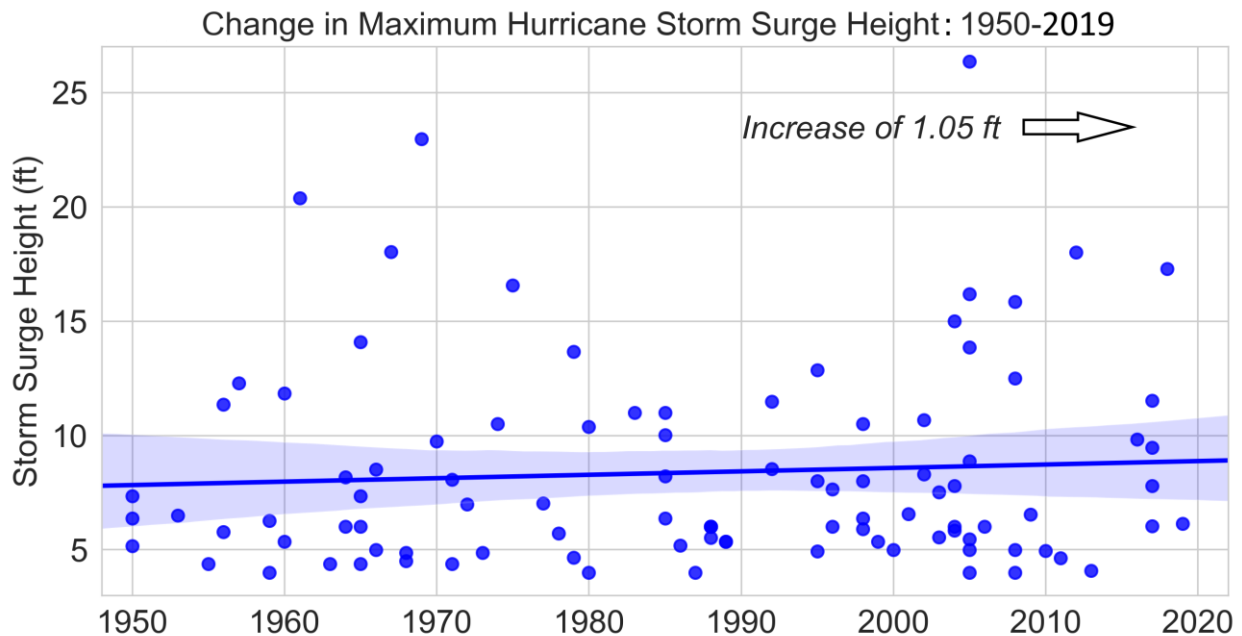


Figure 3: Change in the maximum height of Gulf Coast hurricane storm surges from 1950-2019, using a definition of a 4ft minimum surge height, as per Needham and Keim (2012). The blue line is the trend line, and the blue shading is the confidence interval of the trend line's slope. Data sources: Needham and Keim (2012); NHC (2020).

Hurricanes

1. How do Hurricanes Form?

Hurricanes are tropical weather systems associated with exceptionally heavy rainfall, powerful winds, and high coastal storm surges. This particular hazard has different names depending on location, being called *hurricanes* in the East Pacific and Atlantic Oceans, *typhoons* in the West Pacific, and *cyclones* in the Indian Ocean, but each name describes the same type of event. Hurricane formation requires five key factors:

1. A disturbance, such as “atmospheric waves” moving across the Atlantic from West Africa.
2. An ocean temperature of at least 79°F. Warm ocean water is the fuel of a hurricane.
3. A moist, “unstable” atmosphere, carrying evaporated ocean water high up to form clouds.
4. A lack of “wind shear”, or change in wind speed/direction with height, otherwise clouds are blown away before they can form the towering structure of a hurricane.
5. Being at least 5°N/S away from the Equator. Hurricanes rotate due to the Coriolis effect, an acceleration produced by Earth rotating on its axis, which is stronger at higher latitudes.

Figure 4 illustrates how these ingredients come together to form a hurricane. The warm ocean water heats the air, causing the air to rise and meet the disturbance above. The heated air brings up evaporated water from the ocean, which condenses out to produce clouds and thunderstorms. The air then cools, spreads out, and sinks after its ascent, allowing more warm air to rise and replace it from below, and therefore adding more warm water as fuel. Air pressure above the ocean lowers, causing the water to bulge, which will become the storm surge when the hurricane makes landfall. As this is all happening, the Coriolis effect is rotating the developing tower of clouds, producing the hurricane’s characteristic pinwheel shape and cloudless eye. Trade winds then carry the hurricane westward toward the Gulf Coast States. Hurricane formation continues as long as all 5 key ingredients are present, hence why hurricanes weaken once they make landfall, due to the loss of warm water supply. Generally, the longer all five ingredients are available determines the degree of wind speed strengthening, which in turn sets the difference between a tropical depression (<39 mph winds), a tropical storm (39-73 mph), and a hurricane (>73 mph).

2. Climatology of Hurricanes

Hurricane activity tends to peak in late-summer/early-autumn, when ocean temperatures tend to be highest. Figure 5a shows how around half of all hurricanes in the Gulf Coast States since 1950 made landfall in

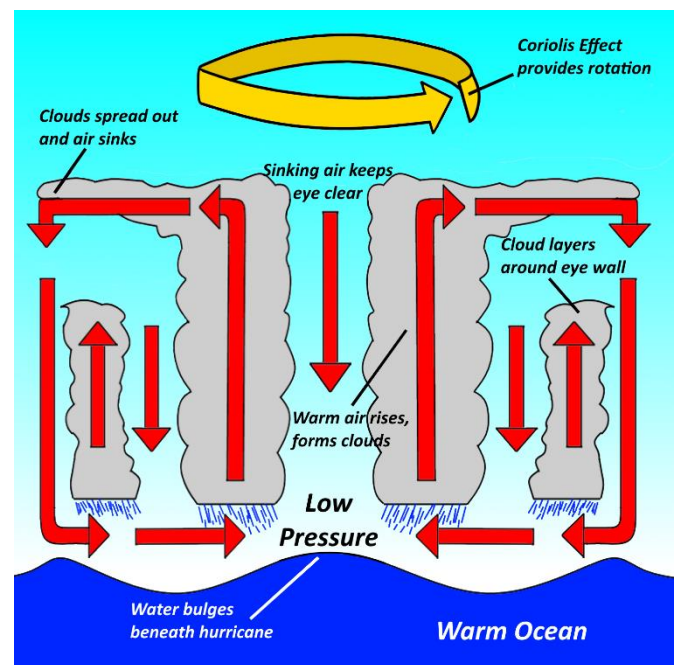


Figure 4: Sketch of the typical hurricane formation process.

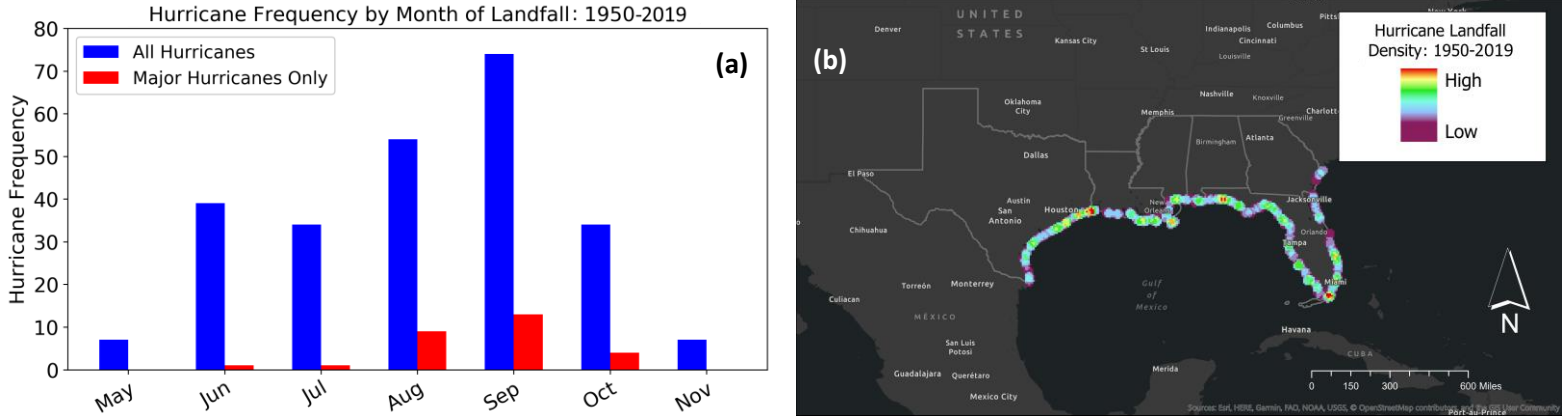


Figure 5: Hurricane frequency by month of landfall for all hurricanes (blue) and major hurricanes only (red) (5a, left), and density of hurricane landfall locations (5b, right), from 1950-2019. Data source: NOAA NOS (2020).

August and September, as did almost all *major hurricanes* (Category 3-5; >110 mph sustained winds). Hurricanes have made landfall across the length of the region’s coastline, as Figure 5b illustrates, with hotspots since 1950 in South Florida, Northwest Florida, South Louisiana, and the Texas-Louisiana border.

Often measuring hundreds of miles across, hurricanes cause widespread devastation upon landfall, their most frequent impacts including property loss, power outages, ecosystem damages, and loss of life. These impacts translate into high financial costs, especially from larger hurricanes that make landfall in urban areas. This was the case for Hurricane Harvey in 2017, which inflicted around US\$125 billion of damage, centered mostly on Southeast Texas (NHC, 2018). Portions of the area received 60 inches of rainfall in four days, enough to flood over 300,000 buildings and claim at least 68 lives, the highest death toll of any hurricane to hit Texas in 100 years (Blake and Zelinsky, 2018).

The last 20 years have seen several high-profile hurricanes with costly impacts across the Gulf Coast States, including Katrina, Harvey, and Irma to name a few. The impacts of these hurricanes seem to be getting worse, not just because of growing urban populations, but also the strengthening of the hurricanes themselves. Figure 6 shows how the properties of hurricanes that made landfall in the Gulf Coast States have changed in the last 70 years. While the number of hurricanes per year has not appreciably changed (Figure 6a), the average maximum wind speed of major hurricanes has made a notable increase (Figure 6b). This strengthening has been attributed to increased ocean temperatures fueling more powerful hurricanes (Elsner et al., 2008; Knutson et al., 2010), though attributing these observed changes to climate change is currently difficult in the absence of sufficient data (IPCC, 2013). However, climate change could alter the frequency and severity of hurricanes impacting the Gulf Coast States in the future. By the end of the 21st Century, the number of Category 4 and 5 hurricanes in the North Atlantic is expected to increase substantially (Bender et al., 2010), as is the intensity of their associated rainfall (Bacmeister et al., 2018). If major hurricanes do become more common, their combined effects with sea level rise could make flooding from storm surges worse in the decades to come (Lin et al., 2012).

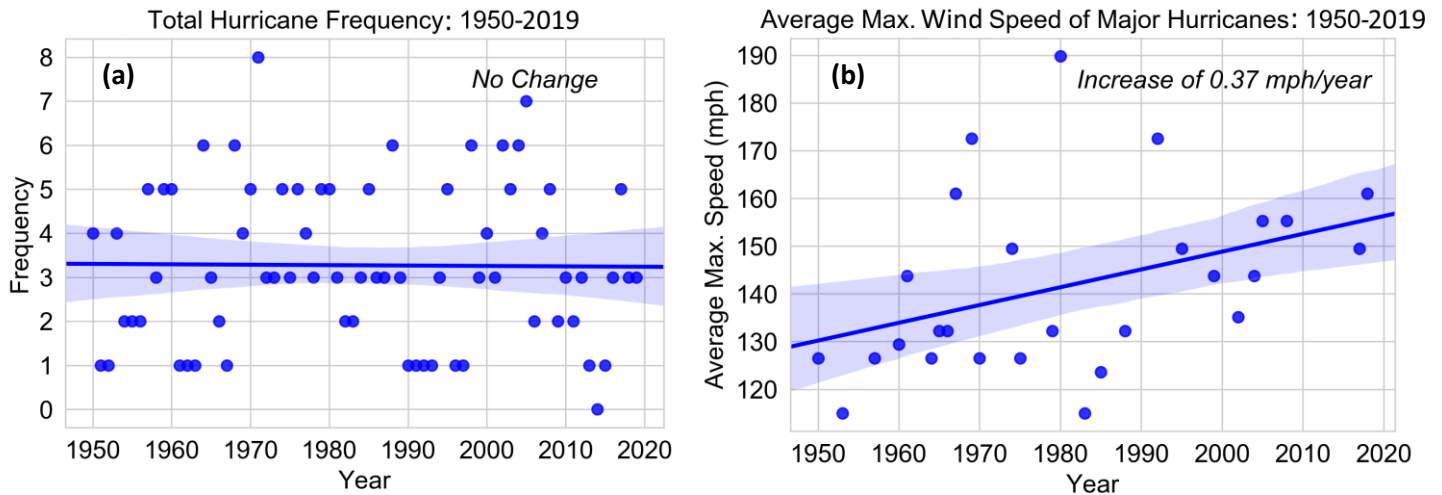


Figure 6: Change of Gulf Coast annual hurricane frequency (6a, left) and change of average maximum wind speed of major hurricanes (6b, right) from 1950-2019. The blue line is the trend line, and the blue shading is the confidence interval of the trend line's slope. Data source: NOAA NOS (2020).

Even with the lack of sufficient data, it is possible that climate change could already be strengthening hurricanes that affect the Gulf Coast States. Studies have shown that climate change increased the heaviness of the rainfall associated with Hurricane Harvey (Emanuel, 2017) and Hurricanes Katrina, Maria, and Irma (Patricola and Wehner, 2018). Furthermore, the 2020 Atlantic Hurricane Season broke multiple records, consisting of 30 named storms, 10 of which rapidly intensified, and five of which made landfall in Louisiana specifically (Cristobal, Laura, Marco, Delta, and Zeta; Caldas, 2020). Frequent rapid intensification of hurricanes is associated with climate change, both in observed (Bhatia et al., 2019) and projected (Bhatia et al., 2018) hurricane activity, meaning that the 2020 Atlantic Hurricane Season could be a window into the increasing risk that climate change poses to the Gulf Coast States.

Droughts and Floods

1. How do Droughts and Floods Happen?

Droughts and floods are somewhat opposites in their posed climate hazards. Whereas a drought is a period of dry conditions associated with low rainfall and plant/soil moisture deficiency, a flood is an excess of water on land that cannot easily drain into the ground or water bodies. These deficits and surpluses of water can last for weeks, even months, costing the United States' economy up to billions of dollars per year (NOAA Climate, 2020²).

Figure 7 illustrates how droughts and floods occur. Droughts typically require a long-term below-average water supply, typically due to reduced rainfall. Although extreme heat worsens drought by evaporating more ground moisture, an effect that has become more prominent in recent years (Alizadeh et al., 2020), drought conditions can also occur in colder, wetter climates. Droughts have myriad effects, such as crop failure, loss of domestic and industrial water supply, and ecosystem stress (NOAA NCEI, 2020³). The left panel of Figure 7 shows how drought dries out the ground as moisture is lost, causing it to crack. The ground can become so dry that when water returns, the ground cannot absorb it as quickly, thus increasing flood risk.

The occurrence of a flood has two requirements: that a large amount of water flows over an area that is typically dry, and that the volume of water is too great to be removed quickly. This rate of water removal is reduced not just by excessively dry ground, but excessively wet ground too. Ground saturation (right panel of Figure 7) commonly results from persistent above-average rainfall, reducing its ability to remove floodwaters, such as during Texas' severe floods of May 2015 (Fournier et al., 2016). There are four different types of events that can produce floods (left to right in Figure 7): breakage of dams or levees, heavy rainfall, runoff produced by melting snow and ice, or storm surges/tidal waves (NOAA NSSL, 2020). Except for dam or levee breakage, these processes are susceptible to the effects of climate change, hence there is concern for the future intensity and frequency of both floods and droughts.

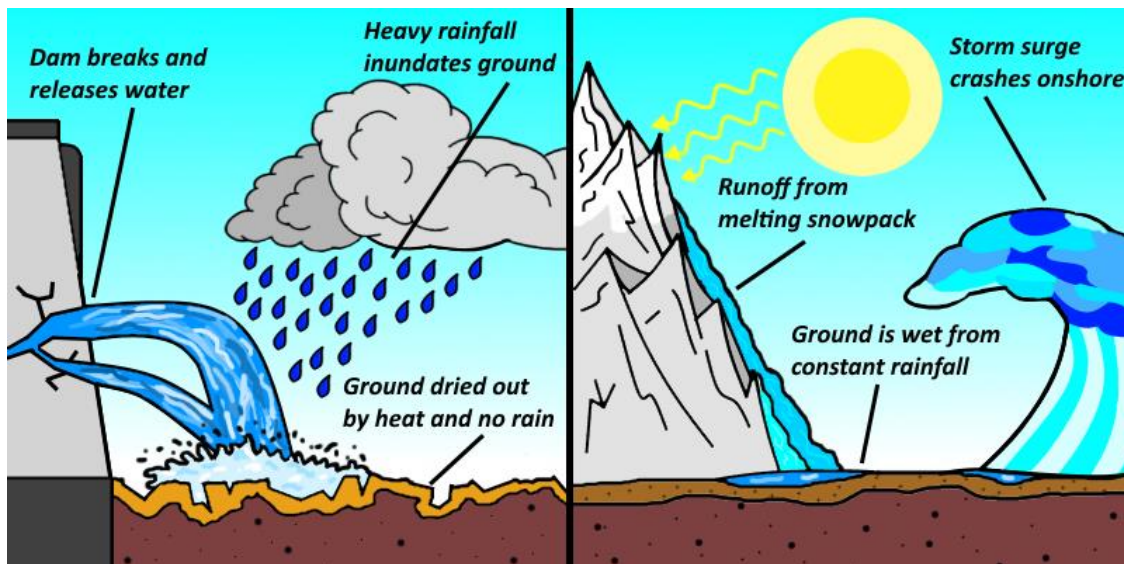


Figure 7: Sketch of the mechanisms that lead to droughts and floods.

2. Climatology of Droughts and Floods

In recent decades, droughts have been more common in warmer seasons than colder ones, according to the Palmer Drought Severity Index (PDSI) analysis in Figure 8a (PDSI > 0 means moister conditions, PDSI < 0 means drier conditions). Droughts from 1950-2014 were least prevalent in winter in all states but Mississippi. Since winter is the Gulf Coast States’ coolest season, and ground moisture is restored by the heavy rains and hurricanes (Maxwell et al., 2013) of prior months, less drought in winter is understandable. Figure 8a also shows that drought was more common further east, with Florida (-0.12) and Georgia (-0.18) having the lowest annual average PDSIs. Since PDSI measures relative dryness (Dai and NCAR Staff, 2019), Texas having a higher annual average PDSI (0.20), despite its drier climate, is not unrealistic, meaning that Texas tends to be less dry relative to its normal conditions, when averaged over the year, than other locations. In fact, drought is enough of an issue in Florida that prescribed wildfires are consistently performed less in drier times (Nowell et al., 2018).

Average flood statistics share little similarity to drought, as shown in Figure 8b, a map of modal (most common) flooding season by county, and state flood frequency per square mile (legend). Although Texas experienced the most floods since 1996, its flood frequency per square mile was low (0.006/mi²), which increased eastward toward Florida (0.016/mi²). Modal flooding season was less consistent, but can be explained. The autumn peak along the Texas coast likely resulted from storm surges and rainfall from hurricanes (Chapter 4 - Hurricanes), the summer/autumn peak in Florida from the state’s wet season, and the spring peak across Mississippi and Alabama from supercell activity (Chaney et al., 2013). However, since these results came from 24 years of flood data, less than the 30-year minimum for assessing climatology (WMO, 2017), this figure could look different with a longer observational record.

Conclusions about changes in flood frequency across the Gulf Coast States are also limited by having only 24 years of data, such as in Figure 9a. The figure suggests that more flood events now occur per year across the region, which makes sense given climate change’s contributions to more powerful storms (Chapter 4 – Hurricanes and Tornadoes), higher tides (Chapter 4 – Sea

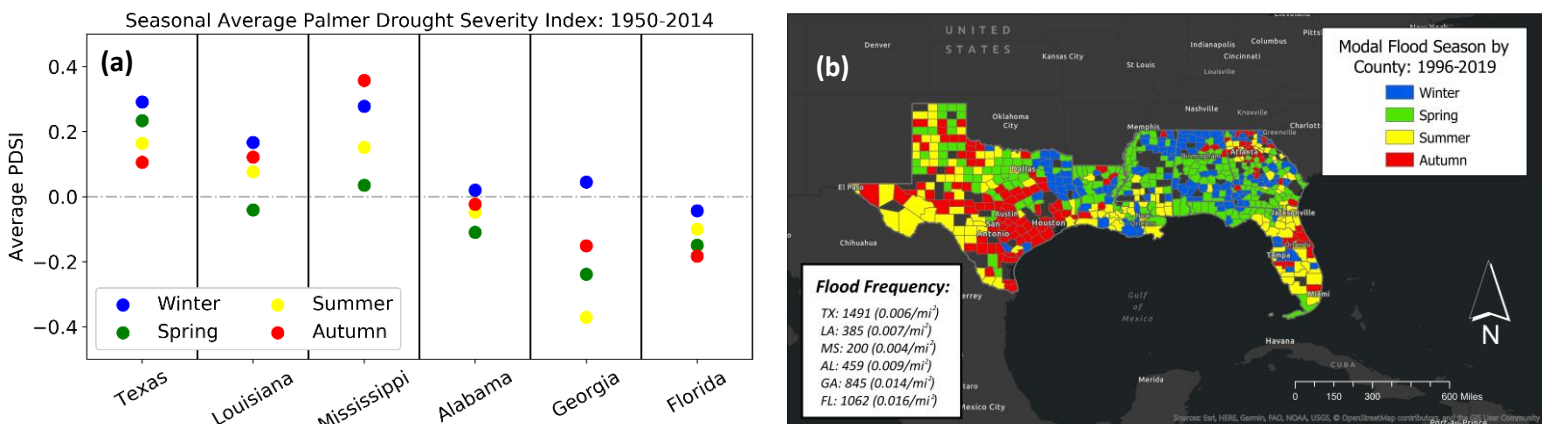


Figure 8: Seasonal average PDSI by state from 1950-2014 (8a, left) and most common flood season by county from 1996-2019 (8b, right; colorless = no floods). Data sources: NOAA PSL (2020); NOAA NCEI (2020⁴).

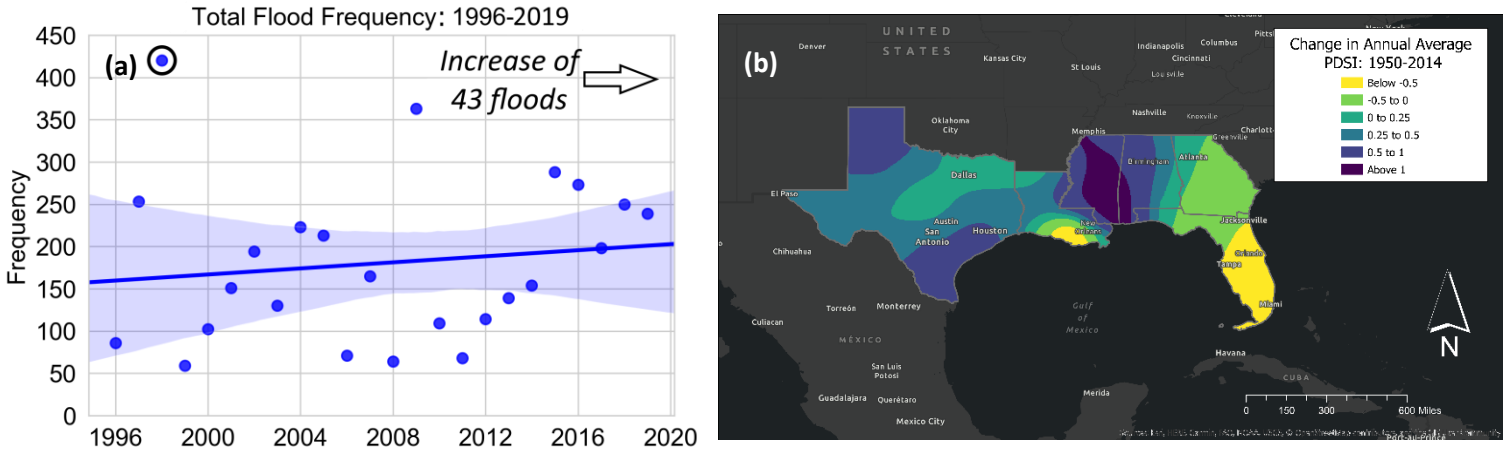


Figure 9: Change of Gulf Coast annual flood frequency from 1996-2019 (9a, left) and change of annual average PDSI from 1950-2014 (9b, right). The blue line in Figure 9a is the trend line, and the blue shading is the confidence interval of the trend line’s slope. Data sources: NOAA NCEI (2020⁴); NOAA PSL (2020).

Level Rise), and heavier rainfall. Despite this positive trend, some years stand out against it, such as 1998 (circled), an El Niño year that brought excessive rainfall to Georgia and Florida from January to March (Bell et al., 1999; NOAA NWS, 2010), and one of the most powerful Atlantic hurricane seasons on record (USGS, 2005). Years like 1998 are why long observational records are essential for assessing flood climatology.

Much like trends in annual flood frequency, annual average PDSI trends from 1950-2014 (Figure 9b) are spatially consistent with those for rainfall. For instance, annual rainfall amount (Chapter 2, Figure 9) has increased across most of Texas and Alabama, states that saw increases in their average PDSI scores, i.e., less drought. Figure 9b suggests that, except for most of Florida and South Louisiana, the Gulf Coast States experience less severe drought now than 65 years ago. This result is supported by several studies of 20th Century drought severity in the United States (Andreadis and Lettenmaier, 2006; Mitra and Srivastava, 2017), although Maleski and Martinez (2016) argue that Alabama’s recent drought variability is within normal climate fluctuations. As such, the effects of climate change on recent drought trends are doubtful.

The picture for the future is climate change exacerbating droughts and floods. A warmer climate increases how much water vapor the atmosphere can hold, which generally results in worsened droughts and floods due to less frequent, more powerful rainfall (Whitfield, 2012). In the decades to come, droughts in the Gulf Coast States could become more intense due to increased evapotranspiration, as noted for Alabama (Mishra, 2015) and the West Texas desert (Venkataraman et al., 2016). As for floods, the Intergovernmental Panel on Climate Change found that future rainfall-driven flooding could increase over the Gulf Coast States (IPCC, 2013), made worse by factors that are heightening the region’s flood risk. From increased populations and assets on flood plains (Wing et al., 2018), to sea level rise worsening tidal floods (McAlpine and Porter, 2018), to the growing flood risk posed by hurricanes (Sajjad et al., 2020), climate change’s effects on flooding threaten the sustainability of Gulf Coast settlements in multiple ways.

Tornadoes

1. How do Tornadoes Form?

Tornadoes are powerful spirals of wind extending to the ground from the cloud base of storms. They can form as part of any storm system that possesses both rotation and a strong updraft of warm air. Although much smaller than hurricanes, tornadoes can possess wind speeds exceeding 300 mph, inflicting serious damage over an area only a few miles across.

The most common mechanism by which tornadoes form is shown in Figure 10. The left panel shows an initial cumulonimbus cloud experiencing rapid changes of wind speed and direction with height (wind shear), initiating rolls of horizontal air rotation within the cloud (red spiral). The cloud derives energy and moisture from a warm updraft (blue arrow), which tilts the rolls upward. Eventually, the rolls are near-vertical and start to rotate the updraft itself (right panel), at which point a mesocyclone has formed and the cumulonimbus cloud has become a supercell. As the updraft sucks warm air into the supercell, the surface air pressure drops, causing the mesocyclone to stretch downward to compensate. As the mesocyclone stretches, its rotation speed increases, producing a funnel at the cloud base. With enough stretching, this funnel cloud reaches the surface, forming a tornado. Most tornadoes last less than 10 minutes, as the supercell's rainfall thrusts a downdraft of cool air toward the ground, felt as a gust front before the rain arrives. This cool air wraps around the tornado, cutting off the warm updraft and leaving the tornado to become rope-like and to gradually decay. It is theorized that the speed of this wrapping is part of the explanation for why some supercells produce tornadoes and others do not.

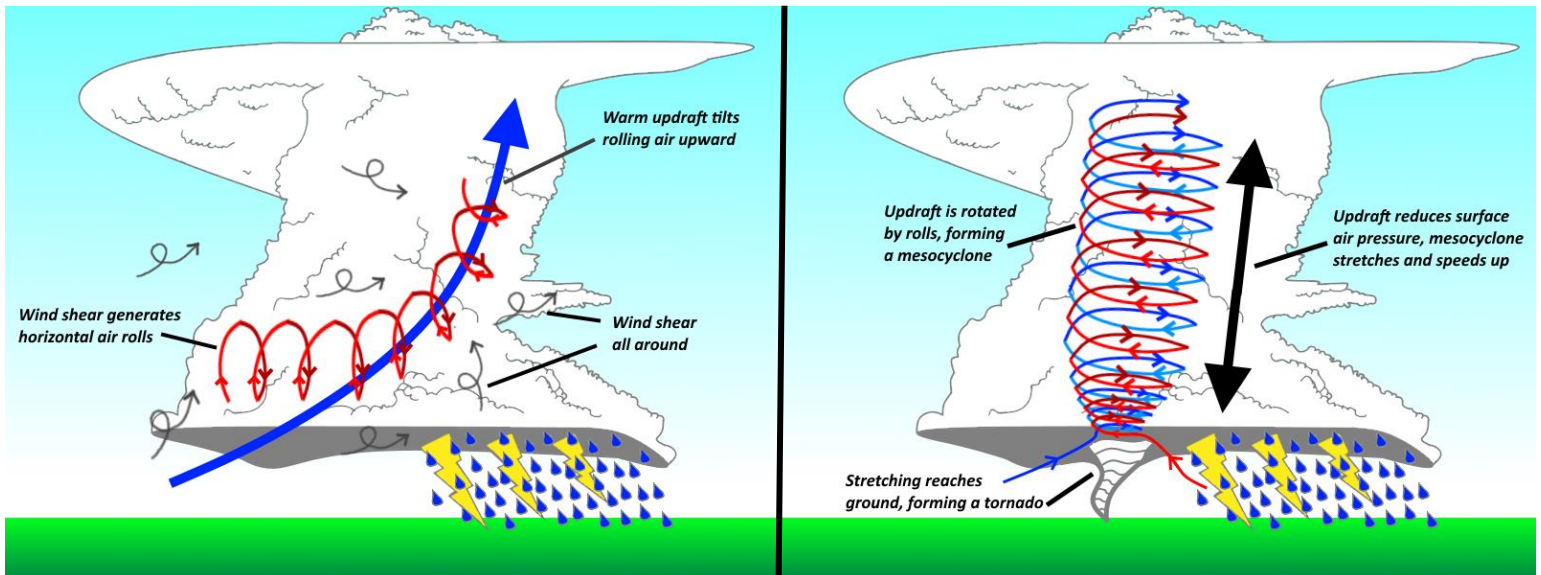


Figure 10: Sketch of the tornado formation process, based on current consensus.

2. Climatology of Tornadoes

Tornado formation in the Gulf Coast States peaks in late-spring and early-summer, when warm, moist air is common over the region. This heat and moisture peaks in the evening, hence why tornadoes often happen near sunset or at night. This peak in spring/summer tornado frequency (from 1950-2018) is shown in Figure 11a. Tornadoes with an Enhanced Fujita rating (the scale for measuring tornado intensity, EF0 = minor damage and EF5 = incredible damage) of EF1 or above (red) occur frequently during this spring/summer peak, when tornadoes form as part of long lines of powerful thunderstorms. By contrast, many tornadoes in summer/early autumn are EF0 (blue), since these tornadoes spawn from landfalling hurricanes, and thus are mostly weak and short-lived. It therefore makes sense that EF0 tornadoes are common across Florida and the Texas coast, whereas EF1+ tornadoes often occur inland (Figure 11b).

Determining change in tornado climatology is difficult, since tornadoes are such small events that their detection in remote places is less guaranteed. This problem was bigger several decades ago when there were fewer storm chasers and urban areas were smaller, hence why weaker (EF0) tornadoes have been reported in greater numbers since the 1970s (Doswell, 2007; NOAA NCEI, 2020¹). Figure 12 thus focuses on changes in the climatology of EF1+ tornadoes from 1970-2018. Tornado frequency across the Gulf Coast States has not changed greatly (Figure 12a), with 100-200 tornadoes per year being typical since the 1980s. What is seemingly true, however, is that the site of greatest tornado frequency has moved eastward, away from Texas and toward Alabama (Agee et al., 2016; Moore and DeBoer, 2019). The April 2011 tornado super outbreak spawned several EF4 and EF5 tornadoes over Alabama and Mississippi, and became the deadliest (316 fatalities), and one of the costliest (\$15.5 billion in damages), tornado disasters in the United States' history (Knupp et al., 2014). An east-shifted “Tornado Alley” could mean more outbreaks of this nature over the Gulf Coast States in the future.

The climatology of the tornado outbreaks themselves has also changed. Figure 12b illustrates how tornadoes across the Gulf Coast States are happening on fewer days than 50 years ago (blue), but the tornado count in outbreaks has increased (red). This figure is inspired by analysis by Brooks et al. (2014), who suggest that climate change could be influencing these trends, but

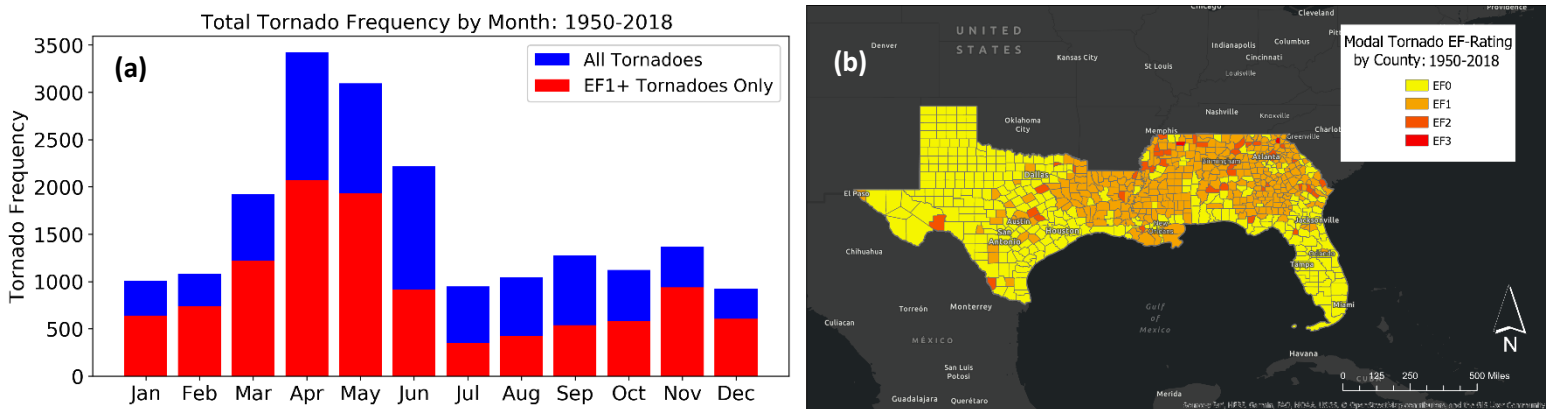


Figure 11: Total tornado frequency by month for all tornadoes (blue) and EF1+ tornadoes (red) (11a, left), and most frequent tornado EF-rating by county (11b, right), from 1950-2018. Data source: SVRGIS (2019).

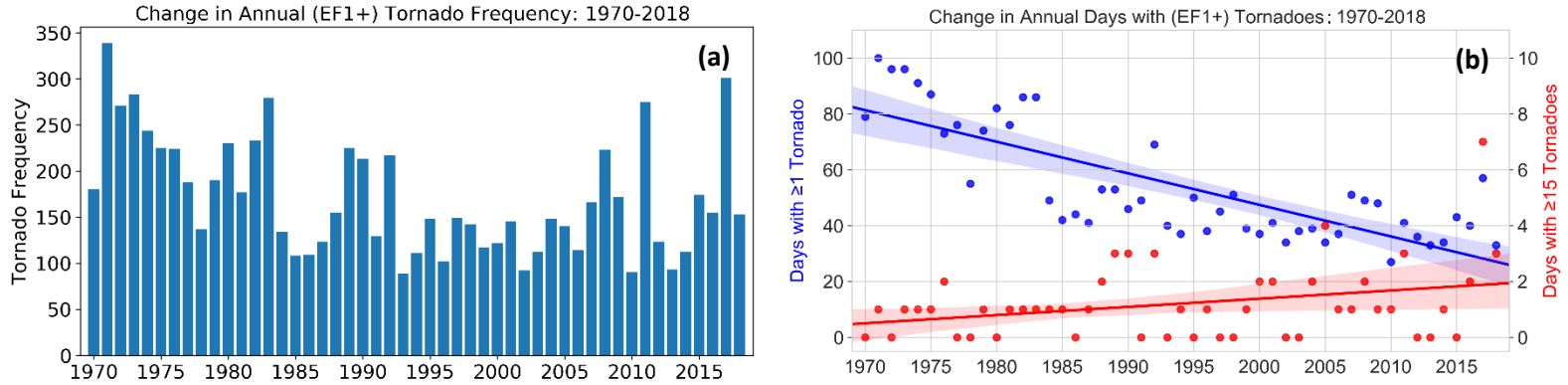


Figure 12: Change in Gulf Coast annual (EF1+) tornado frequency (12a, left), and change in the annual number of days that experience at least one (blue) and at least 15 (red) EF1+ tornadoes (12b, right; inspired by Brooks et al. (2014)) from 1970-2018. The lines in Figure 12b are trend lines, and the shading is the confidence interval of each trend line’s slope. Data source: SVRGIS (2019).

that other factors could be more important. Tippett et al. (2016) agree that long-term natural variability better explains these recent changes, whereas Elsner et al. (2015) are more confident that a warmer, energetic atmosphere is producing these more powerful tornado outbreaks. Climate change’s recent effects on tornadoes in the Gulf Coast States are thus inconclusive.

There is more consensus about the evolution of tornado climatology in the decades to come. Lee (2012) suggests that not only could EF2+ tornado frequency increase by the late-21st Century (including over several Gulf Coast States), but also that these increases could occur mostly in early-spring. This increased intensity will likely result from a warmer climate supporting more convective weather, such as tornado-spawning supercells. Both Hoogewind et al. (2017) and Rasmussen et al. (2020) also came to this conclusion, with the latter finding particular evidence for fewer weak storms and more severe storms, a result that is consistent with the recent changes in tornado outbreaks in Figure 12b. It is stressed by Strader et al. (2017), however, that the increased risks posed by future tornadoes will result more so from increased urbanization than climate change. Given how frequent and damaging tornadoes have historically been across the Gulf Coast States, their intensification due to climate change and a growing urban population presents serious social and economic risks.

Wildfires

1. How do Wildfires Happen?

A wildfire is a type of fire that is uncontrolled, unplanned, and burns large areas of vegetation. Wildfires are distinct from prescribed burns, which National Park Services and the US Forest Service conduct to manage vegetation, remove combustible plant matter, and conduct research (NPS, 2020). Major wildfires are increasingly making headlines, such as California’s 2020 wildfire season being one of the most devastating in its history (Crespo and Kallingal, 2020).

As with any type of fire, wildfires require three key components, as illustrated by Figure 13:

1. *A hot, oxygen-rich atmosphere.* Prolonged periods of high temperature help to dry out vegetation faster, and hot, oxygen-rich days are favorable for the vegetation’s ignition.
2. *A combustible material,* such as the vegetation of forests, wetlands, and steppes. Daytime heat and a lack of rainfall reduce plant moisture content, thus increasing flammability. Peat-filled wetlands, such as Georgia and Florida’s Okefenokee Swamp, are especially vulnerable to catching fire due to their high carbon content (Granath et al., 2016; Blount, 2020).
3. *A source of ignition.* Lightning strikes are the most common ignition source for natural wildfires. Human ignition sources can be unintentional, such as campfires, cooking outdoors, and discarded cigarettes, but also intentional in the case of arson. In recent years, 84% of recorded wildfires in the United States were ignited by humans (Balch et al., 2017).

The spread of wildfires is accelerated by available vegetation to burn, ideal weather conditions (high temperature, strong winds, low humidity), and the presence of uphill terrain (heat rises). Wildfires are an important part of ecosystems, acting as a natural means of removing dead plant matter and recycling nutrients into soils (National Geographic, 2020). However, with so many wildfires now caused by humans, and climate change raising the initial wildfire risk, wildfires are becoming more of a danger to ecosystems than an asset.

2. Climatology of Wildfires

Wildfire conditions across the Gulf Coast States are most commonly found in Texas and Florida, as shown in Figure 14a. The Florida Peninsula and the high plateaus of Texas have been hotspots for large wildfires (>1000 acres burned) since 2002. These hotspots are expected, given Florida’s frequent thunderstorms and its history of fire suppression (Stanturf et al., 2002; Wyman et al., 2012), and

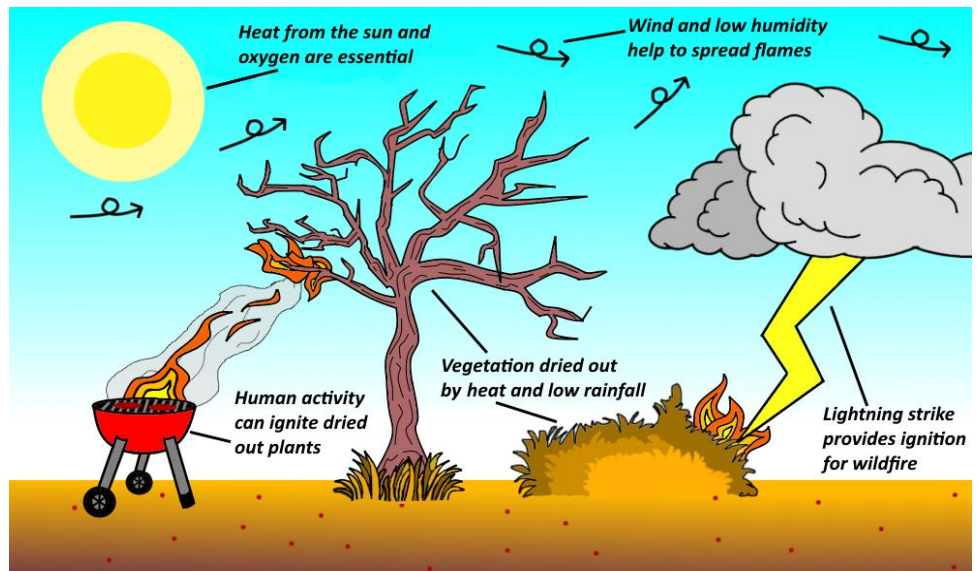


Figure 13: Sketch of the components necessary to start and spread wildfires.

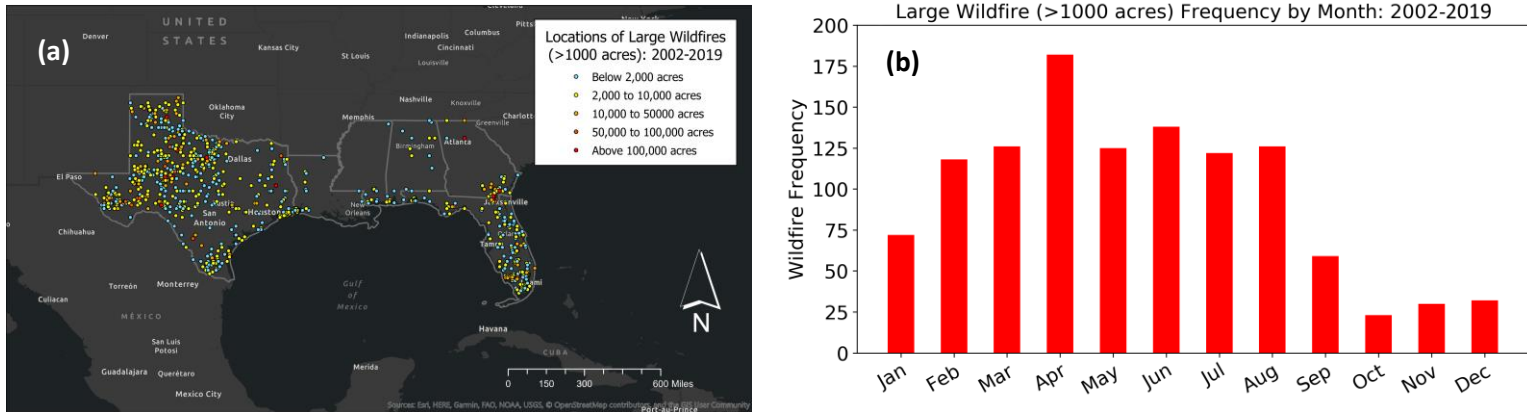


Figure 14: Location and size of large (>1000 acres) wildfires (14a, left) and monthly large wildfire frequency (14b, right) from 2002-2019. Data source: FAMWEB (2020).

Central Texas' grasslands have long been naturally maintained by wildfires (Stambaugh et al., 2014). The Florida hotspot contains a cluster of >100,000-acre wildfires at the Florida-Georgia border, where the Okefenokee Swamp is located. These wetlands have seen devastating wildfires in recent years, such as the Bugaboo Scrub Fire of 2007, with 564,450 acres burned (or >425,000 football fields) and \$65 million worth of lost timber, making it the worst wildfire in Georgia's history (Georgia Forestry Commission, 2007).

These large wildfires have occurred most frequently in mid-spring (Figure 14b). [Climate normal](#) data (NOAA NCEI, 2020²) shows that Central Texas cities are often dry in mid-spring, with any winter storms having passed and the tornado season still to come. Similarly, mid-spring marks the end of Florida's dry season; dry conditions in mid-spring facilitate wildfires in both hotspots, hence the April peak in Figure 14b. Conversely, large wildfires in the Gulf Coast States are less common in autumn and winter, thanks to lower temperatures and reduced drought conditions by months of preceding rainfall. However, these results are based on just 18 years of large wildfire records, a substantially shorter period than the 30-year standard for defining climate normals (WMO, 2017), which means that incorporating more wildfire data in the future could change these findings. Indeed, Labosier et al. (2014) found that some areas of the Gulf Coast States experience a second wildfire peak in autumn.

This short wildfire data record also limits drawable conclusions about changes in wildfire characteristics, such as change in wildfire frequency and area burned. As such, Figure 15 should not be over-interpreted, which shows a slight increase in the annual number of wildfires across the Gulf Coast States (Figure 15a; of all sizes), and a slight decrease in acres burned (Figure 15b). Identifying climate change's effect on recent wildfires is difficult, since modeled wildfire frequency and size has declined significantly in the last 200 years due to greater population density (Grala and Cooke, 2010; Knorr et al., 2014). Nevertheless, human-induced climate change since 1850 has resulted in increased coupling of heatwaves and droughts, especially in the Western Gulf Coast States (Cheng et al., 2019), establishing conditions for larger, more frequent wildfires. Figure 14 also shows that high area burned can result from a relatively small number of wildfires, such as the case for 2011 (circled in Figure 15), one of the Gulf Coast States' worst wildfire years, burning 2.7 million acres of land in Texas (Stambaugh et al., 2017).

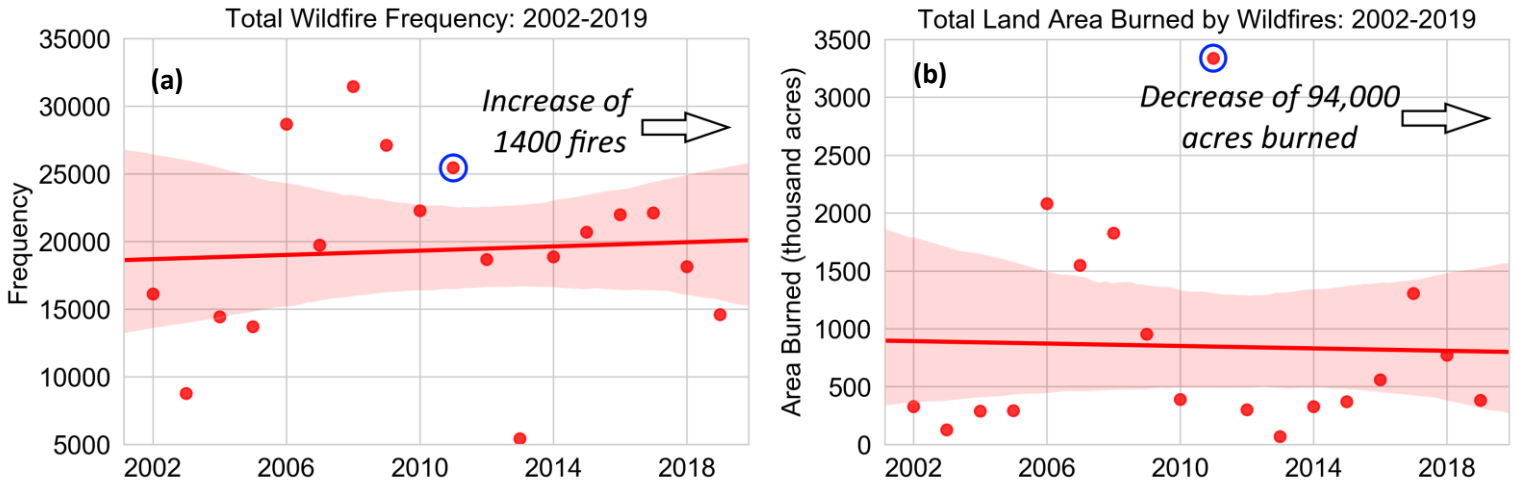


Figure 15: Change of Gulf Coast annual wildfire frequency (of all sizes; 15a, left) and change of annual land area burned by wildfires (15b, right) from 2002-2019. The red lines are trend lines, and the red shading is the confidence interval of each trend line’s slope. Data source: FAMWEB (2020).

Despite uncertainty in climate change’s current role for wildfires in the Gulf Coast States, wildfires are expected to become larger and more frequent in the future. Climate models suggest that, by 2060, the regional annual area burned could increase by 4%, and by up to 15% and 30% in Florida and Louisiana respectively (Prestemon et al., 2016). There is, however, some disagreement in terms of the effects driving this increased future wildfire risk. While Prestemon et al. (2016) found increased winter and spring evaporation (drought) to be an important driver, Liu et al. (2013) suggest that higher temperatures will play a more important role in this region. What all of these studies do agree on is that future increases in temperature and decreases in rainfall are likely to accompany increased wildfire potential (Stambaugh et al., 2018), a risk that everyone from park rangers to community leaders must be prepared to manage.

References

- Agee, E., Larson, J., Childs, S., and Marmo, A. (2016). Spatial Redistribution of U.S. Tornado Activity between 1954 and 2013. *Journal of Applied Meteorology and Climatology*, 55(8), 1681-1697, <https://doi.org/10.1175/JAMC-D-15-0342.1>.
- Alizadeh, M.R., Adamowski, J., Nikoo, M.R., AghaKouchak, A., Dennison, P., and Sadegh, M. (2020). A century of observations reveals increasing likelihood of continental-scale compound dry-hot extremes. *Science Advances*, 6(39), 1-11, <https://doi.org/10.1126/sciadv.aaz4571>.
- Allen, G. (2020, June 13). A \$4.6 Billion Plan To Storm-Proof Miami. *National Public Radio*. Available online at <https://www.npr.org/2020/06/13/875725714/a-4-6-billion-plan-to-storm-proof-miami>.
- Andreadis, K.M., and Lettenmaier, D.P. (2006). Trends in 20th century drought over the continental United States. *Geophysical Research Letters*, 33(10), 1-4, <https://doi.org/10.1029/2006GL025711>.
- Argus, D.F., Shirzaei, M., and Peltier, W.R. (2018). Subsidence along the Gulf and Atlantic coast of the United States exacerbates ocean inundation of the land produced by sea level rise. *Fall 2018 Meeting of the American Geophysical Union*, <https://agu.confex.com/agu/fm18/meetingapp.cgi/Paper/388158>.
- Bacmeister, J.T., Reed, K.A., Hannay, C., Lawrence, P., Bates, S., Truesdale, J.E., Rosenbloom, N., and Levy, M. (2018). Projected changes in tropical cyclone activity under future warming scenarios using a high-resolution climate model. *Climatic Change*, 146, 547-560, <https://doi.org/10.1007/s10584-016-1750-x>.
- Balch, J.K., Bradley, B.A., Abatzgolou, J.T., Nagy, R.C., Fusco, E.J., and Mahood, A.L. (2017). Human-started wildfires expand the fire niche across the United States. *PNAS*, 114(11), 2946-2951, <https://doi.org/10.1073/pnas.1617394114>.
- Bell, G.D., Halpert, M.S., Ropelewski, C.F., Kousky, V.E., Douglas, A.V., Schnell, R.C., and Gelman, M.E. (1999). Climate Assessment for 1998. *Bulletin of the American Meteorological Society*, 80(5s), S1-S48, <https://doi.org/10.1175/1520-0477-80.5s.S1>.
- Bender, M.A., Knutson, T.R., Tuleya, R.E., Sirutis, J.J., Vecchi, G.A., Garner, S.T., and Held, I.M. (2010). Modeled Impact of Anthropogenic Warming on the Frequency of Intense Atlantic Hurricanes. *Science*, 327(5964), 454-458, <https://doi.org/10.1126/science.1180568>.
- Bhatia, K.T., Vecchi, G.A., Murakami, H., Underwood, S., and Kossin, J. (2018). Projected Response of Tropical Cyclone Intensity and Intensification in a Global Climate Model. *Journal of Climate*, 31(20), 8281-8303, <https://doi.org/10.1175/JCLI-D-17-0898.1>.
- Bhatia, K.T., Vecchi, G.A., Knutson, T.R., Murakami, H., Kossin, J., Dixon, K.W., and Whitlock, C.E. (2019). Recent increases in tropical cyclone intensification rates. *Nature Communications*, 10, 635, <https://doi.org/10.1038/s41467-019-08471-z>.

Blake, E.S., and Zelinsky, D.A. (2018). *National Hurricane Center Tropical Cyclone Report – Hurricane Harvey*. (Report No. AL092017). National Oceanic and Atmospheric Administration. https://www.nhc.noaa.gov/data/tcr/AL092017_Harvey.pdf.

Blount, S. (2020). Wetlands of the United States - The National Environment Education Foundation. Accessed 3 October 2020. Available online at <https://www.neefusa.org/nature/land/wetlands-united-states#Florida>.

Blum, M.D., and Roberts, H.H. (2009). Drowning of the Mississippi Delta due to insufficient sediment supply and global sea-level rise. *Nature Geoscience*, 2, 488-491, <https://doi.org/10.1038/ngeo553>.

Boon, J.D., Mitchell, M., Loftis, J.D., and Malmquist, D.M. (2018). *Anthropocene Sea Level Change: A History of Recent Trends Observed in the U.S. East, Gulf, and West Coast Regions* (Special Report in Applied Marine Science and Ocean Engineering (SRAMSOE) No. 467). Virginia Institute of Marine Science, College of William and Mary. <https://doi.org/10.21220/V5T17T>

Brooks, H.E., Carbin, G.W., and Marsh, P.T. (2014). Increased variability of tornado occurrence in the United States. *Science*, 346(6207), 349-352, <https://doi.org/10.1126/science.1257460>.

Burkett, V.A., Wilcox, D.A., Stottlemeyer, R., Barrow, W., and Fagre, D. (2005). Nonlinear dynamics in ecosystem response to climatic change: case studies and management implications. *Environmental Science and Ecology Faculty Publications*, 2, 357-394, https://digitalcommons.brockport.edu/cgi/viewcontent.cgi?article=1074&context=env_facpub.

Caldas, A. (2020). Rapid Intensification and Number of Storms Make 2020 a Record Hurricane Season. *Union of Concerned Scientists*. Available online at <https://blog.ucsusa.org/astrid-caldas/rapid-intensification-unprecedented-number-of-storms-make-2020-a-record-hurricane-season>.

CBS News (2018, August 22). Big oil asks government to protect its Texas facilities from climate change. *CBS News*. Available online at <https://www.cbsnews.com/news/texas-protect-oil-facilities-from-climate-change-coastal-spine/>.

Chaney, P.L., Herbert, J., Curtis, A. (2013). A climatological perspective on the 2011 Alabama tornado outbreak. *Journal of Operational Meteorology*, 1(3), 19-25, <http://dx.doi.org/10.15191/nwajom.2013.0103>.

Cheng, L., Hoerling, M., Liu, Z., and Eischeid, J. (2019). *Journal of Climate*, 32(14), 4431-4443, <https://doi.org/10.1175/JCLI-D-18-0611.1>.

Crespo, G., and Kallingal, M. (2020, October 3). 2 California wildfires remain out of control. *Cable News Network*. Available online at <https://www.cnn.com/2020/10/03/us/california-wildfires-saturday/index.html>.

Dahl, K.A., Fitzpatrick, M.F., and Spanger-Siegfried, E. (2017). Sea level rise drives increased tidal flooding frequency at tide gauges along the U.S. East and Gulf Coasts: Projections for 2030 and 2045. *PLoS One*, 12(2), 1-23, <https://doi.org/10.1371/journal.pone.0170949>.

Dai, A., and NCAR Staff. (2019). The Climate Data Guide: Palmer Drought Severity Index (PDSI). Accessed 7 October 2020. Available online at <https://climatedataguide.ucar.edu/climate-data/palmer-drought-severity-index-pdsi>.

DeSantis, L.R.G, Bhotika, S., Williams, K., and Putz, F.E. (2007). Sea-level rise and drought interactions accelerate forest decline on the Gulf Coast of Florida, USA. *Global Change Biology*, 13(11), 2349-2360, <https://doi.org/10.1111/j.1365-2486.2007.01440.x>.

Donoghue, D.F. (2011). Sea level history of the northern Gulf of Mexico coast and sea level rise scenarios for the near future. *Climatic Change*, 107, 17-33, <https://doi.org/10.1007/s10584-011-0077-x>.

Doswell, C.A.III. (2007). Small Sample Size and Data Quality Issues Illustrated Using Tornado Occurrence Data. *Electronic Journal of Severe Storms Meteorology*, 2(5), 1-16, <https://ejssm.org/ojs/index.php/ejssm/article/view/26/26>.

Elsner, J.B., Elsner, S.C., and Jagger, T.H. (2015). The increasing efficiency of tornado days in the United States. *Climate Dynamics*, 45, 651-659, <https://doi.org/10.1007/s00382-014-2277-3>.

Elsner, J.B., Kossin, J.P., and Jagger, T.H. (2008). The increasing intensity of the strongest tropical cyclones. *Nature*, 455, 92-95, <https://doi.org/10.1038/nature07234>.

Emanuel, K. (2017). Assessing the present and future probability of Hurricane Harvey's rainfall. *PNAS*, 114(48), 12681-12684, <https://doi.org/10.1073/pnas.1716222114>.

FAMWEB. (2020). National Fire and Aviation Management Web Applications – ICS-209 Database. Accessed 3 October 2020. Available online at https://fam.nwcg.gov/fam-web/hist_209/report_list_209.

Fournier, S., Reager, J.T., Lee, T., Vazquez-Cuervo, J., David, C.H., and Gierach, M.M. (2016). SMAP observes flooding from land to sea: The Texas event of 2015. *Geophysical Research Letters*, 43(19), 10338-10346, <https://doi.org/10.1002/2016GL070821>.

Georgia Forestry Commission. (2007). *The Historic 2007 Georgia Wildfires: Learning from the Past – Planning for the Future* (Georgia Forestry Commission Report P1-300-01-08). https://web.archive.org/web/20111006063416/http://www.wildfirelessons.net/documents/Historic_2007_GA_Wildfires.pdf.

Grala, K., and Cooke, W.H.III. (2010). Spatial and temporal characteristics of wildfires in Mississippi, USA. *International Journal of Wildland Fire*, 19(1), 14-28, <https://doi.org/10.1071/WF08104>.

Granath, G., Moore, P.A., Lukenbach, M.C., and Waddington, J.M. (2016). Mitigating wildfire carbon loss in managed northern peatlands through restoration. *Scientific Reports*, 6(24898), 1-9, <https://doi.org/10.1038/srep28498>.

Hoogewind, K.A., Baldwin, M.E., and Trapp, R.J. (2017). The Impact of Climate Change on Hazardous Convective Weather in the United States: Insight from High-Resolution Dynamical

Downscaling. *Journal of Climate*, 30(24), 10081-10100, <https://doi.org/10.1175/JCLI-D-16-0885.1>.

IPCC. (2013). *Climate Change 2013: The Physical Science Basis. Contribution of Working Group I to the Fifth Assessment Report of the Intergovernmental Panel on Climate Change* [Stocker, T.F., D. Qin, G.-K. Plattner, M. Tignor, S.K. Allen, J. Boschung, A. Nauels, Y. Xia, V. Bex and P.M. Midgley (Eds.)]. Cambridge University Press, Cambridge, United Kingdom and New York, NY, USA, 1535 pp.

Knorr, W., Kaminski, T., Arneeth, A., and Weber, U. (2014). Impact of human population density on fire frequency at the global scale. *Biogeosciences*, 11, 1085-1102, <https://doi.org/10.5194/bg-11-1085-2014>.

Knupp, K.R., Murphy, T.A., Coleman, T.A., Wade, R.A., Mullins, S.A., Schultz, C.J., Schultz, E.V., Carey, L., Sherrer, A., McCaul, E.Jr., Carcione, B., Latimer, S., Kula, A., Laws, K., Marsh, P.T., and Klockow, K. (2014). Meteorological Overview of the Devastating 27 April 2011 Tornado Outbreak. *Bulletin of the American Meteorological Society*, 95(7), 1041-1062, <https://doi.org/10.1175/BAMS-D-11-00229.1>.

Knutson, T.R., McBride, J.L., Chan, J., Emanuel, K., Holland, G., Landsea, C., Held, I., Kossin, J.P., Srivastava, A.K., and Sugi, M. (2010). Tropical cyclones and climate change. *Nature Geoscience*, 3, 157-163, <https://doi.org/10.1038/ngeo779>.

Labosier, C.F., Frauenfeld, O.W., Quiring, S.M., and Lafon, C.W. (2014). *International Journal of Climatology*. 35(9), 2620-2634, <https://doi.org/10.1002/joc.4160>.

Langston, A.K., Kaplan, D.A., and Putz, F.E. (2017). A casualty of climate change? Loss of freshwater forest islands on Florida's Gulf Coast. *Global Change Biology*, 23(12), 5383-5397, <https://doi.org/10.1111/gcb.13805>.

Lee, C.C. (2012). Utilizing synoptic climatological methods to assess the impacts of climate change on future tornado-favorable environments. *Natural Hazards*, 62, 325-343, <https://doi.org/10.1007/s11069-011-9998-y>.

Lin, N., Emanuel, K., Oppenheimer, M., and Vanmarcke, E. (2012). Physically based assessment of hurricane surge threat under climate change. *Nature Climate Change*, 2, 462-467, <https://doi.org/10.1038/nclimate1389>.

Liu, Y., Goodrick, S.L., and Stanturf, J.A. (2013). Future U.S. wildfire potential trends projected using a dynamically downscaled climate change scenario. *Forest Ecology and Management*, 294, 120-135, <https://doi.org/10.1016/j.foreco.2012.06.049>.

Maleski, J.J., Martinez, C.J. (2016). Historical trends in rainfall, temperature and drought in the Alabama-Coosa-Tallapoosa and Apalachicola-Chattahoochee-Flint river basins. *International Journal of Climatology*, 37(2), 583-595, <https://doi.org/10.1002/joc.4723>.

Marsooli, R., and Lin, N. (2018). Numerical Modeling of Historical Storm Tides and Waves and Their Interactions Along the U.S. East and Gulf Coasts. *Journal of Geophysical Research: Oceans*, 123(5), 3844-3874, <https://doi.org/10.1029/2017JC013434>.

- Maxwell, J.T., Ortegren, J.T., Knapp, P.A., and Soulé, P.T. (2013). Tropical Cyclones and Drought Amelioration in the Gulf and Southeastern Coastal United States. *Journal of Climate*, 26(21), 8440-8552, <https://doi.org/10.1175/JCLI-D-12-00824.1>.
- McAlpine, S.A., and Porter, J.R. (2018). Estimating Recent Local Impacts of Sea-Level Rise on Current Real-Estate Losses: A Housing Market Case Study in Miami-Dade, Florida. 37, 871-895, <https://doi.org/10.1007/s11113-018-9473-5>.
- Mishra, N. (2015). *What do climate projections say about future droughts in Alabama and the Apalachicola-Chattahoochee-Flint River Basin?* (Master's thesis, Auburn University, Auburn, AL, USA). Available online at <https://pdfs.semanticscholar.org/a5e5/6ad1f0504dbb125371829eeae8721bc0f460.pdf>.
- Mitra, S., and Srivastava, P. (2017). Spatiotemporal variability of meteorological droughts in southeastern USA. *Natural Hazards*, 86, 1007-1038, <https://doi.org/10.1007/s11069-016-2728-8>.
- Moore, T.W., and DeBoer, T.A. (2019). A review and analysis of possible changes to the climatology of tornadoes in the United States. *Progress in Physical Geography: Earth and Environment*, 43(3), 365-390, <https://doi.org/10.1177%2F0309133319829398>.
- National Geographic. (2020). The Ecological Benefits of Fire. Accessed 3 October 2020. Available online at <https://www.nationalgeographic.org/article/ecological-benefits-fire/>.
- Needham, H.F., and Keim, B.D. (2012). A storm surge database for the US Gulf Coast. *International Journal of Climatology*, 32(14), 2108-2123, <https://doi.org/10.1002/joc.2425>.
- NHC. (2018). Costliest U.S. tropical cyclones tables updated. Accessed 12 September 2020. Available online at <https://www.nhc.noaa.gov/news/UpdatedCostliest.pdf>.
- NHC. (2020). National Hurricane Center Data Archive – Tropical Cyclone Reports. Accessed 26 September 2020. Available online at <https://www.nhc.noaa.gov/data/#tcr>.
- NOAA Climate. (2020¹). Climate Change: Global Sea Level. Accessed 26 September 2020. Available online at <https://www.climate.gov/news-features/understanding-climate/climate-change-global-sea-level>.
- NOAA Climate. (2020²). 2010-2019: A landmark decade of U.S. billion-dollar weather and climate disasters. Accessed 8 October 2020. Available online at <https://www.climate.gov/news-features/blogs/beyond-data/2010-2019-landmark-decade-us-billion-dollar-weather-and-climate>.
- NOAA Inundation Dashboard. (2020). Coastal Inundation Dashboard. Accessed 26 September 2020. Available online at <https://tidesandcurrents.noaa.gov/inundationdb/>.
- NOAA NCEI. (2020¹). U.S. Tornado Climatology – Historical Records and Trends. Accessed 18 September 2020. Available online at <https://www.ncdc.noaa.gov/climate-information/extreme-events/us-tornado-climatology/trends>.

- NOAA NCEI. (2020²). Data Tools: 1981-2010 Normals. Accessed 4 October 2020. Available online at <https://www.ncdc.noaa.gov/cdo-web/datatools/normals>.
- NOAA NCEI. (2020³). DROUGHT: Monitoring Economic, Environmental, and Social Impacts. Accessed 8 October 2020. Available online at <https://www.ncdc.noaa.gov/news/drought-monitoring-economic-environmental-and-social-impacts>.
- NOAA NCEI. (2020⁴). Storm Events Database. Accessed 7 October 2020. Available online at <https://www.ncdc.noaa.gov/stormevents/>.
- NOAA NOS. (2020). Historical Hurricane Tracks – Database. Accessed 12 September 2020. Available online at <https://coast.noaa.gov/hurricanes/>.
- NOAA NSSL. (2020). Severe Weather 101 – Flood Basics. Accessed 8 October 2020. Available online at <https://www.nssl.noaa.gov/education/svrwx101/floods/>.
- NOAA NWS. (2010). El Niño and its Effect on the Southeast U.S. Accessed 9 October 2020. Available online at <https://www.weather.gov/tae/enso>.
- NOAA PSL. (2020). Dai Palmer Drought Severity Index data provided by the NOAA/OAR/ESRL PSL, Boulder, Colorado, USA. Accessed 7 October 2020. Available online at <https://psl.noaa.gov/data/gridded/data.pdsi.html>.
- NOAA SLR VIEWER. (2020). Sea Level Rise Viewer – Sea Level Rise. Accessed 26 September 2020. Available online at <https://coast.noaa.gov/slr/#>.
- Nowell, H.K., Holmes, C.D., Robertson, K., Teske, C., and Hiers, J.K. (2018). A New Picture of Fire Extent, Variability and Drought Interaction in Prescribed Fire Landscapes: Insights From Florida Government Records. *Geophysical Research Letters*, 45(15), 7874-7884, <https://doi.org/10.1029/2018GL078679>.
- NPS. (2020). National Park Service - Wildland Fire: What is a Prescribed Fire? Accessed 3 October 2020. Available online at <https://www.nps.gov/articles/what-is-a-prescribed-fire.htm>.
- Patricola, C.M., and Wehner, M.F. (2018). Anthropogenic influences on major tropical cyclone events. *Nature*, 563, 339-346, <https://doi.org/10.1038/s41586-018-0673-2>.
- Prestemon, J.P., Shankar, U., Xiu, A., Talgo, K., Yang, D., Dixon, E.IV., McKenzie, D., and Abt, K.L. (2016). Projecting wildfire area burned in the south-eastern United States, 2011-60. *International Journal of Wildland Fire*, 25, 715-729, <https://doi.org/10.1071/WF15124>.
- Rasmussen, K.L., Prein, A.F., Rasmussen, R.M., Ikeda, K., and Liu, C. (2020). Change in the convective population and thermodynamic environments in convection-permitting regional climate simulations over the United States. *Climate Dynamics*, 55, 383-408, <https://doi.org/10.1007/s00382-017-4000-7>.
- Sajjad, M., Lin, N., and Chan, J.C.L. (2020). Spatial heterogeneities of current and future hurricane flood risk along the U.S. Atlantic and Gulf coasts. *Science of The Total Environment*, 713, 1-11, <https://doi.org/10.1016/j.scitotenv.2020.136704>.

Stambaugh, M.C., Sparks, J.C., and Abadir, E.R. (2014). Historical Pyrogeography of Texas, USA. *Fire Ecology*, 10, 72-89, <https://doi.org/10.4996/fireecology.1003072>.

Stambaugh, M.C., Creacy, G., Sparks, J., and Rooney, M. (2017). Three centuries of fire and forest vegetation transitions preceding Texas' most destructive wildfire: Lost Pines or lost oaks? *Forest Ecology and Management*, 396, 91-101, <https://doi.org/10.1016/j.foreco.2017.04.017>.

Stambaugh, M.C., Guyette, R.P., Stroh, E.D., Struckhoff, M.A., and Whittier, J.B. (2018). Future southcentral US wildfire probability due to climate change. *Climatic Change*, 147, 617-631, <https://doi.org/10.1007/s10584-018-2156-8>.

Stanturf, J.A., Wade, D.D., Waldrop, T.A., Kennard, D.K., and Achtemeier, G.L. (2002). Fire in Southern Forest Landscapes. In D.M. Wear, J. Greis (Eds.). *Southern Forest Resource Assessment* (pp. 607-630). Ashville, NC: U.S. Dept. Agric., Forest Service, Southern Research Station.

Strader, S.M., Ashley, W.S., Pingel, T.J., and Kremenec, A.J. (2017). Projected 21st century changes in tornado exposure, risk, and disaster potential. *Climatic Change*, 141, 301-313, <https://doi.org/10.1007/s10584-017-1905-4>.

SVRGIS. (2019). NOAA Storm Prediction Center – SVRGIS Page. Accessed 18 September 2020. Available online at <https://www.spc.noaa.gov/gis/svrgis/>.

Sweet, W.V., Dusek, G., Obeysekera, J., and Marra, J.J. (2018). *Patterns and Projections of High Tide Flooding Along the U.S. Coastline Using a Common Impact Threshold* (NOAA Technical Report NOS CO-OPS 086). National Ocean Service – Center for Operational Oceanographic Products and Services. https://tidesandcurrents.noaa.gov/publications/techrpt86_PaP_of_HTFlooding.pdf

Tippett, M.K., Lepore, C., and Cohen, J.E. (2016). More tornadoes in the most extreme U.S. tornado outbreaks. *Science*, 354(6318), 1419-1423, <https://doi.org/10.1126/science.aah7393>.

Törnqvist, T.E., Jankowski, K.L., Li, Y.-X., and González, J.L. (2020). Tipping points of Mississippi Delta marshes due to accelerated sea-level rise. *Science Advances*, 6(21), 1-7, <https://doi.org/10.1126/sciadv.aaz5512>.

USGS. (2005). *Summary of Significant Floods in the United States and Puerto Rico, 1994 Through 1998 Water Years*. (Report No. 2005-5194). U.S. Department of the Interior. <https://pubs.usgs.gov/sir/2005/5194/pdf/sir2005-5194.pdf>.

Venkataraman, K., Tummuri, S., Medina, A., and Perry, J. (2016). 21st century drought outlook for major climate divisions of Texas based on CMIP5 multimodel ensemble: Implications for water resource management. *Journal of Hydrology*, 534, 300-316, <https://doi.org/10.1016/j.jhydrol.2016.01.001>.

Wdowinski, S., Bray, R., Kirtman, B.P., and Wu, Z. (2016). Increasing flooding hazard in coastal communities due to rising sea level: Case Study of Miami Beach, Florida. *Ocean & Coastal Management*, 126, 1-8, <http://dx.doi.org/10.1016/j.ocecoaman.2016.03.002>.

- Whitfield, P.H. (2012). Flood in future climates: a review. *Journal of Flood Risk Management*, 5(4), 336-365, <https://doi.org/10.1111/j.1753-318X.2012.01150.x>.
- Wing, O.E.J., Bates, P.D., Smith, A.M., Sampson, C.C., Johnson, K.A., Fargione, J., and Morefield, P. (2018). Estimates of present and future flood risk in the conterminous United States. *Environmental Research Letters*, 13(3), 1-7, <https://doi.org/10.1088/1748-9326/aaac65>.
- WMO. (2017). WMO Guidelines on the Calculation of Climate Normals (WMO Report WMO-No. 1203). World Meteorological Organization. https://library.wmo.int/doc_num.php?explnum_id=4166.
- Wyman, M., Malone, S., Stein, T., and Johnson, C. (2012). Race and Wildfire Risk Perceptions Among Rural Forestland Owners in North-Central Florida. *Society & Natural Resources*, 25(12), 1293-1307, <https://doi.org/10.1080/08941920.2012.681752>.

Glossary

Bermuda-Azores High – An area of semi-permanent high air pressure situated over the subtropical North Atlantic Ocean. Its westward expansion during the summer months directs warm, moist air and hurricanes toward the Gulf Coast States. Also known as the “North Atlantic Subtropical High” or simply the “Azores High”.

Bias – A systematic error that exists in the raw data output of a climate model, judged by the difference between these data and observations of the same variable (e.g., temperature, rainfall). Due to coarse model resolution, the simplification of climate physics in model equations, and incomplete climate system knowledge, biases in climate model outputs are very common.

Bias Correction – The practice of minimizing systematic biases that exist within climate model data. The two commonest bias correction techniques are delta approaches (an additive/subtractive or factor change to a dataset) and quantile mapping (performing different correction regimes for different magnitudes of a given variable). Quantile mapping is the typical approach for stochastic (random) variables like rainfall.

Climate Forcing – The influence of an external process on Earth’s climate system, in terms of the energy gained/lost and the temperature change that results. A climate forcing can be natural in origin, such as solar output variations and volcanic eruptions, or its origin can be human, such as the industrial emission of greenhouse gases.

Climate Normal – A three-decade long average of a given climate variable, whether obtained from climate models or observations. Climate normals are a product developed by NOAA’s National Centers for Environmental Information.

Coupled Model Intercomparison Project (CMIP) – A globally coordinated effort to develop, test, and run climate models to a common set of standards that furthers humanity’s understanding of climate change. Developed by the World Climate Research Program, all data produced by climate models participating in the CMIP are publicly available online. The project is currently entering its Sixth Phase (CMIP6) since beginning in 1995.

Downscaling – The practice of increasing the horizontal and/or vertical resolution of a climate model, thereby improving the model’s depiction of smaller climate features (e.g., land surface, clouds) and ensuring the end-use of produced datasets. Dynamical downscaling applies a GCM’s equations and assumptions to an RCM with a higher-resolution grid. By contrast, statistical downscaling constructs statistical relationships between observations and climate model data to produce a higher-resolution dataset.

General Circulation Model (GCM) – One of the common types of models developed by research institutes participating in the CMIP. These models use our current understanding of climate physics to construct and apply equations that describe behaviors of and interactions between the atmosphere, oceans, land, and ice. These models are ran over the entire planet in order to recreate past states, and project future states, of the climate system. Also known as a “Global Climate Model”.

(The) Greenhouse Effect – The trapping of heat emitted from Earth’s surface by greenhouse gases in the atmosphere. This heat is re-emitted by these gases out into space but more importantly back toward Earth’s surface, thus maintaining a habitable surface temperature. The accumulation of greenhouse gases in the atmosphere from human sources (e.g., transportation, agriculture, and industrial activity) is producing climate change due to the consequent enhancement of the greenhouse effect.

Greenhouse Gases – Gases that enable the trapping and re-emission of heat between the Earth’s atmosphere and surface. Common greenhouse gases include carbon dioxide (CO₂), methane (CH₄), nitrous oxide (N₂O) and water vapor (H₂O). These gases occur naturally in Earth’s atmosphere, but their concentration can be affected by human activity, e.g., livestock farming is a major source of methane and nitrous oxide.

Hazard – A natural event that has the potential to negatively impact humans, animals, and/or the environment. Hazards relevant to the Gulf Coast States include hurricanes, floods, tornadoes, droughts, and wildfires. A hazard becomes a disaster when significant negative impacts take place, e.g., destroyed homes, economic costs, and forced evacuations.

Initial Conditions – The starting values for a given set of variables in a climate model; these values evolve with time as the model’s run progresses. Initial conditions are typically based on observations of variables, such as surface temperature and daily rainfall totals, so that a climate model’s run begins from a basis in reality.

Intergovernmental Panel on Climate Change (IPCC) – An intergovernmental body within the United Nations that is tasked with providing information about current knowledge, risks, and strategies for addressing human-induced climate change worldwide. The IPCC releases Assessment Reports every several years that update said knowledge, risks, and strategies, using the latest climate model data courtesy of the CMIP.

Köppen-Geiger Climate Classification System – A system of succinctly describing general climate properties around the world based on a given region’s typical temperature and rainfall climatology, developed by Wladimir Köppen and Rudolf Geiger. Under this system, most of the Gulf Coast States are classified as having a “humid subtropical” climate, characterized by warm, moist summers and mild winters.

Multi-Model Ensemble – A collection of climate models, often developed by different research institutes, whose outputs together represent the range of possible futures (and sometimes histories) for Earth’s climate system. Multi-model ensembles can also be used to create ensemble datasets by averaging and weighting the outputs of the climate models comprising them, to both mitigate the effects of climate model biases and identify the likeliest climate futures.

North American Monsoon – An annual wind direction change over the western Gulf Coast States that brings warm, moist air from the tropics overland during summer and autumn. This event is responsible for the powerful July-September rainfall that occurs

over West Texas. When the land cools in autumn, the wind direction reverts to former conditions and the warm, moist air supply disappears until next summer.

Projection – The practice of using one or more climate models to simulate the future state of a given variable or component of the climate system. Projection is distinct from prediction because, whereas a prediction assumes that the climate’s future state is determined by initial conditions (what *will* happen), a projection also accounts for changes in the climate system that are independent of the initial conditions (what *could* happen based on what we know).

Regional Climate Model (RCM) – A type of climate model that is developed, tested, and ran to represent a particular region of Earth’s climate, as opposed to the global climate as with GCMs. RCMs use the same equations, assumptions, and conditions as GCMs, but their higher resolution means that regional, small-scale components of the climate system can be more precisely represented, e.g., mountains, coastlines, and clouds.

Regridding – Interpolation of a climate model dataset in order to increase its spatial and/or temporal resolution. The general approach is to use data values for two (or more) grid cells, or points in time, to infer values in between those cells/points, thereby increasing the dataset’s resolution. Regridding is distinct from downscaling because regridding is performed on a climate model dataset, whereas downscaling is performed prior to dataset production.

Representative Concentration Pathways (RCPs) – The greenhouse gas emissions scenarios used by climate models that participated in CMIP5 to drive model projections of the future climate state. The four major RCP scenarios, RCP 2.6, RCP 4.5, RCP 6.0, and RCP 8.5, represent decreasing global efforts to reduce future human greenhouse gas emissions by the year 2100. RCP 8.5 was used for *Climate of the Gulf Coast States* to represent possible but extreme climate change due to little effort to reduce global emissions.

Resolution – The number of grid cells and/or the number of points in time within a dataset of a given spatial domain and/or duration. Increasing the number of model grid cells within a 100 square mile area, or generating data on an hourly rather than a daily timescale, are examples of producing data with a higher resolution. Higher spatial and/or temporal resolution allows a climate model to capture smaller-scale features of Earth’s climate system, which generally increases the model’s precision.

Simulation – The practice of running a climate model to generate data, regardless of the variable, spatial domain, or timeframe desired. Common simulation purposes include testing a model’s performance against observations, or projecting a range of possible futures for an aspect of Earth’s climate system.

Vulnerability – The potential for a given location to be negatively impacted by a hazard. Vulnerability is a product not just of a hazard’s proximity, magnitude, and duration, but also socio-economic factors that increase the likelihood of negative consequences, such as poverty, minority status and political stability.

Acknowledgements

This project is funded by the National Academy of Sciences, Engineering, and Medicine Gulf Research Program. Research reported on this website is supported by the Gulf Research Program of the National Academy of Sciences, Engineering, and Medicine under the Grant Agreement Number 200010878. The content is solely the responsibility of the authors and does not necessarily represent the official views of the Gulf Research Program or the National Academies of Sciences, Engineering, and Medicine.



(End of report)